INSTITUTO SUPERIOR DE ENGENHARIA DE LISBOA

Departamento de Engenharia Eletrónica e Telecomunicações e Computadores

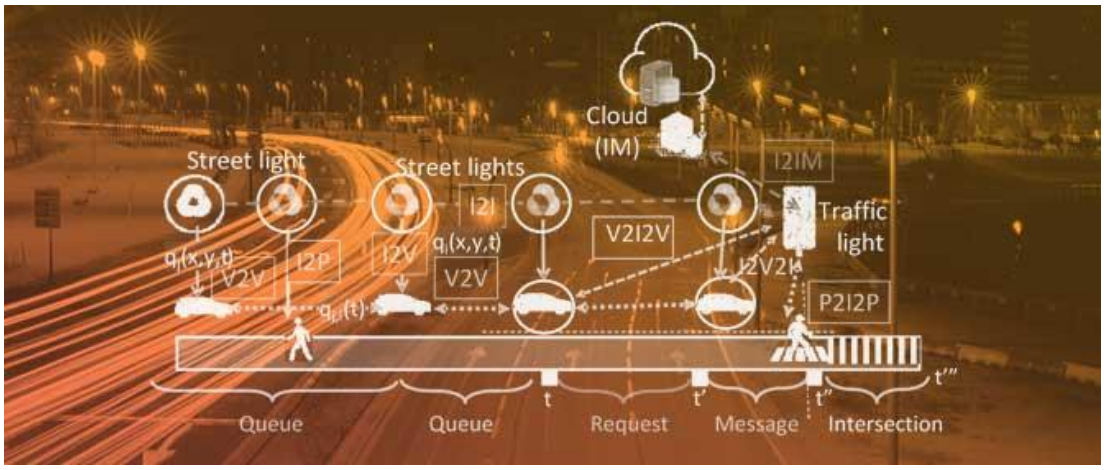

Adaptive Traffic Control in Visible Light Connected Vehicles (VLC)

Gonçalo Baltazar Galvão

Master's Degree in Electronics and Telecommunications Engineering

Supervisors:
Professor Maria Manuela de Almeida Carvalho Vieira
Professor Paula Maria Garcia Louro
Professor Mário Pereira Véstias

Jury:
Professor Rui António Policarpo Duarte
Professor Manuel Martins Barata

07/2024

Acknowledgements

This project's development was a journey filled with many obstacles as well as plenty of opportunities for learning. When I was younger, I never imagined that one day I would have the opportunities that I have had throughout my academic journey, which I hope is nearing an intermission stage.

This Dissertation would not have been possible without the collaboration, encouragement, and commitment of a number of people. As a result, I'd like to express my gratitude and appreciation to everyone who, directly or indirectly, contributed to the happy ending of this story. I'd like to express my heartfelt gratitude to everyone.

First of all, I would like to thank the Professors Doctors and Engineers that supervised me during this period: Manuela Vieira, Paula Louro and Mário Véstias. They were always there to help and I would like to thank them for giving me the opportunity to work with them.

Also take this opportunity to thank Professor and Doctor Manuel Augusto Vieira, who, despite not being my supervisor, was always present at the work meetings and was a key element in the project, as he helped me a lot along the way and I am very grateful. Has been and will continue to be a pleasure to work with the professors.

I now thank ISEL, the institution that welcomed me during the last years, not only for my academic process, but also for the attribution of the Research Fellowship. This work was sponsored by FCT – Fundação para a Ciência e a Tecnologia, within the Research Unit CTS – Center of Technology and Systems, reference “UIDB/00066/2020”.

Last but not least, I thank my family, especially my father, to the one who I dedicate this work, who has always helped me with everything and motivated me to invest in my education.

ABSTRACT

With the modernization of vehicles, new opportunities have emerged when it comes to automotive innovation. Due to the technological evolution of today's new vehicles, it is possible for vehicles to be connected (CV) to each other, exchanging traffic and safety information. This exchange of information, together with the sensor technology applied, makes it possible for autonomous vehicles (AV) to travel from one place to another safely without human intervention. Combining these two technologies it is possible to achieve connected and autonomous vehicles (CAVs).

New communication technologies between vehicles and/or infrastructures can increase safety, comfort, accessibility, and data privacy while traveling. With a connected traffic environment, it is expected to obtain important information about the vehicular and pedestrian traffic flow in order to optimise it. So visible light communication (VLC) is then proposed as an integrated approach to optimize traffic signals and vehicle trajectory at urban intersections. Using the LED technology implemented in road infrastructures like streetlamps and traffic lights and in vehicles on headlights, it is possible to establish various types of communications.

With this amount of information collected via VLC it is necessary to have a system that intelligently controls in real time all traffic and responds to all incoming vehicle's manoeuvring requests. A two connected four-arm intersection scenario with two lanes in both directions is considered. It is assumed that communication between infrastructure and vehicles exists, resulting in a cooperative environment of information sharing. The simulation process of the referred system involves using the SUMO urban mobility simulator to create the traffic scenario and generate traffic flows. A reinforcement learning system, with a Deep Q-Learning algorithm is used to control both intersections, optimising traffic flows and minimise congestion during peak hours.

A comparative analysis of the simulation results highlights the benefits of the proposed approach in terms of throughput, reducing delays and minimising vehicle stops, revealing improved patterns for optimising signals and trajectories. Evaluation on separate training and test sets guarantees the model's reliability and effectiveness.

Keywords : Visible Light Communication, Traffic Control, Connected Vehicles, SUMO, Reinforcement Learning, Deep Q-Learning.

Resumo

Com a modernização dos veículos, surgiram novas oportunidades no que diz respeito à inovação automóvel. Devido à evolução tecnológica dos novos veículos atuais, é possível que os veículos estejam ligados (CV) entre si, trocando informações de trânsito e de segurança. Esta troca de informações, juntamente com a tecnologia de sensores aplicada, permite que os veículos autónomos (AV) se desloquem de um local para outro em segurança, sem intervenção humana. Combinando estas duas tecnologias, é possível obter veículos conectados e autónomos (CAV).

As novas tecnologias de comunicação entre veículos e/ou infraestruturas podem aumentar a segurança, o conforto, a acessibilidade e a privacidade dos dados durante a deslocação. Com um ambiente de tráfego conectado, espera-se obter informações importantes sobre o fluxo de tráfego de veículos e peões, a fim de o otimizar. Assim, a comunicação por luz visível (VLC) é então proposta como uma abordagem integrada para otimizar os sinais de trânsito e a trajetória dos veículos nos cruzamentos urbanos. Utilizando a tecnologia LED implementada nas infraestruturas rodoviárias, como postes de iluminação pública e semáforos, e nos faróis dos veículos, é possível estabelecer vários tipos de comunicações.

Com esta quantidade de informação recolhida através do VLC, é necessário dispor de um sistema que controle de forma inteligente e em tempo real todo o tráfego e responda a todos os pedidos de manobra dos veículos que se aproximam. Considera-se um cenário de intersecção de dois braços ligados com duas faixas de rodagem em ambos os sentidos. Assume-se que existe comunicação entre a infraestrutura e os veículos, resultando num ambiente cooperativo de partilha de informação. O processo de simulação do referido sistema envolve a utilização do simulador de mobilidade urbana SUMO para criar o cenário de tráfego e gerar fluxos de tráfego. Um sistema de aprendizagem por reforço, com um algoritmo Deep Q-Learning, é utilizado para controlar ambas as intersecções, otimizando os fluxos de tráfego e minimizando o congestionamento durante as horas de ponta.

Uma análise comparativa dos resultados da simulação destaca os benefícios da abordagem proposta em termos de rendimento, redução dos atrasos e minimização das paragens dos veículos, revelando melhores padrões para otimizar os sinais e as trajetórias. A avaliação em conjuntos de treino e de teste separados garante a fiabilidade e a eficácia do modelo.

Palavras-chave: Comunicação por luz visível, controlo de tráfego, veículos conectados, SUMO, Reinforcement Learning, Deep-Q Learning

CONTENTS

LIST OF FIGURES

LIST OF TABLES

List of Acronyms

AAC	Adaptive Cruise Control
ADAS	Advanced Assisted Driving System
ADS	Automated Driving System
AI	Artificial Intelligence
AV	Autonomous Vehicle
BER	Bit Error Value
CAV	Connected and Autonomous Vehicle
CRCS	Connected Roadway Classification System
CSMA/CA	Carrier Sense Multiple Acess with Collision Avoidance
CV	Connected Vehicles
DSRC	Dedicated Short Range Communications
ECU	Eletric Control Unit
FCLN	Fully Connected Layer Network
FOV	Field Of View
GNSS	Global Navigation Satellite System
I2IM	Infrastruture-to-Intersection Manager
I2V	Infrastruture-to-Vehicle Communication
IM	Intersection Manager
IR	Infrared
ITS	Intelligent Transport Systems
LCA	Lane Centring Assist
LDW	Lane Departure Warning
LED	Light Emitting Diode
LIDAR	Light Detection and Ranging
Li-Fi	Light Fidelity
LKS	Lane Keeping System
LOS	Line of Sight
MAS	Multi Agent Systems
MSE	Mean Squared Error
NN	Neuronal Network
OFDM	Orthogonal Frequency Division Multiplexing
OOK	On-Off Keying Modulation
RADAR	Radio Detection and Ranging

ReLU	Rectified Linear Unit
RF	Radio Frequency
RL	Reinforcement Learning
RSU	Road Side Units
SAE	Society of Automotive Engineers
SNR	Signal-to-Noise Ratio
SUMO	Simulator of Urban Mobility
USDOT	United States Department of Transportation
V2I	Vehicle-to-Infrastruture Communication
V2V	Vehicle-to-Vehicle Communications
V2X	Vehicle-to-Anything Communication
VLC	Visible Light Communication
VSCC	Vehicular Safety Communications Consortium
V-VLC	Vehicular Visible Light Communications
WLED	White Light Emitting Diode

1

INTRODUCTION

This first chapter serves as the introduction to the document, where the motivations for writing it, the proposed objectives, how it is organized are revealed and the publications that arose from it.

1.1 Motivation

Visible light can be modulated in time and frequency appropriately as a communication technology. Visible Light Communication (VLC) is therefore presented as a communication technology that can complement RF communications when applied in a traffic scenario.

This proposal aims to take advantage of the rise of the Intelligent Transport System (ITS) technology to optimize road safety and traffic management on public roads through communication between vehicles (V2V), from vehicles to infrastructures (V2I) and from infrastructures to vehicles (I2V).

As it is well known, the density of vehicles on public roads tends to increase and the referred technology has characteristics that allow better traffic control, as well as mitigation of possible accidents. Currently it is already possible to collect traffic information through Road Side Units (RSU) such as sensors, but it is still very limited. The introduction of visible light communications in this context should be seen as an opportunity for optimization of connected vehicles.

VLC has several potential applications that are achieved with relative simplicity of design, energy efficiency, low cost, among others. In the case of vehicular communications, the necessary equipment for the emission is already assured considering that there is an increasing number of exterior lightings, traffic lights and vehicles' lights that use LED technology.

Much of the content related to VLC physical transmission has already been properly tested and worked on. However, there is a lack of research to be done in the field of vehicular and pedestrian traffic control, especially when it comes to pedestrians, which is why a large part of the project is focussed on the implementation of a traffic control system model with a VLC system that can serve both vehicles and pedestrians. Traffic control should be adaptive, responding in real-time to traffic demands by

processing and analysing information collected in the field. Compared to the use of sensors, this approach not only provides more detailed information thanks to the VLC's accuracy in collecting the vehicles' position, speed, etc., but also, by analysing the data collected over time, it can decide appropriate to the traffic at any given moment.
The operation of the system should be based on a Reinforcement Learning (RL) method, with Deep Q-Learning algorithms, taking advantage of the information gathered over time to decide the most correct action. The result of the action taken is collected as a reward sample and compared with previous ones, making it possible for the algorithm to understand whether the decision taken was best or not.

1.2 Objectives

This document serves as a proposal for the Master's Thesis whose name is: Adaptive Traffic Control in Visible Light Connected Vehicles (VLC).
Its purpose is to introduce a scenario of an intelligently controlled intersections. A Visible Light Communication (VLC) system that supports safe vehicle management through junctions is considered and uses Vehicle-to-Vehicle, Vehicle-to-Infrastructure, and Infrastructure -to-Vehicle communications for this purpose. By adopting the concept of cooperative communication, it is feasible to access a significant amount of information that was not available before. In this sense, traffic control can be optimized, improving not only its own but also the safety of circulation on public roads. It is intended to implement an intelligent system to manage traffic at the intersections. Artificial intelligence, more especially deep learning, can bring many advantages to the system, especially in critical decision making for traffic control.

1.3 Document Outline

This paper is organized into six chapters, the first of which serves as an introduction. The second chapter is dedicated to the contextualization of concepts addressed such as connected vehicles and VLC, as well as intelligent systems. Chapter 3 describes the system’s design and development process, describing the considered V-VLC scenario and results from the VLC transmission from the lab trials. On chapter 4 a dynamic traffic control system is implemented with different vehicle and pedestrian scenarios. In Chapter 5, the intelligent traffic control system created are demonstrated through simulation to show their effectiveness. The final chapter acts as a conclusion, outlining the key ideas for future work.

1.4 Resulting Outputs

This work was presented under project IPL/2022/POSEIDON ISEL of the IDICA program, 7th Edition. The participation in this project resulted in the submission, publication, and conference presentation of several papers as outputs. Their descriptions follow:

1. G. Galvão, M. Vieira, P. Louro, M. A. Vieira, M. Véstias and P. Vieira, "Visible Light Communication at Urban Intersections to Improve Traffic Signaling and Cooperative Trajectories," 2023 7th International Young Engineers Forum (YEF-ECE), Caparica / Lisbon, Portugal, 2023, pp. 60-65, doi: 10.1109/YEF-ECE58420.2023.10209320.

2. "Traffic flow control on road intersections: Communication through Visible Light ", M. A. Vieira, M. Vieira, P. Louro, P. Vieira, G. Galvão. Comunicação em poster apresentado na conferência 2023 Spring Meeting do European Materials Research Society (E-MRS) que decorreu em Estrasburgo, França de 28 de maio a 2 de junho.

3. M. A. Vieira, G. Galvão, M. Vieira, M. Véstias P. Vieira, and P. Louro "Traffic Signaling and Cooperative Trajectories based on Visible Light Communication" 9th International Conference on Sensors and Electronic Instrumentation Advances (SEIA' 2023), 20-22 September 2023, Funchal (Madeira Island), Portugal. Pp 23-28. ISBN: 978-84-09-53746-4

4. Manuel Augusto Vieira, Manuela Vieira, Paula Louro, Gonçalo Galvão Pedro Vieira, "Smarter Intersections with Cooperative Vehicular Visible Light Communication", SENSORDEVICES 2023 : The Fourteenth International Conference on Sensor Device Technologies and Applications, September 25, 2023 to September 29, 2023, Porto-Portugal, pp. 7-12, Copyright I IARIA, 2023. ISBN: 978-1-68558-091-9.

5. M. A. Vieira, G. Galvão, M. Vieira, M. Véstias P. Vieira, and P. Louro , "*Enhancing Traffic Management through Visible Light Communication-Driven Signaling and Cooperative Trajectories"* Sensors & Transducers journal,Vol. 263, Issue 4, December 2023, *pp. 58-66.*

6. Vieira, M.A.; Galvão, G.; Vieira, M.; Louro, P.; Vestias, M.; Vieira, P., *"Enhancing Urban Intersection Efficiency: Visible Light Communication and Learning-Based Control for Traffic Signal Optimization and Vehicle Management."* Symmetry 2024, 16, 240.

7. G. Galvão, M. A. Vieira, M. Vieira, P. Vieira, P. Louro, M. Vestias, P. Lourenço Traffic “Signals and Cooperative Trajectories at Urban Intersections: Leveraging Visible Light Communication for Implementation”, Light-Emitting Devices, Materials, and Applications XXVIII, edited by Jong Kyu Kim, Michael R. Krames, Martin Strassburg, Proc. Of SPIE Vol. 12906, 129060O © 2024 SPIE · 0277-786X · doi: 10.1117/12.3000529 .

8. Vieira, M.A.; Galvão, G.; Vieira, M.; Louro, P.; Vestias, M.; Vieira, P. “Enhancing Urban Intersection Efficiency: Visible Light Communication and Learning-Based Control for Traffic Signal Optimization and Vehicle Management”. Symmetry 2024, 16, 240. https://doi.org/10.3390/sym16020240

9. Vieira, M.; Vieira, M.A.; Galvão, G.; Louro, P.; Vestias, M.; Vieira, P. “Enhancing Urban Intersection Efficiency: Utilizing Visible Light Communication and Learning-Driven Control for Improved Traffic Signals Performance.” Vehicles 2024, 6, 666–692. https://doi.org/10.3390/vehicles6020031

10. Vieira, M.A.; Vieira, M.; Galvão, G.; Véstias, M.; Vieira, P; Louro, P. “Unlocking Traffic Efficiency: Visible Light Communication for Urban Intersection Optimization”, Presentation ate the SPIE West 2024 Optics and Photonics Conference and Exhibition in Strasbourg, France 7-11 April 2024.

11. Vieira, M.A.; Vieira, M.; Galvão, G.; Véstias, M.; Vieira, P; Louro, P. “Optimizing urban intersection management: a visible light communication approach for cooperative trajectories and traffic signals.”, Presentation ate the SPIE West 2024 Optics and Photonics Conference and Exhibition in Strasbourg, France 7-11 April 2024.

12. Vieira, M.; Vieira, M.A.; Galvão, G.; Louro, P.; Vieira, P.; Fantoni, A. “Enhancing indoor navigation in multi-terminal airports through visible light communication signals.”, Presentation ate the SPIE West 2024 Optics and Photonics Conference and Exhibition in Strasbourg, France 7-11 April 2024.

13. Galvão, M. Vieira, M. A. Vieira, P. Louro, M. Véstias, P. Vieira, “Multi Agent Reinforcement Learning System for Vehicular, Pedestrian Traffic Control with Visible Light Communication,” 2024 8th International Young Engineers Forum (YEF-ECE), Caparica / Lisbon, Portugal, 2024

14. Manuel A.Vieira, Manuela Vieira, Gonçalo Galvão, Paula Louro, Pedro Vieira, Mário Véstias, “Exploring Intersection Dynamics with Visible Light Communication”, 6th International Conference on Microelectronic Devices and Technologies (MicDAT ‘2024) 25-27 September 2024, Ibiza (Balearic Islands), Spain.

15. Manuela Vieira, Manuel A. Vieira, Gonçalo Galvão1 Paula Louro, Pedro Vieira, Mário Véstias “Enhancing Airport Management Using Visible Light Communication” , “Exploring Intersection Dynamics with Visible Light Communication”, 6 th International Conference on Microelectronic Devices and Technologies (MicDAT ‘2024) 25-27 September 2024, Ibiza (Balearic Islands), Spain

16. Manuel A.Vieira, Manuela Vieira, Gonçalo Galvão, Paula Louro, Mário Véstias, “Unlocking Traffic Control: Exploring Intersection Dynamics with Visible Light Communication”, Book of Abstracts, VI International Conference on Applications of Optics and Photonics, AOP2024, Aveiro, Portugal, July 16-19, 2024. ISBN: 978-989-9798-09-1

17. Gonçalo Galvão, Manuela Vieira, Manuel A. Vieira, Paula Louro, Mário Véstias, “Enhancing Urban Traffic Management with Visible Light Communication and Reinforcement Learning “ ”, Book of Abstracts, VI International Conference on Applications of Optics and Photonics, AOP2024, Aveiro, Portugal, July 16-19, 2024. ISBN: 978-989-9798-09-1

18. Manuela Vieira, Manuel A. Vieira, Gonçalo Galvão, Paula Louro, Mário Véstias, “Enhancing Airport Navigation Using Visible Light Communication” ”, Book of Abstracts, VI International Conference on Applications of Optics and Photonics, AOP2024, Aveiro, Portugal, July 16-19, 2024. ISBN: 978-989-9798-09-1

2

STATE OF ART

2.1 Connected Vehicles

Vehicular communication is one of the key enabling technologies for future intelligent transportations systems (ITS) [1][2]. The term connected vehicles refers to applications, services, and technologies that connect a vehicle to its surroundings. The main objective of the ITS technology is to optimize traffic safety and efficiency on public roads by increasing situation awareness and mitigating traffic accidents through Vehicle-to-vehicle (V2V), Infrastructure-to-vehicle (I2V) and Vehicle-to-infrastructure (V2I) communication, as show in Figure 2.1.

The most recurrent 7pportunnalities in connected vehicles may consist of, for example: automatic braking, traffic warnings, GPS, blind spot display, various cameras and sensors from different angles, among others. This is something that, is made possible by the technologies and equipment available in modern vehicles.

Although these already ensure some safety, it is important to add some extra features to improve it even more. With V2V communications, is possible to vehicles to share information with each other along the road. With the adaptive cruise control and automated platooning implemented in these modern vehicles, will result in an increase on lanes capacity. So V2V communications are particularly important for cooperative factors and safety functionalities, such as pre-crash sensing and forward collision warning, by knowing in real time, the location, speed, and direction of nearby vehicles.

I2V communications provide the connected vehicles with a variety of useful information regarding traffic control. The traffic lights should provide status information in real time, displaying warnings inside the vehicle for signal violations, weather condition, or other driving advice to drivers. There are also functions concerning fleet management of vehicle routing and scheduling, enabling also I2V cooperative adaptive cruise control with the current track situation information, provided in real-time. This should hopefully signify the end of queues on the road.

The vehicles' connectivity to the infrastructures (V2I) can provide detailed traffic information (speed, Volume, travel time, queue length, stops, among others) or road surface condition information (pavement roughness or slippery conditions) to the control system. This can only be achieved thanks to the technological enhancements on most recent vehicles, allowing such information acquisition. It can also be used for distress calls and concierge services, as well as automatic payments for tolls or parking spots. Last but not least, the vehicles would be able to request priority signals to the traffic lights.

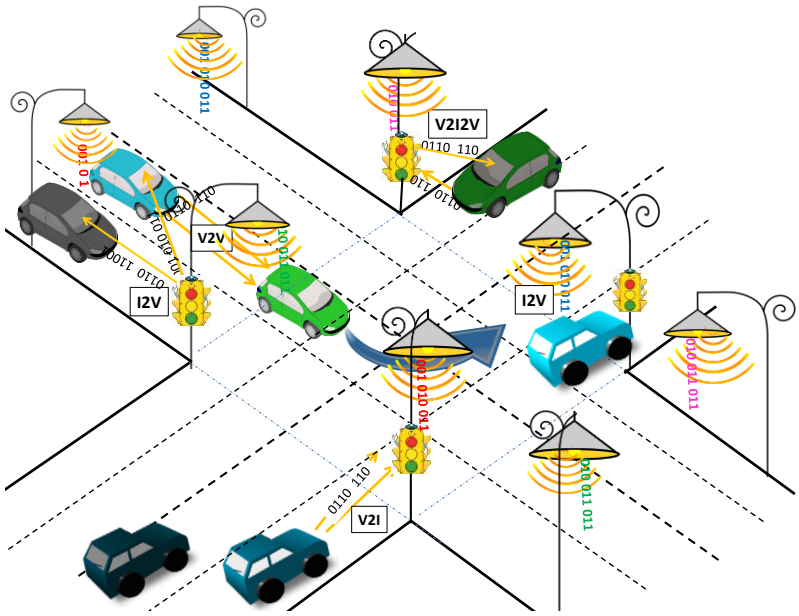

Figure 2.1 – Representation of an intelligent traffic system environment with V2V, I2V and V2I communications

It is considered by many entities that connected vehicles could dramatically reduce the number of fatalities and serious injuries caused by accidents on public roads and highways. Instead of helping people survive crashes, this initiative will prevent crashes from even happening.

On these communications, information is exchanged with the aid of transmitters and receivers strategically placed to allow data transmission with minimal disturbance. On the vehicle side, the headlights are used as transmitters, and receive the signal from other vehicles via sensors at the rear. The vehicles receive the signal from the infrastructure via photodetectors on the vehicle roof. On the infrastructure side, they are also equipped with sensors near their light emitters.

These connectivity types in connected-vehicle systems can be achieved on a variety of wireless communication technologies. Initially, it was thought that mobile radio communications were sufficient to serve the needs. Since then, it has become evident that there is a wider range of wireless

technologies, differing strengths and weaknesses. This has made the spectrum in this frequency range saturated, showing that some alternatives are needed. Section 2.2 will explain in detail what advantages the VLC technology will bring to such a system.

In addition to CV, there are also autonomous vehicles (AV). The difference between the two is that CV use communication technologies to establish connections with other vehicles and infrastructures. On the other hand, autonomous vehicles can go from one place to another, processing only the information collected by sensors and cameras, without human intervention.

Bringing together both technologies, it is possible to transform CV and AV in connected and autonomous vehicles (CAV).

In this chapter a general explanation about connected and autonomous vehicles technology evolution, applications and safety developments, will be given.

2.1.1 Advancement In vehicle automation and their benefits

Over the last decades, progressive technological development has brought human-driven vehicles to the pilot program stage of fully Avs. The active and passive safety systems in modern vehicles initiated advancements in automation [3]. The active safety system is related with airbag and security belts protocols. Active safety is associated to monitoring the environment around the vehicle and controlling its controls to avoid accidents. This system includes an advanced assisted driving system (ADAS) which is a set of functions incorporated into the modern vehicles, being an integrated part of ITS, assisting the human driver in driving functions.

The main ADAS functions are adaptive cruise control (AAC), which aims to accelerate or stop the vehicle. Back-up cameras/sensors that help with parking by allowing you to see the rear of the vehicle. Adaptive headlights that adjust the headlights on bends and corners.

With ADAS it is also possible to help the driver to keep the vehicle safely on the road through Lane Departure Warning (LDW), which alerts the driver when they are leaving the road. Lane centring assist (LCA) which keeps the vehicles in the center of the lane. Lane keeping system (LKS) that confines the vehicles in the lane width. Automatic parking, blind spot monitoring, emergency braking, and pedestrian detection are some other functions implemented too.

The main goal of AD”S is“to ”ransform vehicles from human-driven to fully autonomous conditions. Transportation sectors have already entered into a new era of automation technology by the successful transformation of ADAS into fully automated driving systems (ADS). The Society of Automotive Engineers (SAE), a global platform comprising scientists and engineers, classify passenger transport automation into six levels. These autonomy levels have been adopted by the United States Department of Transportation (USDOT) and the United Nations [4].

The SAE level 0 (ADA") is"pre"ent In most modern vehicles and consists in sensing the surroundings of the vehicle using various sensors. With microcontrollers and an Electric Control Unit (ECU) implemented in the vehicle, sensor data is processed and alerts the human driver to an obstacle, not having any real control over driving functions.

In SAE level 1 (ADAS) microcontrollers process the data of multiple sensors and map the environment around the vehicle. ECU makes the interpretation of the scenario and performs the safest action like steering and braking. ACC, LKS, and collision avoidance are considered as Level 1.

SAE levels 2 (ADAS) and 3 (ADS) can be found in many vehicles manufactured by Audi, Tesla, GM (Cadillac), Lexus, Porsche, BMW, Volvo. Both use advanced algorithms and artificial intelligence to process the information received by various sensors to perform different complex tasks like automatic lane changes and automatic parking.

The last levels are still being tested. Level 4 (ADS) can perform most driving functions, but the vehicles are limited for good weather conditions, and human has the option to take control. Level 5 (ADS) is considered a fully autonomous vehicle. The experimental program of CAVs (Level 4 and 5) is growing tremendously, and the feasibility of commercial deployment has been a reality from the technological point.

ADAS systems are a pointer to a future in which drivers will increasingly rely on ADAS autonomous driving technology. This system will have the ability to not only improve the individual driver experience, but also reduce traffic congestion and pollution. By co-ordinating and synchronizing with infrastructure and other vehicles, traffic flow can be optimized and made more efficient.

Despite ADAS being relatively new, driver acceptance of self-driving technology is rising. A recent study [5] by MIT's Human Centered AI Institute on Tesla journey data found drivers relied on Tesla's Autopilot for over 30% of their total miles driven, which means that over one billion miles have been completed by this feature.

Consumer interest varies by ADAS feature and their associated autonomy levels. Two of the most popular ADAS functions today are blind spot warning (Level 0) and parking assist (Level 1), which achieve 84% and 81% customer satisfaction, respectively. Informational ADAS features are now widely accepted whilst newer, more advanced ADAS features are gaining acceptance, with Level 1 features such as ACC and automatic emergency braking achieving 75% and 69% customer satisfaction, respectively.

Implementation of the autonomous vehicle has potential benefits in various aspects. The positive aspects of CAVs are presented in five major perspectives- road safety, highway capacity, mobility, environmental, and economic.

Road safety is a significant consideration for the transition of human drivers to connected and autonomous drivers. Human drivers and their driving habits are the most influential factors of the crash on the road [6]. Globally there are over a million road fatalities every year and adopting driverless

cars, can potentially reduce if not eliminate, the most significant cause of car accidents, that are human errors. Studies estimate that a significant number of crashes could be avoided as a result of autonomous braking.

The automatic braking configured in the AV system can also have other advantages, for example increase highway capacity. This increased capacity may further induce an overuse of the practical roads, reducing the safe distance between vehicles and increasing vehicle speed [7]. Applications of ACC systems in CAVs increase highway capacity by 80% compared to human-driven traffic [8].

Due to an improvement in mobility, environmental benefits are expected to increase by reducing traffic congestion and smoothening traffic from minimizing stop-and-go driving behaviour. CAVs can potentially reduce the negative environmental impact of the transportation industry and thereby contribute to environmental sustainability, reducing carbon emissions.

The economic benefits of the CAVs are associated with reduced congestion and reduced travel time, and its reliability. Can also allow for more inclusive economic growth through greater accessibility to transport. CAVs open up accessibility to new user groups who were previously unable to drive, such as the elderly and handicapped, which makes it possible to achieve a more inclusive society [9].The increase in vehicle use might also be the result of a modal shift from conventional public transport. For example, buses could be gradually replaced by more flexible, less costly, and easier to operate automated ride-sharing and vehicle-sharing services. The use of high capacity public transport systems, such as trains and metro might also drop after the introduction of automated vehicles, if ride-sharing or vehicle-sharing could adequately serve high-demand corridors.

2.1.2 Sensors and road Infrastructure technology

Although there are differences in the architecture of the various manufacturers, CAVs move on the road based on the same systems. Sensors are used to collect information about the environment around the vehicle. The control system with advanced software to process the information from the sensors to make decisions, such as which way to go on a journey, and finally the actuators to operate the steering wheel, wheels and brakes.

These sensors, used in the recognition phase, can be of different types such as stereo cameras, IR, light detection and ranging (LIDAR), radio detection and ranging (RADAR), ultrasonic sensors and global navigation satellite system (GNSS). They are used to detect and calculate the distance to obstacles, people, roads, and signals from other vehicles, as illustrated in Figure 2.2.

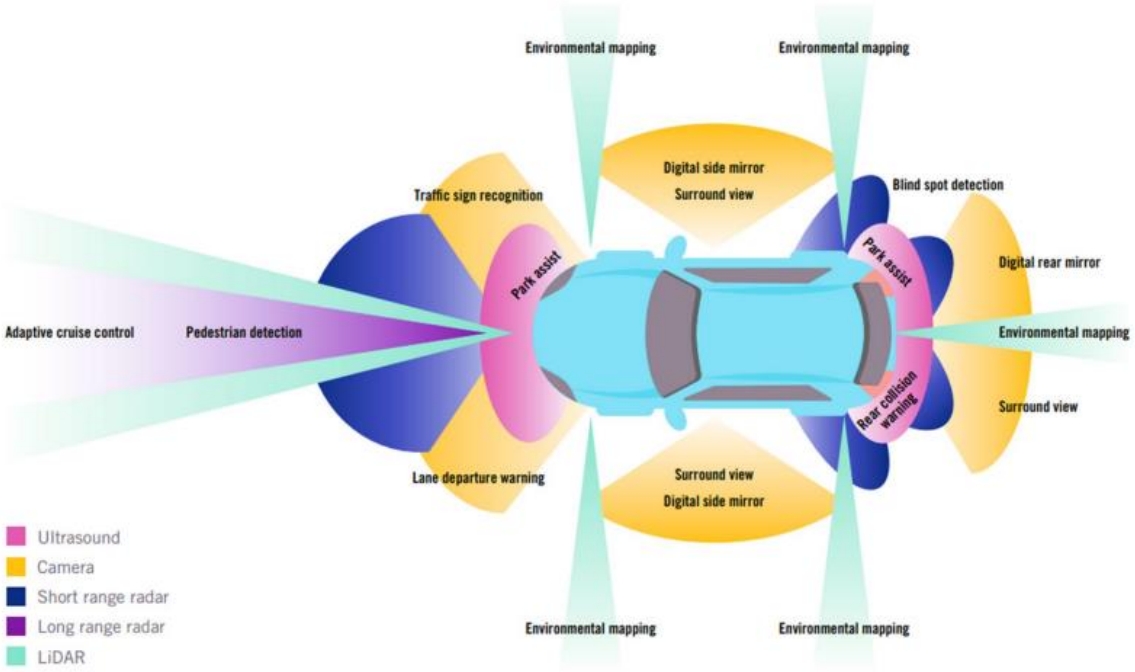

Figure 2.2 – Sensors used in recognising phase of the environment around of an AV and their applications [3].

With the evolution of the vehicles and their implemented technology leads to an improvement of the roads infrastructures to make sure that it is possible to establish communication with the vehicles through V2I and I2V. These advancements are in the planning/study phase to find out the likely impacts of CAVs on physical infrastructures and find out a way out of these limitations.

The United States Transportation Research Board coordinated with the National Cooperative Highway Research Program, are developing a connected roadway classification system (CRCS). This research program developed the framework with three approaches concerning the establish of communication with CAVs.

The first approach is the improvement in the roadway infrastructure, adding communication technology along the roadway, making it possible the establishment of communications of CAVs with infrastructures (V2I) and other vehicles (V2V) on the road. This solution is independent of the technology. Two current approaches are dedicated short-range communication (DSRC) using the 5.9 GHz bandwidth and cellular communication, often identified as C-V2X [10].

The12pportd approach is to enhance the roadway infrastructure to improve safety and operation of CAVs, whether radar, machine vision, or LIDAR, are interpreting the driving environment. Improvements in the infrastructure can enhance the performance and accuracy of these sensors. Examples could be changes in the shape, size, or materials of signs, pavement markings, and traffic signal control systems.

The third approach is to adjust the roadway geometric design to simplify the navigation of CAVs on the roadway. Simplifying the roadway could include changing usage or user access, changing the roadway control to improve the vehicle safety and performance.

Regarding communication between vehicles, in [11] several solutions are proposed. 5.9 GHz Dedicated Short Range Communications (DSRC) based on the IEEE 802.11p standard [12] is often considered as the most promising solution in V2V and I2V communications. DSRC use Orthogonal Frequency Division Multiplexing (OFDM) and is robust to interferences and it is adapted for fast movement conditions. The DSRC channel is divided in 7 channels of 10 MHz, with each channel divided into 52 sub-channels. To comply with the imposed safety requirements, the data is classified in 4 priority categories. Thus, the information required in communication based safety applications is considered to have high priority data and it is transmitted using the center channel (the control channel). To prevent data collisions, DSRC uses Carrier Sense Multiple Access with Collision Avoidance (CSMA/CA). Although several mechanisms are used to improve the reliability of the link and to enable the DSRC technology to provide trustworthy data transfer, reliability issues still arise. Thus, in high traffic densities, packet collisions can occur affecting the reliability and increasing the latencies.

An alternative to DSRC could be represented by the 5G cellular network technology [13], [14]. In this fifth generation mobile communication system it is used millimiter wave radio access with very wide frequency bandwidths of more than 1 GHz, achieving higher data rates and lower latency. Ericsson has recently provided a demonstration using 5G technology in which a truck in Gothenburg (Sweden) is remotely controlled 2500 km away from Barcelona (Spain). This demonstration has as a purpose to show that their 5G services can deliver a high transfer rate that can carry a large amount of data and provide a low latency. These features are essential in automotive applications where real-time data processing is imperative . Nevertheless, it is not sure for now that a similar approach could be used to control an entire vehicle network and to provide reliability in high traffic densities.

In addition to radio frequency and millimiter waves signals, the usage of nanometer waves for short range wireless communication is currently under intense research investigations. The VLC technology uses the visible light (380 – 780 nm) as a carrier for the data and it has already been standardized by the IEEE (IEEE 802.15.7 standard). This is the proposed communication technology of this thesis and an analysis of it is given in the next section, which covers various topics such as is composition, the benefits of this technology in relation to radio frequency communication and how it fits into CAVs and some applications.

2.2 Visible Light Communication (VLC)

As mentioned earlier, the main goal of ITS is to improve road safety, traffic efficiency and driving comfort. By using I2V/V2I and V2V communications, ITS continuously collects traffic data, analyses it and distributes it, in order to increase the vehicle awareness. This collected information enables an efficient management of the transportation system, increasing efficiency and reducing traffic congestion [15]. The data gathered is used to automatically adjust the transport system to different traffic situations [16], [17]. Therefore, a crucial aspect for ITS is its widespread distribution. However, to ensure its effectiveness, the system requires a wide geographical distribution of intelligent vehicles and infrastructures, which allows it to collect more data and distribute it effectively. This distribution of important information can be achieved by using RF communications but with the exponential increase in mobile data traffic over the last two decades, the limitations of RF-only mobile communications were identified. Even with efficient reuse of frequency and space, the current RF spectrum is proving to be too scarce to satisfy the ever-increasing traffic demand. Compared to this, the visible light spectrum, which includes hundreds of terahertz of unlicensed bandwidth is completely untapped for communications. VLC can complement RF-based mobile communication systems in the design of high-capacity mobile data networks. Because of this, the interest in VLC as growing up in the last years [18]. With the evolution of Light Emitted Diodes (LED) technology, these are used as transmitters, allowing visible light to be transmitted and modelled in intensity at high speeds, imperceptible to the human eye. As for the receiver, a photodetector or a camera sensor are used to decode the signal.

Combining the VLC technology with V2V and I2V/V2I communications, it is expected to prevent 81% of vehicles crashes [19]. The VLC technology has the potential to significantly enhance the performances of vehicular networks, especially in high traffic densities, increasing road safety and supporting the distribution of the important traffic information to all intelligent vehicles.

VLC can have indoor and outdoor applications. The first one has received more attention due to the great evolution of the concept of Li-Fi (Light Fidelity), which is a bidirectional wireless system that transmits data via visible light or IR. The second application, and the one that will be studied in this project, has been developed more slowly as it faces more challenges in terms of the environment in which it is used, the type of mobility and the weather conditions.

ITS is the most important outdoor application of VLC, since vehicular network applications can take advantage of the use of LED communication to realise Vehicular Visible Light Communication (V-VLC). The VLC applications for vehicular communication fall into two categories: I2V/V2I and V2V. For I2V/V2I applications, they focus on using the traffic related infrastructure, such as street lights and traffic lights to provide useful information. Both infrastructures have to be LED-based street lights, whose main goal is to provide illumination, can be used for data communication with cars and

pedestrians. These can typically provide coverage in 50 – 100 meters range, creating a VLC cell with nine possible footprints. Each footprint is composed of a set of colours from the infrastructure's lamps, which are modulated in intensity to transmit information to vehicles.
The traffic lights can also communicate with vehicles and because they are always on, they are more suitable for applications such as vehicle safety and traffic information broadcast.
For the V2V applications, they mainly work on exploiting the headlights and taillights on automobile as transmitter, and the photodiode or image sensor as the receiver to provide reliable communications between vehicles.
The following sub-chapters discuss the transmitters and receivers used in VLC communications and how this communication is carried out. It also covers some applications of VLC in vehicle traffic environments and how important this technology can be when applied to communicating with pedestrians so that they can circulate safely both on pavements and on pedestrian crossings.

2.2.1 VLC Transmitter and Receiver

VLC is a medium range optical wireless communication technology which uses the 380-780 nm wavelength of the electromagnetic spectrum, as illustrated in Figure 2.3. To be possible to have visible light communications is necessary to have a transmitter and a receiver.
To transmit the light is used LEDs that are an optoelectronic device that transduces electrical energy into optical energy by emitting incoherent light when driven under forward current controlled by a driver circuit. An important component fo the VLC emitter is the encoder which as the function to convert the data into a modulated message. The encoder commands the switching of the LEDs according to the binary information and the required data rate. The binary data are thus converted into a modulated light beam. For the modulation is used an On-Off-Keying Modulation (OOK) where the bit ''0'' and ''1'' means two different levels of intensity of the light [20].

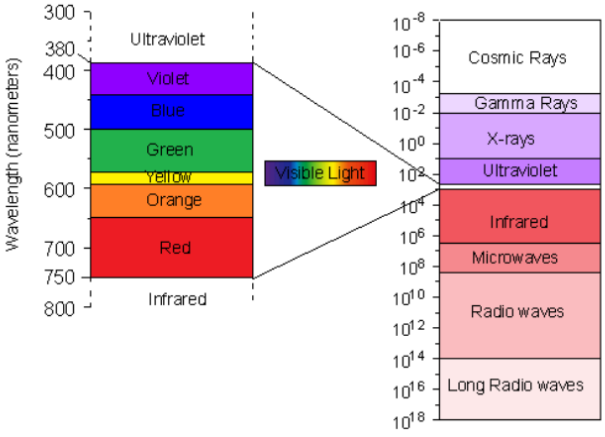

Figure 2.3 - Electromagnetic spectrum zooming at the visible light spectrum.

The LEDs used in VLC have two main purposes: to illuminate and to communicate. So based on these two objectives, white light is therefore the ideal colour to use in both cases and there are two techniques to producing it.

The first one requires the proper combination of two or more LEDs of different colour in a single chip. The most common implementation of this technique is the combination of red, green and blue LEDs to obtain trichromatic white led (WLED). The presence of multiple LEDs in a single chip is advantageous for communication as it allows the use of modulation techniques that can modulate each of the individual LEDs, hence provide higher data rates. On the other hand, increases complexity and the cost of such devices.

The second technique to produce white light using LEDs, is to use phosphor coating with one or more monochromatic or ultraviolet LEDs. The most popular implementation of phosphor coated WLED is the coating of blue led with yellow phosphor layer. In this configuration, some of the converted yellow photons as they interact with the phosphor layer, whereas other photons result in white light. The major limitation of this technique is its limited bandwidth (few MHz) due to slow time response of the yellow phosphor.

As for the receiver, its function is to receive the modulated light and decode it, and there are two types of devices considered. The cheapest and most used is the photodetector, usually composed by positive intrinsic negative (PIN) photodiodes. This component is a semiconductor device that converts the received optical power into electrical current. With the current technology, photodetectors can sample the received visible light at the very high rates of tens of MHz.

The other type of receiver is a camera sensor, that are used in current mobile devices like smartphones to capture images and videos. These devices are composed of many photodetectors arranged in a matrix on and integrated circuit. Besides its price, the main limitation is the very high number of

photodetectors, which significantly reduces the sample rate to a maximum of 40 frames per second. This means that the camera sensor can only communicate using visible light at a very low data rate. Fortunately, camera sensors have a property called ”rolling shutter” that can increase the received data rate. It makes it possible to receive information from different sets of photodiodes. This is a procedure that cannot be done in parallel but must be done sequentially.

In [21] it is explained some major differences between photodiode and camera sensors VLC receiver. In the case of photodiode-based receivers, the background noise is received and processed simultaneously with the data signal, whereas the camera-based receivers can spatially isolate the noise sources. Further on, in photodiode-based receivers the data is recovered by using different types of analog and/or digital signal processing techniques, whereas in the second case, the information is obtained based on high complexity image processing techniques. In some cases, the increased complexity of these procedures does not allow real time data decoding or, when it does, it requires a powerful and thus expensive data processing unit. Because of this, at the moment it is more favourable to use photodetector-based receivers for VLC.

2.2.2 Applications of VLC

As V-VLC uses the visible light portion of the electromagnetic spectrum, the different characteristics of the light waves can help to complement RF technologies. In general, RF technologies in the sub-6 GHz-band as used for vehicular networking have non-directional propagation, relatively long communication range, and can penetrate objects. RF has been very well investigated over the last decades and the technology is quite mature. At the same time, the limited available radio spectrum as well as the congestion level in medium and high node density scenarios are limiting the scalability of RF-based solutions.

The V-VLC can bring some benefits to traffic communication because of the line of sight (LOS) property, its directionality, and the smaller collision domain substantially reducing interferences. Simultaneously, the massive bandwidth available in the visible light spectrum allows huge potential data rates. On the other hand, V-VLC requires LOS, which might not always be available in outdoor scenarios, due to mobility and environmental impact such as heavy snow.

Both technologies can complement each other. RF can make up for VLC short communication range and inability to propagate through opaque objects and V-VLC can offer high data rates with very low interference in LOS scenarios.

RF-based communication technologies such as IEEE 802.11p and C-V2X have been developed specifically for vehicular networking applications. However, RF technologies might not always be able to support all types of applications, especially those which require frequent transmissions in dense scenarios, where safety-critical metrics can suffer due to channel congestion. In such cases V-VLC can

be used to complement RF to decrease the RF channel load and improving the overall system reliability. In [22] some of the most important V-VLC applications are appointed like awareness, sharing sensorial data, safety and informational applications.

Cooperative awareness applications like forward collision warning or emergency vehicle warning, requires communication with the direct vehicle neighbours. V-VLC can be used to exchange messages and therefore reduce channel congestion that would be caused by RF transmissions.

Cooperative Sensing/Perception applications, like see-through video streaming, which includes the sharing of sensory data with vehicles in the vicinity, or collective collection of sensor data to perceive a bigger picture of the driving situation. In this context, headlights and rear lights can be used to transmit high throughput data via V-VLC to the vehicles in front and back, respectively.

Emergency electronic brake light is a safety application that notifies the driver in case that a vehicle ahead brakes suddenly. In these cases, the V2V communication via V-VLC can be used to transmit the emergency brake messages from the vehicle ahead to the following vehicles.

Information query applications use V-VLC for the query and dissemination of information in the scope of the traffic information system. These applications do not have a strong latency and reliability requirements, but they require high scaling throughout the entire network, and for that it is used V2V, V2I and I2V communications.

Intersection Assistance application, like intersection collision avoidance, are used to improve the safety in intersections by providing means of coordination and waring between the vehicles. In these scenarios, vehicle and traffic lights communication via I2V and V2I are important.

VLC can also be used for positional recognition. It enables a more accurate measurement of the distance and position of vehicles with sub-meter resolution given the high directivity of visible light. The VLC capabilities, when combined with the latest equipment in vehicles, enables communication and position acquisition capable of building a map of the vehicle's surroundings. In [23], the results show that it is possible to achieve centimetre-level accuracy with the proposed V2V VLC positioning method. In this way, vehicles can not only obtain the distance to other vehicles, but also transmit this information in real time to nearby vehicles. These vehicles, upon receiving this information, will be able to adjust their speed to maximise fuel efficiency and minimise the risk of accidents.

In terms of data security, given the need to communicate in line-of-sight, an attacker on a VLC communication would require greater exposure compared to RF. Even without considering the available bandwidth, transmission speed or modulation/encoding mechanism. VLC already proves to be a more secure option.

Although VLC is currently being studied for its strong application in communications between vehicles and infrastructures, this technology can also be used to establish communications with pedestrians.

Pedestrian traffic control is also an important topic when it comes to road safety. In [24], the impact that pedestrians have on accidents is studied. In these cases, accidents are often caused by vehicles,

but the fault is not directly related to the driver, but rather to the pedestrian's behaviour on the road. In [25]Europe road fatalities statistics are analysed, in specific in urban areas, and among the various road users, drivers, pedestrians, cyclists and motorcyclists, 40% of all fatalities are pedestrians, which demonstrates their vulnerability on the roads.

Improving vehicles, road infrastructure and integrating intelligent technologies into road safety applications are the most concrete solution. These are fully compatible with the current trend towards smart cities and wireless communication technologies in order to improve the safety of vulnerable road users.

This means that pedestrian traffic control also needs to be treated with the most importance in order to guarantee pedestrian safety, avoiding accidents that can have serious consequences for people's lives as well as for the flow of traffic on the roads. This requires a strict phase control for both vehicles and pedestrians, as well as a good way of detecting pedestrians, whether at pedestrian crossings and on pavements, implemented in intelligent vehicles and traffic signals.

A pedestrian detection system is proposed in [25]. The pedestrian detection is done on the pavements, even before the persons reaches the crosswalk. The detection was tested with various sensors, such as LIDAR, Ultrasonic, Passive Infra-red (PIR) and Microwaves sensors, placed in a crosswalk traffic signal. After the pedestrian detection, a VLC transmitter, also placed in the traffic signal, emitted the information to a VLC receiver, in this case, a photodetector, implemented in a vehicle. The test results show that the pedestrians are detected with high percentage of success. As for the VLC system , the results are variable, with better BER (Bit Error Value) values in night time conditions, around 10^{-5}, regarding daytime BER values reaching 10^{-3}. As the vehicle continues to move forward, the VLC distance, between the transmitter and receiver, is decreasing and the SNR is improving, enabling in turn BER around 10^{-6} , even in daytime conditions.

Despite all these outdoor applications that VLC can have, it still faces many challenges. One of them was observed in this test and is related to sunlight, which affects the quality of the received signal sent by the transmitter. In the next section explores other challenges that VLC faces caused by the outdoor environment.

2.2.3 Major challenges in VLC outdoor applications

Despite VLC being a single communication technology, thus a similar operating principle, outdoor and indoor applications assume different expectations, dissimilar channel conditions and therefore rather different challenges.

First of all, indoor applications are expected to provide very high data rates (Gb/s) for distances that are usually bellow 2 or 3 meters. On the other hand, outdoor applications are expected to provide

significantly larger communication distances, and in consequence, lower data rates can be achieved, and that can be a problem. In vehicles safety communication it Is required a very high packet delivery ratio and latencies as low as 20 ms, meaning that a higher robustness to disturbances is expected.

Another major difference between both environments comes from the totally dissimilar channel conditions. In indoor applications, the influence of external light interferences is negligible, as the light of the VLC transmitter is usually the main source of light. The outdoor channel is far more problematic, as it is strongly influenced by the numerous sources of external lights [26], especially background solar radiation, and because of that, one of the main goals on vehicular communication is to is to mitigate the21pportts of the intense ambient interferences and to ensure a reliable long range link. The parasitic lights incident on the VLC receiver, in this case a photodetector, introduces a very strong DC component. Although this DC component can be easily removed, the generated current also produces a noise component, being this the dominant noise source. Moreover, if the sunlight is directly facing the receiver, it can saturate the photodetector, obstructing the communication.

There are many approaches to decrease this noise effects. In [27] is discussed this problem and the solution consists of reducing the field of view (FOV). In general, the power of the received noise is strictly dependent of the receiver FOV. The implemented solution was to reduce it, and in consequence, the environmental light coming from the sides. Test results show that by decreasing the FOV, a communication distance of up to 50 meters is achieved, whereas the BER is maintained lower than 10^{-7}, even in outdoor sunny conditions. Although this solution significantly enhances the SNR, it has as disadvantage fact that it proportionally reduces the mobility. A good signal detection is always obtained in VLC when the transmitter and receiver are in s LOS configuration. This allows the receiver to operate in a narrow FOV, being a good solution for an efficient data transmission, but in other hand, reduces the mobility of both transmitter and receiver [28].

Another challenge is related with the dynamic nature of the vehicular environment and the diverse weather conditions making the VLC channel very unpredictable. Besides sunlight, VLC can also be affected by snow or by heavy dust, which can obstruct the communication path, and therefore, influence the power of the received signal. Moreover, the water particles from fog or from rain drops, affect the light passage through a combination of absorption, reflection and scattering, increasing the channel unpredictability.

Other main challenge to enable the usage of the VLC technology in automotive application is increasing the communication distance. Vehicle Safety Communications Consortium (VSCC) has concluded that the safety and the efficiency of the transportation system can be substantially increased by using wireless communications to enable real-time data exchange between the vehicles and the traffic infrastructures. Furthermore, VSCC has published a report, where it has defined a preliminary

vehicular communication requirement [29]. For high priority safety applications, a communication distance bellow 300 meters is required, as is possible to see at Table 2.1.

Table 2.1 - The high priority safety applications and the respective maximum communication distance

Applications	Max. Range [m]	Type
Traffic Signal Violation Warning	250	I2V
Curve Speed Warning	200	I2V
Emergency Electronic Brake Light	300	V2V
Pre-Crash Sensing	50	V2V
Cooperative Forward Collision Warning	150	V2V
Left Turn Assistance	300	I2V and V2I
Lane Change Warning	150	V2V
Stop Sign Movement Assistance	300	I2V and V2V

However, it is also defined that in particular traffic situations and conditions, most of them involve shorter distances, as it is possible to see in Table 2.2.

The existing VLC prototypes achieve low error communication distances that can go up to 100 meters in the case of the camera-based systems, and 40-60 meters for the photodiode based systems. Therefore, in order to be fully compatible with the automotive domain, the communication distance needs to be further enhanced.

Table 2.2 - Inter-vehicle distance in different traffic conditions

Conditions	Inter-vehicle distance [m]
Traffic Jam	<35
Roadway in urban areas	35 – 49
Urban highways rush hours	50 – 66
Urban highway	67 – 100
Rural highway	101 – 159
Rural areas	> 160

The communication distance can be increased by using optical lenses at the receiver side. This solution is very efficient and for this reason, this technique is used in most of the VLC receivers intended for long distance applications. The demonstration showing the impact of optical lenses usage can be found in [30]. In the test, by narrowing the beam divergence and by using a 25 mm focal length lens at the receiver, the communication distance is increased from 1 to 31 meters.

Another technique to increase the communication distance, especially for high priority messages, is by using multi-hop transmissions. Such structures are normally used to extend the signal coverage for limited power transmissions, but in the case of VLC applications these structures could also be used to address network nodes that are not within the transmitter's LOS. In such cases, the source of information, for example a traffic light, transmits a message which is received by the vehicles in its vicinity. The vehicles receiving the message, recognize its high priority, and forward it to the vehicles behind, creating a relay-assisted network, with a I2V2V communication.

2.3 Traffic Light Control System

Transport is directly related to people's daily lives and people depend heavily on transport resulting in the increasing number of vehicles on the roads, which leads to an increase in traffic congestion. This scenario mostly prevails during the morning time when majority of the people are heading towards their workplaces and at the evening times when they are heading back towards their homes. The most widely used traffic control scheme is the fixed-time traffic control system, and it cannot meet the requirements of optimal waiting times on roads. Due to its non-adaptive nature, it easily causes traffic congestions when the traffic flow is uneven on the roads. This system does not have any provisions to make an estimate of the traffic loads. As a result, for variable traffic densities these systems continue to work with their fixed timed phases and do not adapt to the present traffic load. Thus, the roads with minimum traffic loads are also served with the same time durations as that of the roads with high traffic. Therefore, the people on roads with high traffic have to wait unnecessarily for that excess amount of time when there is almost no vehicle on the road being served. This leads to wastage of time and thus increases the total travelling time. So, it is necessary a more rigorous control of phases, where their activation would be based on observation of road occupancy with phase times that adapt to traffic density. With this implementation would be possible to improve the system and traffic flow on the roads.

A traffic phase is of a set of traffic light signals that control the flow of vehicle and pedestrian traffic passing through them. Figure 2.4 represents a set of possible phases at an intersection, which may vary in number, in order to control the traffic circulating there, thus increasing the safety of the intersection.

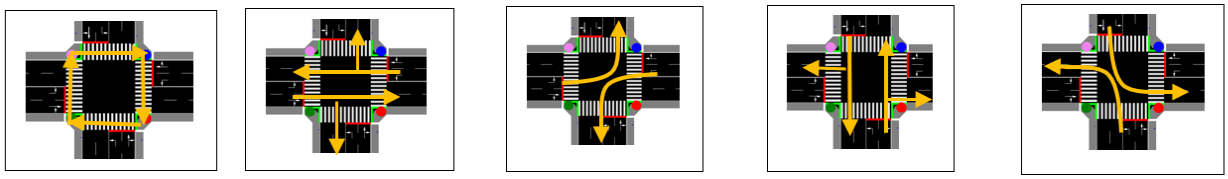

Figure 2.4 - Possible phases activated by traffic lights to control traffic at an intersection

The system currently in place also do not have provisions to provide any traffic related information to users either through a broadcast scheme or on-demand on the mobile phones. Thus, in case of high traffic situations and congestions more vehicles accumulate on the congested road and the problem becomes more severe. This leads to more waiting time and rise in pollution. If people get the traffic information well in advance, then they can easily avoid high traffic and congested roads by taking an alternate route.

A traffic control system does not only control the flow of the vehicles on the roads but also it manages the phases of signalization for pedestrians in crosswalks. Good control of pedestrian movement on the roads is extremely important. The main causes of conflict involving pedestrians and vehicles are due to poor control of phases and their activation times. Long waiting times for the green light for pedestrians can lead to a lack of patience on the part of pedestrians to wait, leading them to cross at a red light. In cases of large concentrations of people in waiting areas, due to the fixed green time for the phases without adapting to the density of pedestrians, this time can be too short for everyone to pass safely within the time limit, causing some to cross when the phase is no longer active, which reduces pedestrian safety. Also, activating phases for vehicles and pedestrians at the same time reduces safety on the roads, since the left or right turning movement of a vehicle in permissive green mode collides with a pedestrian phase.

To reduce this traffic congestion and increase travel safety, an intelligent traffic light control system needs to be implemented. With this system it is possible to control each phase that is activated by the traffic lights, by varying the time they are active, depending on various aspects of the flow of vehicles, such as speed or the number of cars waiting, and can prioritise a phase in order to ensure that the environment is balanced.

In order to develop a fully adaptive traffic system, it is necessary to turn to the field of artificial intelligence. One of the acceptations of the goals of AI is to develop machines that resemble the intelligent behaviour of a human being. In order to achieve this goal, an AI system should be able to interact with the environment and learn how to correctly act inside it. An established area of AI that has been proved capable of experience-driven autonomous learning is reinforcement learning.

2.3.1 Reinforcement Learning and Deep Q-Learning

For traffic control problems, Reinforcement Learning (RL) based approaches usually take the traffic flow states around the intersections as the observable states, the change of signal timing plans as actions, and the traffic control performance as feedback [31].

RL is a type of machine learning paradigm where an agent learns to make decision by interacting with an environment. The agents learn to achieve a goal in an uncertain, potentially complex environment by receiving feedback in the form of rewards or punishments. The fundamental idea is for the agent to learn optimal behaviour or strategies through trial and error. At each time step t, the agent receives a state input s_t, based on the observation of the environment and then executes an action a_t, that transforms the state observed to a next state s_{t+1}. Then the reward r_t, a metric that defines how good the action was for the environment, is calculated. In most cases, the reward is defined by the equation

(1), where tw_t and tw_{t-1} represent the total waiting time of all the vehicles in the intersection captured respectively at *t* and *t-1*.

$$r_t = tw_{t-1} - tw_t \quad (1)$$

If the agent's behaviour leads to positive environmental reward, which indicates that the waiting time is longer in the past, *t-1*, than at the present moment, *t*, then the tendency of producing this behaviour by the agent will be strengthened, and vice versa. The goal is to maximize the cumulative discounted reward.

This experience $e_x = (s_t, a_t, r_t, s_{t+1})$ will be stored in the replay memory, to be used in the future to train the agent. The replay memory is a dataset of an agent's experiences $D_t = (e_1, e_2, \dots, e_t)$, which are gathered when the agent interact with the environment as time goes by (t = 1, 2…, n). In training, a mini batch of random samples are chosen. This random selection of samples breaks the temporal correlation between consecutive samples. If the agent learned only from consecutive samples of experiences, as they occurred sequentially in the environment, the samples would be highly correlated and would therefore lead to inefficient learning. The replay memory buffer is filled until a specific length and when it is full, old experiences are overwritten by new ones.

To train the agent, the deep Q-Learning technique is employed, leveraging the Q-Learning algorithm. The Q-value (Quality-value) represents the expected cumulative reward of taking a particular action in a particular state and following the optimal policy thereafter. In traditional, Q-Learning algorithm stores the Q-value associated with each state-action pair in a look-up table. Therefore, it is also called tabular Q-Learning. This method guarantees convergence to the optimal value with infinite visits to state-action pairs. However, this tabular approach is effective only for problems with small-scale state and action spaces. Real-world challenges with continuous and large-scale state and action spaces led to the adoption of deep Q-Learning networks. In this approach, instead of estimating the Q-Value of each state-action separately, Q-values are predicted by a neural network (NN) that takes the state as input and outputs Q-values for each possible action.

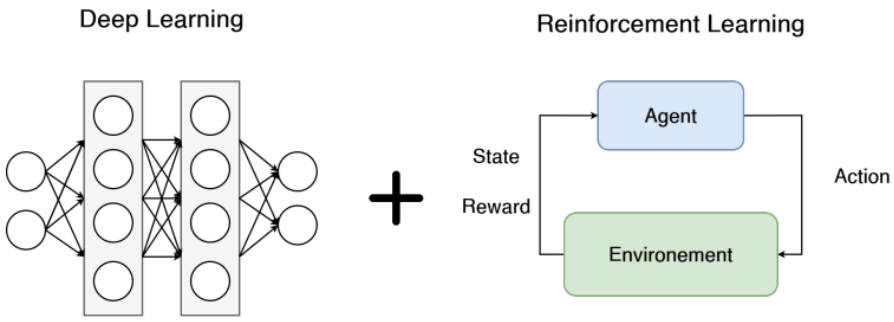

Figure 2.5 - Deep Reinforcement Learning

The neural network architecture consists of a fully connected layer network (FCLN), and the weights θ_k of the FCLN are used to approximate its Q-values Q(s, a; θ_k). The first layer of the network is the input layer, representing the state of the environment. Following this, there are several hidden layers, each with rectified linear unit (ReLU), an activation function commonly used in deep neural networks, with the ability to introduce non-linearity to the network, allowing the NN to learn complex patterns and representations in the data. Finally comes the output layer, which will display the Q-Values for each action. The next action that the agent will choose is determined by the maximum Q-Value output. To improve this prediction of Q-Values it is used a Mean-Squared-Error function that is a mathematical function that quantifies the difference between the predicted Q-values and the target Q-values, as it is possible to see in equation (2).

$$MSE\ Loss = \frac{1}{N}\sum_{i=1}^{N}(Q_{target} - Q_{pred})^2 \quad (2)$$

Where N is the number of samples in the memory, Q_{target} and Q_{pred} are the target and predicted value, respectively. After each episode of training the target Q-Values for action-state pairs are calculated based on the following equation (3).

$$Q_{target} = r_t + \gamma . maxQ_{pre}(s_{t+1}, a') \quad (3)$$

Where r_t is the reward obtained, γ is a discount factor applied to the $maxQ_{pred}$ value, lowering the importance of the future reward compared to the immediate reward.

The MSE loss function calculates the squared difference between each predicted and target value. The goal during training is to minimize this loss, meaning the model aims to make its predictions as close as possible to the true target values. This function is decreasing the difference between the initial prediction and the target by the learning rate. With the repetition of the updating process, the weights θ_k of the neurons in the neural network are adjusted in order to make the approximation of the Q-value predicted to the target Q-value. The loss will decrease, and the prediction will be better, which means that the agent will take better decisions in choosing actions based on the observed environment.

2.3.2 Intelligent control CV systems

In a reinforcement learning problem, an autonomous agent is inserted into a given environment, in this case, a traffic scenario such as an intersection [32]. The agent observes the scenario and controls it by activating the traffic light phase that it believes will bring the most benefit to the environment. To train the agent, the field of reinforcement learning comprises a number of algorithms that employ slightly different methodologies. Their approaches to navigating their environments account for the majority of the differences. Reinforcement learning can be applied in many different ways, but some are more flexible than others. Q-Learning and Deep Q-Learning are two different approaches that can be considered, where the second one considers Deep Q-Networks, combining RL with neural networks. In [33][34] is aborded the reinforcement learning and deep Q-Learning techniques and it is developed a traffic scenario in SUMO of a four-arm intersection which is controlled by an agent trained by a neural network. Depending on the observed scenario, the agent chooses the best action from an action set. This action represents an activation of a green phase for a set of lanes for a fixed amount of time. After taken an action the agent receives a reward that qualifies it based on the vehicles avarage time waiting. The results show that as the training progresses, the agent makes better decisions lowering the avarage queue lengths and waiting times, demonstrating that this is a reliable method to improve traffic flow.

In more complicated traffic scenarios like multi-intersection systems, a more complex approach has to be considered. The complex intersections features, heterogeneous intersection structures, and dynamic coordination for multiple intersections pose challenges for reinforcement learning-based algorithms. Many real problems require the interaction of multiple agents to maximize the learning performance [35], [36]. Reaching a globally optimum solution when considering other agent's actions is a challenging task. This is even more the case, when, for scalability, increasing the 'umber of agents also makes the state-action dimensions soar.

The first main issue with high-dimensional systems is the stability. When each agent optimizes its action without considering close agents, the optimal learning for the overall system would eventually

become non-stationary. This central problem in Multiagent Systems (MAS) also leads to the inadaptation of agents into the environment. There are several approaches to address this, such as distributed learning, cooperative learning and competitive learning [37].

In [38] for an adaptive multi-intersection signal control it is proposed a cooperative deep Q-Network with Q-value transfer, where the traffic scenario is modelled as a multi-agent reinforcement learning system. Each agents searches the optimal strategy to control an intersection by a deep Q-network, taking discrete state encoding of traffic information, like vehicle position in intersection approaching lanes and normalized speed as network inputs. To work cooperatively, the agent considers the influence of the latest actions of its adjacencies in the process of policy learning. Especially, the optimal Q-values of the neighbour agents at the latest time step are transferred to the loss function of the Q-network. The performance results of the Cooperative Deep Q-Learning with Q-Value transfer (QT-CDQN) are compared with other algorithms, including coordinated deep reinforcement learners (CDRL), multi-agent deep Q-Learning (MADQN) and distributed Q-Learning and shows that QT-CDQN is competitive and efficient in terms of different metrics.

Several approaches in a two connected intersection scenario are considered in [35]. In the first one, each intersection is associated with an independent agent and each one is unaware of what the other agent is doing and how their actions might affect itself. The training process is done by using an Independent Deep Q-Network where each agent trains is own network. A second solution is an enhanced representation of the environments state observed by the agent. The state becomes composed, when the agent uses information from its neighbours to compose the state information. The last approach consists in two new different definitions of the reward. With a multi-agent controlled intersection, the hypothesis of a new local reward is tested. The idea is to have a hybrid metric that could deal with both the measured queue length along each incoming lane and the cumulative delay of the vehicles. This reward is defined in the equation (4), where *c* is a fixed factor that works as a trade-off coefficient, *tw* is the total waiting time of the vehicles and *queue* is the measured queue length along each incoming lane.

$$r_t = (c.tw_{t-1} + queue_{t-1}) - (c.tw_t + queue_t) \quad (4)$$

Other type of reward is also tested and it is a shared reward, defined in equation (5), where a_n is the agent n with n = 1,2, ${r_t}^{a1}$ the reward obtained by the agent a_1 at time *t,* and α a discounted factor which is set arbitrarily, at 0.5. The objective of this test is to analyse the behavior of the agent's learning ability in case they share the same reward, potentially leading to some collaborative behavior since both of them would be linked by the metric.

$$\begin{cases} {r_t}^{a1} = {r_t}^{a1} + \alpha . {r_t}^{a2} \\ {r_t}^{a2} = {r_t}^{a2} + \alpha . {r_t}^{a1} \end{cases} \quad (5)$$

The results of these various approaches mentioned above turn out not to be as exciting as expected. The agents show difficulties in learning throughout the training process, which results in poor decisions being made in their actions, affecting the traffic flow, increasing the queue lengths as well as waiting times for vehicles. This demonstrates that inserting agents into this type of complex environments is not as straightforward as it might seem.

3 VEHICULAR-VISIBLE LIGHT COMMUNICATION

In the previous chapter, it was possible to inform and contextualize the reader to the main areas that make up the project in question With this, it is possible to begin the description of the work conducted. First, we address the V-VLC communication and how it would be implemented and carried out on the various roadways of the considered traffic scenario. Next, the description of the communication protocol created for V2V, V2I/I2V, and P2I/I2P communications for vehicles and pedestrians, respectively, is presented. Lastly, experimental results from simulations of the various communications for a specifically designed scenario are analysed.

3.1 V-VLC Communication Link

The proposed V-VLC system, as illustrated in Figure 3.1 , employs a mesh cellular hybrid structure featuring two distinct controllers: the “mesh” controller situated at streetlights, responsible for relaying messages to vehicles, and the “mesh/cellular” hybrid controller at streetlights, serving as a border-router for edge computing [39]. This architectural framework facilitates Infrastructure-to-cloud communication (I2IM), utilizing embedded computing platforms for tasks like processing, interfacing with sensors, and enabling geo-distribution and real-time load balancing. By processing data at the edge, the system enhances response times and alleviates the load on central cloud infrastructure [40]. Additionally, the design fosters peer-to-peer communication (I2I) among vehicles, promoting advanced data sharing and collaboration within the network.

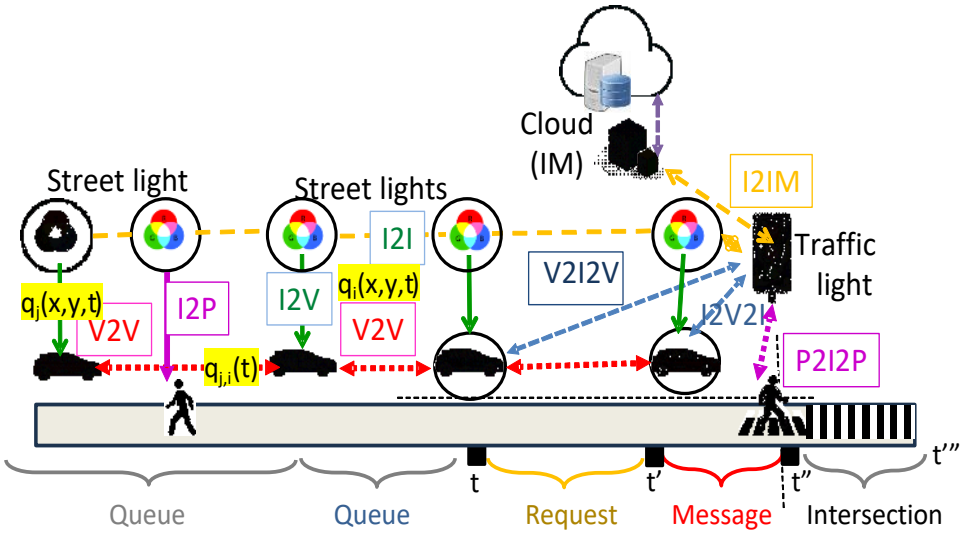

Figure 3.1 - 2D Graphical representation of the simultaneous localization as a function of node density, mobility and transmission range.

The Vehicular VLC system (V-VLC) comprises a transmitter that generates modulated light and a receiver located in infrastructures, driving to detect the received light variation, as illustrated in Figure 3.2. Both the transmitter and receiver are connected through the wireless channel. In this system, the light produced by the LED is modulated using ON-OFF-keying (OOK) amplitude modulation. The environment is defined by a cluster of square unit cells arranged in an orthogonal geometry. Different data channels are provided by tetra-chromatic white light (WLEDs) sources positioned at the corners of the square unit cells distributed along the road and at the crossroads. The white WLEDs sources consist of Red (R: 626 nm), the Green (G: 530 nm), the Blue (B: 470 nm) or the Violet (V: 390 nm) chips and combine the lights in correct proportion to generate white light.

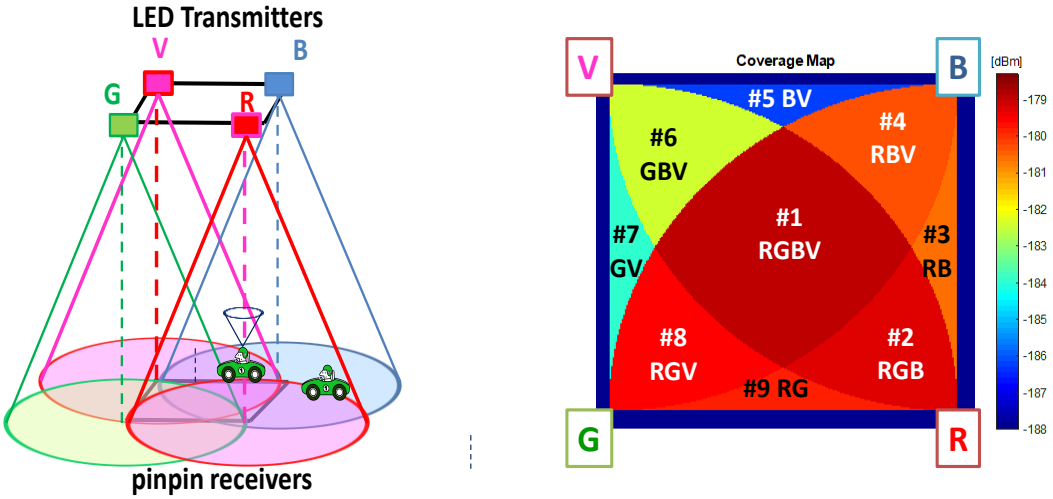

Figure 3.2 - Illustration of the coverage map in the unit cell: footprint regions (#1-#9).

The V-VLC system operates on coded signals transmitted by devices like streetlights and traffic lights. These signals serve to communicate directly with identified vehicles (I2V) and pedestrians (I2P), or indirectly between vehicles through their headlights (V2V).

Upon entry into the capture range of a streetlight, a vehicle or pedestrian triggers a response from the receiver, which assigns a distinctive ID and traffic message. To regulate vehicle passage through intersections, the system employs queue/request/response mechanisms and temporal/space relative pose concepts. In this zones, illustrated in Figure 3.1, important V2I, V2V and I2V communications are carried out to inform the intersection manager (IM) about the state of the lane, exchanging information on various traffic metrics that help with decision-making about which phases to activate.

Pin-Pin photodetectors with light-filtering properties, embedded within mobile receivers, receive, and decode the coded signals[41]. A MUX receiver multiplexes various optical channels, performs filtering processes (such as amplification and switching), and identifies the centroid of received coordinates. This information is stored as reference point positions. Nine reference points are identified within each unit cell, offering fine-grained resolution in localizing mobile devices across the network. This input, comprising coded signals from transmitters to identify vehicles/pedestrians (I2V/P), facilitates pinpointing positions within the network ($q(x_i, y_j, t)$) within specific unit cells (#1-#9) and provides directional guidance (cardinal points) for drivers/pedestrians along their paths.

Vehicle speed is determined using transmitter IDs for tracking ($q_i(x,y,t)$), while mesh nodes estimate indirect V2V relative poses ($q_{ij}(t)$) in scenarios with multiple neighboring vehicles. Various notations ($q(t)$, $q(t')$, $q(t'')$, $q(t''')$) represent vehicle pose estimations at different times. Requests include positions, directions, and speeds, with leader-follower information aiding V2I request confirmation.

Delays are determined by observing vehicle queues in each cell at the beginning and end of green times through V2V2I mechanisms, as illustrated in Figure 3.1.
The integration of VLC facilitates direct monitoring among pedestrians, vehicles, and infrastructure, focusing on critical aspects such as queue formation, speed thresholds, inter-vehicle spacing, and pedestrian corner density to enhance road safety. V2I2V/P2I2P communication enables travel time calculations, while real-time data on speed and waiting times are analyzed using transmitter tracking IDs. Receivers compute geographical positions over time, allowing for inference of pedestrian speed.

3.2 Communication Protocol

To encode the information, an On-Off Keying (OOK) modulation scheme was employed, utilizing synchronous transmission with a 64-bit data frame[42]. To transmit the signals, each infrastructure is equipped with tetrachromatic LEDs, enabling the simultaneous transmission of four signals. This configuration requires a receiver capable of actively filtering each channel, providing a four-fold increase in bandwidth.
Each of the RGBV signals sent has a wavelength calibrated amplitude that defines it. Since each VLC infrastructure has four independent emitters, the optical signal generated in the receiver can have one, two, three, or even four optical excitations, resulting in 2^4 different optical combinations and 16 different photocurrent levels at the photodetector. Filtering is accomplished using a PIN-PIN demultiplexer. The PIN-PIN demultiplexer plays a crucial role in the decoding process, ensuring accurate retrieval of the original message. It receives the combined OOK signals and armed with prior knowledge of the calibrated amplitudes, decodes the sent message.
The communication protocol defines the structure and rules governing the exchange of Information. It includes specifications for the synchronization, identification, and payload portions of the transmitted frame. The communication protocol is presented in Table 1.
Each frame depends on the kind of communication (1-6) and starts with a synchronization block, followed by various identification blocks, and ends with an EoF block. The traffic message contains critical information related to vehicles and pedestrian's movements. The entire structure ensures a systematic and standardized communication protocol for the VLC system [43].

Table 3.1 – Message protocol defined for each of the V-VLC communications

		COM	Position												
L2V	Sync	1	x	y	END	Hour	Min	Sec	Payload (32 bits)						EOF
V2V	Sync	2	x	y	Lane (0–7)	N° Veic.	END	Hour	Min	Sec	Car IDx	Car IDy	n° behind		EOF
V2I	Sync	3	x	y	TL (0–15)	N° Veic.	END	Hour	Min	Sec	Car IDx	Car IDy	n° behind		EOF
I2V	Sync	4	x	y	TL (0–15)	ID veic	END	Hour	Min	Sec	Car IDx	Car IDy	n° behind	Phase	EOF
P2I	Sync	5	x	y	TL (0–15)	Direct.	END	Hour	Min	Sec	payload				EOF
I2P	Sync	6	x	y	TL (0–15)	Phase	END	Hour	Min	Sec	Payload				EOF

Starting the analysis of the communication protocol by examining the frame structure it begins with a synchronization block (Sync) of five bits, indicated by the pattern [10101]. This is used to synchronize the receivers and identify the start of a new frame.

Advancing to the identification blocks (ID), these encode information using binary representation for coded decimal numbers. Information includes the type of communication (COM), localization of transmitters (x, y coordinates), and timeline information (END, Hour, Min, Sec). The time sub-block begins with the pattern [111] to alert the decoder that the following bit sequence (6+6+6) corresponds to time identification rather than payload.

Other ID blocks include the necessary number and temporary identification of vehicles following the leader. Include also information related to the occupied lane (Lane 0-7), traffic light (TL) signal requested (TL 0-15), cardinal direction, or active phase provided by the infrastructure in a “response” or “request” message at the intersection.

In relation to the traffic messages of the communication protocol, this block includes vehicle information such as x, y coordinates and order of cars behind the leader that request/receive permission to cross the intersection (CarIDx, CarIDy, nº behind). It also includes traffic information (payload) such as road Conditions, average waiting time or weather conditions.

The frame concludes with a 4-bit EoF block, defined by the pattern [0000], indicating the end of the frame.

3.3 V-VLC Experimental Results

The traffic scenario used for study in this project is displayed in Figure 3.3. It considers two four-arm connected intersections, with two lanes per arm, totaling 160 meters in length, intended for vehicles and pavements on each side of the road for pedestrians to walk around the environment. Right lanes are used to go straight or turn right and left lanes only to turn left. Each lane also contains the footprint cells (1-9) where the vehicles will be detected. The positions of the respective streetlights (R,G,B,V), identified with the respective colors that will be modulated for communication, are also shown throughout the environment. These streetlights work as a geo-transmitters and for that reason they are strategically positioned along the roadside, 20 meters apart [44]. Each LED transmitter emits an I2V message, sending synchronization, physical ID and traffic information. When a vehicle or a pedestrian enters the capture range of a streetlight, the receiver promptly responds by assigning a unique ID (x, y, t) and providing relevant traffic information.

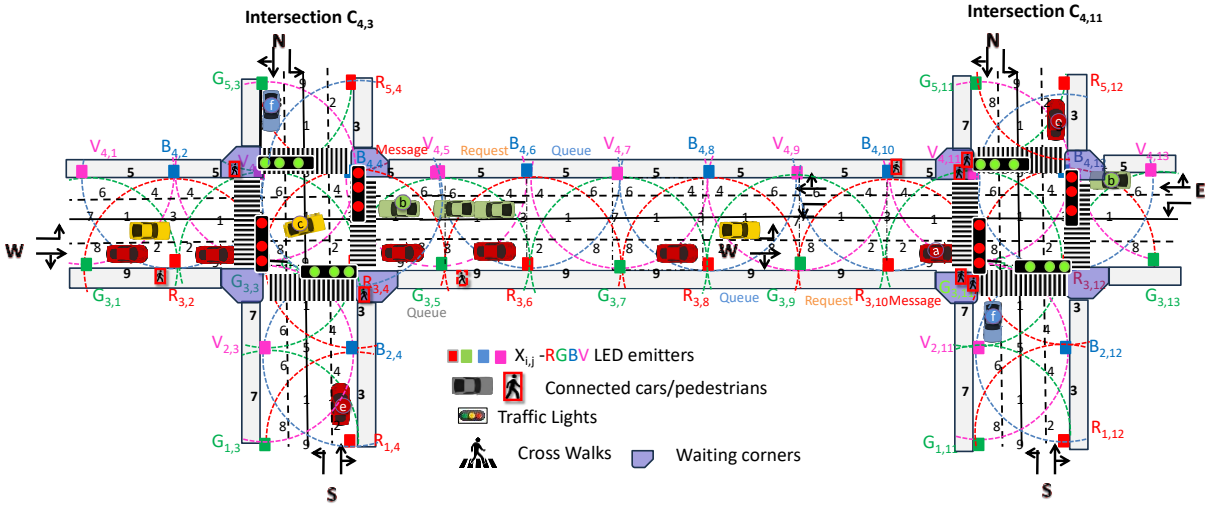

Figure 3.3 - Traffic scenario considered with the respective footprints (1-9), connected vehicles and pedestrians.

As the vehicle or pedestrian approaches an intersection, they initiate a request for permission to cross (V/P2I). In response, an acknowledgment (response, I2V/P) is dispatched from the traffic signal to the head vehicle's in-car application or to the pedestrians.

If a crossing request poses a potential collision risk with approved vehicles, the intersection manager that controls the junction, exercises caution by delaying the response until the risk is adequately mitigated. Vehicle speed is calculated by measuring the actual travelled distance over time, utilizing the IDs (x, y, t) of transmitters for tracking. In scenarios involving multiple neighbouring vehicles, the mesh node employs indirect V2V relative pose estimations, leveraging data from each neighbouring vehicle. All requests include vehicle positions, directions and approach speeds. In cases where

followers exist, the request message from the leader, i.e. the first vehicle in the queue, includes the poses and speed previously received by V2V. This information serves as an alert to the controller for a subsequent request message (V2I) confirmed by the following vehicle. To determine delays, the number of vehicles queuing in each cell at the beginning and end of the green time is ascertained through V2V2I observation.

The introduction of VLC between pedestrians, vehicles and the surrounding infrastructure allows the direct monitoring of critical points that are related to the queue formation and dissipation, relative speed thresholds, inter-vehicle spacing and pedestrian corner density increasing the road safety. Critical points where traffic conditions may change include instances where a pedestrian stops and joins the waiting corners. Through P2I2P communication, the travel time influencing different sidewalks can be calculated, and real-time data about speed and waiting times are analyzed using the ID's transmitter tracking [45]. Receivers compute geographical positions in successive instants (path) and infer the pedestrian's speed.

Some laboratory tests were then carried out, in a controlled environment, where the various existing communications considering vehicles and pedestrians were simulated.

Based on the measured photocurrent signal by the receiver the transmitted information must be decoded, requiring a predefined calibration curve for this purpose. The bit sequence for this curve was chosen to allow all the *on/off* sixteen possible combinations of the four optical channels (2^4). Each of the 16 distinct photocurrent levels on the calibration curve corresponds to one of the 2^4 possible RGBV channel combinations. By matching the sixteen calibrated levels with their respective 4-digit RGBV binary codes, the decoding process becomes straightforward, allowing the message to be deciphered. Subsequently, decoding the MUX signals and analyzing the frame structure (refer to Table 3.1) unveils details such as the communication type, transmitter positions, frame time and traffic messages.

Considering Figure 3.3 with the respective vehicle positions, and the communication protocol in Table 3.1 along with the technique for decoding calibrated signals emitted by transmitters, Figure 3.4 displays the decoded optical signals and the signals received (MUX) by the receivers in a V2V (COM 2) and V2I (COM 3) communication scenario involving a leader vehicle a_o at position ($R_{3,10}$, $G_{3,11}$, $B_{4,10,}$). This vehicle is communicating with the IM at the second intersection (C2) on lane L0 (direction E) at 10:25:46 and is followed by three other vehicles (Veic. Nr) V_1, V_2, and V_3 with the same direction, located at positions (Idx,y) $R_{3,8}$, $G_{3,6}$ and $R_{3,4}$, respectively.

In Figure 3b, the responses (I2V and I2P) from two traffic lights (TL10 and TL13) to the crossing request from the preceding vehicle a_o ($R_{3,10}$, $G_{3,11}$,$B_{4,10,}$) and a pedestrian q_1 located in the "waiting corner" of the first intersection ($R_{3,4}$, $G_{3,5}$) are exemplified. The timestamps "10:25:46" and "10:28:66" represent the times at which the two responses were sent and provide a reference point for when each response was generated.

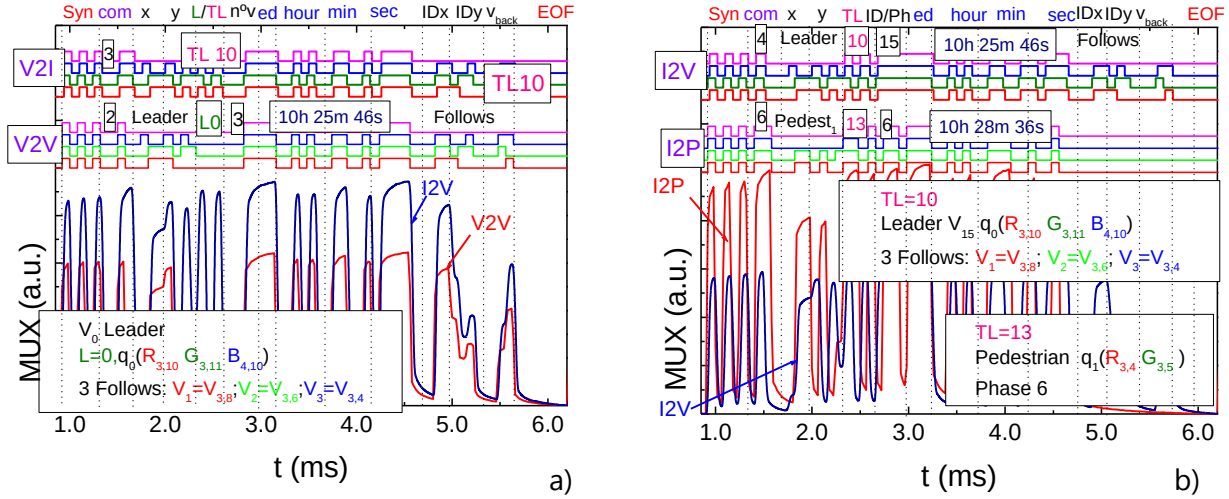

Figure 3.4 - MUX signal request (a) and responses (b) assigned to different types of V-VLC communication.

Figure 3.5 a) illustrates the MUX signal sent to the traffic lights (TL's) by pedestrians to cross both intersections (C1 and C2) while waiting in the corners ($P_{1,2}2I$). In this figure, the top part displays the decoded messages, and on the right-hand side, the content of the message is outlined. Furthermore, Figure 3.5 b) demonstrates the MUX signal received by the traffic lights ($I2P_{1,2}$). The top part of the figure showcases the decoded messages, while the right-hand side provides a draft of the message content. This visual representation helps to understand the communication between pedestrians waiting in the corners and the corresponding traffic lights, providing insights into the signals exchanged for pedestrian crossings at both intersections (C1 and C2).

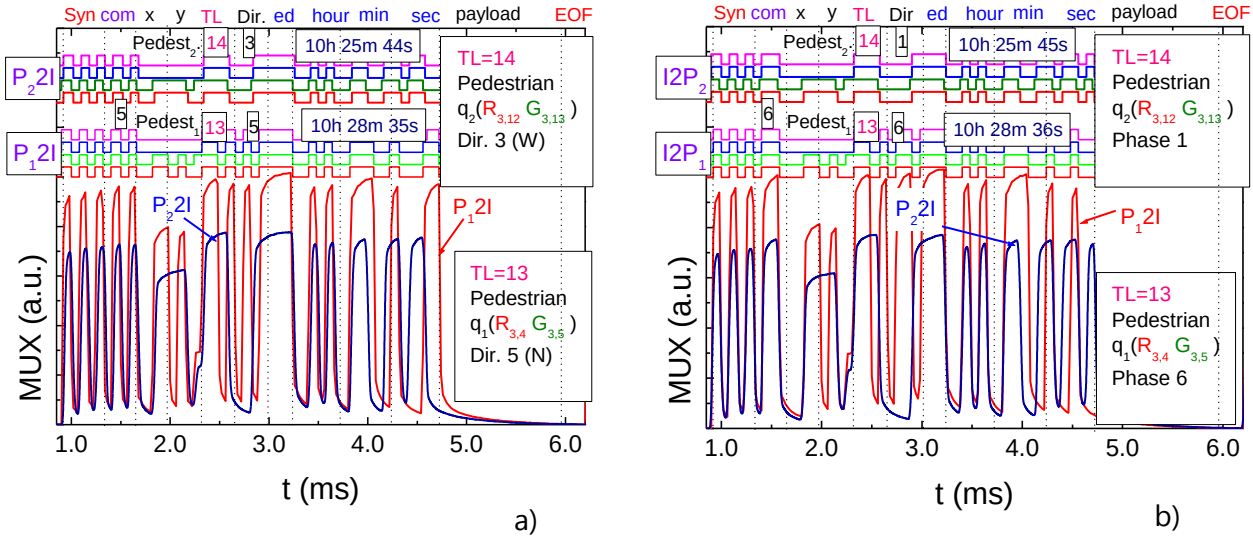

Figure 3.5 - Normalized MUX signal responses and the corresponding decoded messages, sent by pedestrians waiting in the corners (a) and acquired by them (I2P1,2) (b) at various frame times.

This representation provides insight into the communication dynamics between pedestrians and traffic lights at different intersections. The results reveal that the pedestrian begins walking on the sidewalk lane towards the west (W) with the intention of crossing at C2, waiting in the designated area at positions $R_{3,12}$-$G_{3,13}$. At precisely 10:25:44, the pedestrian initiates communication with the traffic light ($P_2$2I), and within a second, by "10:25:45", a response is received (I2P_2). The pedestrian patiently remains in the waiting zone until the pedestrian phase becomes active. Upon receiving information from the traffic light, it becomes evident that the current active phase is N-S (Phase 1), signifying that the pedestrian did not arrive in time "or their"designated phase (Phase 0). Consequently, the pedestrian is required to wait for an "stimated"120 seconds before being granted the 41pportunityy to cross. Subsequently, the pedestrian crosses the crosswalk, covering the distance to the next intersection in approximately 1 minute and 50 seconds. Upon arrival, the pedestrian waits in the designated waiting zone at position $R_{3,4}$-$G_{3,5}$ until the pedestrian phase becomes active once again. At "10:28:35", the pedestrian establishes communication with traffic light at the C1 ($P_1$2I). The traffic light promptly responds (I2P_1) at "10:28:36", providing crucial information that the currently active phase is the final one in the cycle (Phase 6). These interactions highlight the effectiveness of the pedestrian's communication with the traffic lights, enabling them to stay informed about the active phase, waiting time, and make decisions accordingly.

4 DYNAMIC TRAFFIC CONTROL SYSTEM

This section is dedicated to the description of the work developed within the dynamic traffic control system. This system serves as a basis for comparison with the intelligent control system in the following chapter. The results are obtained through a simulation and, to this end, a brief introduction to the simulation tool SUMO is given in the first subchapter as well as the traffic scenario considered for this work. Next, it is described the traffic flow scenarios of vehicles and the results obtained from the simulation.

4.1 Traffic Environment and Cycle Phases

Simulation of Urban Mobility (SUMO) is an open source, highly portable, microscopic and continuous traffic simulation package designed to handle large networks. It allows for intermodal simulation including vehicles and pedestrians and comes with a large set of tools for scenario creation.
The considered environment for simulation, represented in Figure 4.1, is a two four way connected intersections (C1 and C2), where two lanes per arm approach the junction, leading to two lanes per arm leaving the intersection. Each arm is 160 meters long and each lane defines the possible directions that a vehicle can follow. The right lane enables vehicles to turn right or going straight while on the left the left turn is the only direction allowed. In the center of the intersections, a traffic light system, controlled by the IM, manages the approaching traffic. This scenario turns out to be somewhat different from the traffic scenarios observed in the state of the art, where each arm of the road is usually made up of more than two lanes with the option to go straight and a left-turn lane. This change is made because the scenario created is thought to be the most appropriate for autonomous vehicles to circulate. Before reaching the continuous line, they must already be properly positioned in the lane that corresponds to their intended destination. Once in the correct position, it then communicates via V2I with the IM indicating that it wants to cross the intersection in the respective direction.

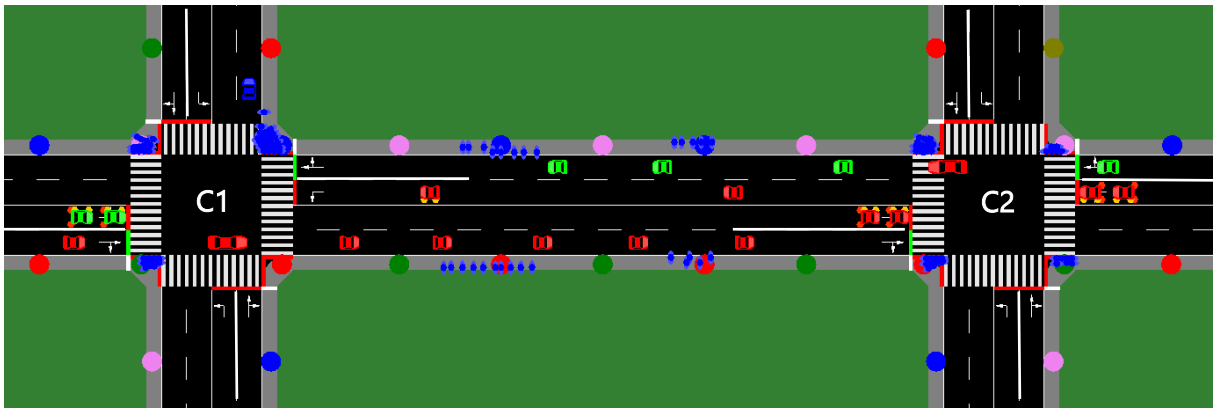

Figure 4.1 – Traffic scenario considered build on SUMO

A traffic control system made up of sixteen traffic lights has been implemented to control traffic arriving at the intersections. These are numbered as shown in Figure 4.2 a), where it is also illustrated the numbering of the considered lanes, the same for both junctions. With these sixteen traffic lights it is possible to implement the phases that will control the flow of traffic and pedestrians as shown in the Figure 4.2 b).

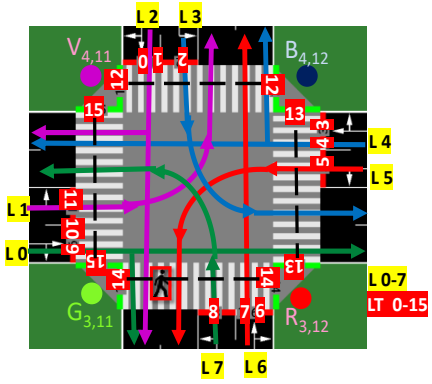

a)

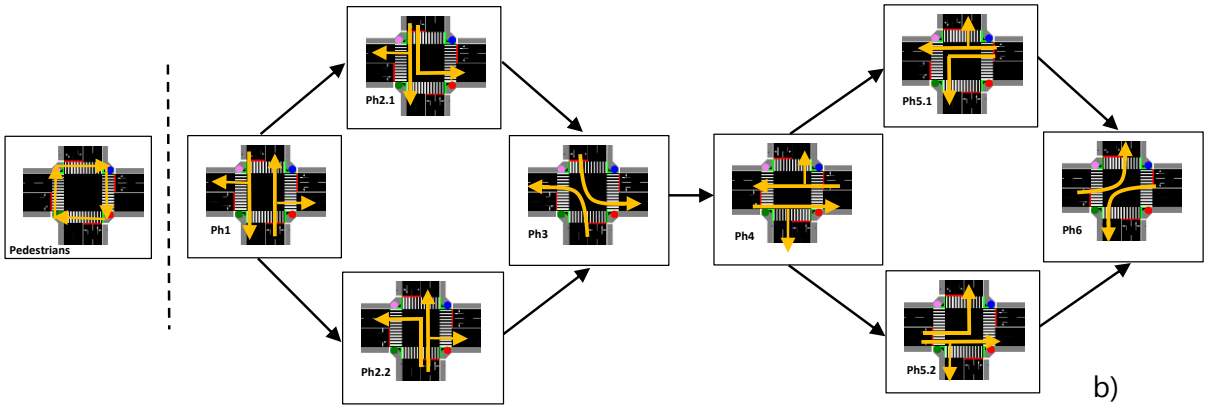

Figure 4.2 - Schematic diagram of the intersection with coded traffic lights (TL 0-15) and lanes (L 0-7) (a). Diagram of the considered phase (b)

The cycle of the phases starts always with the pedestrian phase (Ph 0), where the traffic lights 12-15 are set to a green signal, enabling pedestrians to cross at crossings. The other traffic lights are set to red, not allowing any vehicles to cross the junction. This ensures and increases the safety of pedestrians when travelling on the roads, since they have a phase reserved for their movement. This implemented phase is different from the pedestrian phases in the state of the art, where pedestrians were considered to have more than one phase, which was active together with a vehicle phase. This would result in some vehicles meeting pedestrians at pedestrian crossings, which is not very safe for them.

The next phase in the cycle is the phase North-South (Ph 1) where only the traffic lights 0-1 and 6-7 are set to green. This enables vehicles to cross the intersection by going straight ahead or turning right. After this phase a decision has to be made by the intersection manager where he has to choose between the phase North to all direction (Ph 2.1), where the traffic lights 0-2 are set to green, or South to all directions (Ph 2.2), with the respective traffic lights 6-8, and only one phase can be active in the respective cycle. This choice is based on the number of cars waiting in the respective lanes. If the L2 lane has more waiting vehicles than the L6 lane so the phase 2.1 is active, otherwise phase 2.2 is activated. After that the North-South left turn phase (Ph 3) is actuated, where only the traffic lights 2 and 8 are set to a green signal.

When all the north-south phases have been activated, the system moves on to the West-East phase (Ph 4), where only the traffic lights 3-4 and 9-10 are set to green. After this the same decision as before has to be made between the West all direction phase (Ph 5.1) and the Wast all direction phase (5.2). Then, as the last phase of the cycle, West-East phase (Ph 6) is activated, returning again to the pedestrian phase, completing a cycle.

Between each phase transition an intermediate phase is active, where the respective traffic lights with a green light are turned yellow, after the phase time has ended, turning red when the new phase is active. These intermediate phases have a fixed time duration of 4 seconds, except the intermediate

phase of pedestrians, between Ph 0 and Ph 1, where it is 6 seconds. This extra time is given to ensure that people on the zebra crossing can leave it before the vehicle phase is active, ensuring pedestrian safety.
The duration of one of each phase is determined dynamically depending on the number of cars waiting to cross the junction, in the respective lane for the corresponding phase, and also depending on the traffic scenario in question, as will be seen in the next subchapter, as well as the duration of the respective cycle, which will be important for the development of the intelligent system.

4.2 Traffic Scenarios with Vehicles

In order to analyse the functioning of the dynamic system, several traffic scenarios involving only vehicles were developed. These scenarios involved the generation of vehicles in specific quantities and lanes, according to the parameters intended for the study of each scenario. Scenarios of high, medium, and low traffic were developed to observe the decision-making of the IM and to verify and adjust the duration of each phase so that the cycle duration aligned with the desired goals. It was predefined that a cycle for a high-traffic scenario should have a duration of approximately 120 seconds, while a low-traffic scenario should have a duration of 80 seconds. For scenarios with medium traffic, a duration of approximately 100 seconds was established.
To align with the defined cycle times, the phase durations had to be adjusted based on the number of cars transversing the environment. Additionally, the time each vehicle in the waiting queue, where the respective phase would be active, would take to cross the traffic light of the respective lane had to be considered and adjusted accordingly. In order to gain additional time during the transition between phases, intermediate phases were added to avoid unnecessary red signals. For example, during an active North-South phase (PH 1) transitioning to an all-direction north phase (PH2.1), an intermediate phase was introduced. This prevents the traffic lights 0-1 from unnecessarily turning red since they will turn green again in the next active phase. During this phase, the signals for these lanes remain green, with only the signals from traffic lights 6-7 changing to yellow. Subsequently, when phase 3 becomes active, these turn red. In Table 4.1 all phases are represented in the order in which they occur throughout the cycle. The ‘next’ column indicates which phase will be active next after the current one concludes.

Table 4.1 - Order of phases and intermediate phases during the cycle

State ID	Traffic Light State	Phase	Next
0	Pedestrian	0	1
1	Pedestrian Red	--	2
2	North-South	1	3 or 6
3	North Straight	--	4
4	North All Directions	2.1	5
5	North Left	--	9
6	South Straight	--	7
7	South All Directions	2.2	8
8	South Left	--	9
9	North-South Left	3	10
10	North-South Left Yellow	--	11
11	West-East Straight	4	12 or 15
12	West Straight	--	13
13	West All Directions	5.1	14
14	West Left	--	18
15	East Straight	--	16
16	East All Directions	5.2	17
17	East Left	--	18
18	West-East Left	6	19
19	West-East Left Yellow	--	0

Table 4.2 and Table 4.3 show the various simulated scenarios in which the different times were collected for each of the triggered phases at intersections C1 and C2, respectively. The green lines of the tables represent the phase times that can be manipulated so that the system is better adapted to the traffic scenario presented to it. The column of fixed times indicates the duration of the intermediate phases, which remain the same regardless of the scenario in question. This time results in 38 seconds of the total cycle time, for each scenario.

For the low-traffic scenario, 44 vehicles were generated throughout the environment, with a greater number of vehicles coming from West and East of intersections C1 and C2, respectively, where it was possible to obtain a cycle length of 86 seconds, which is approximately in line with the time defined for this type of scenario.

Regarding the medium traffic scenarios, North-South and West-East scenarios were simulated. In each of these, 66 vehicles were generated, but with a higher generation of vehicles in the lanes to turn left and go straight. It was possible to achieve a cycle length of approximately 100 seconds, which aligns with the desired time.

Moving on to the analysis of the highest traffic scenario, 76 cars circulating in the environment were considered, with higher number of vehicles in the West and East direction of both intersections, resulting in a cycle duration of approximately 120 seconds.

Table 4.2 - Phase times for intersection C1 in various scenarios

State ID	Low Traffic Scenario (s)	N-S Medium Traffic Scenario (Turn Left) (s)	N-S Medium Traffic Scenario (Straight) (s)	E-W Medium Traffic Scenario (Turn Left) (s)	E-W Medium Traffic Scenario (Straight) (s)	High Traffic Scenario (s)	Fixed Time (s)
0	--	--	--	--	--	--	8
1	--	--	--	--	--	--	6
2	6	9	14	12	14	14	--
3	--	--	--	--	--	--	4
4	3	6	5	5	5	5	--
5	--	--	--	--	--	--	4
6	--	--	--	--	--	--	--
7	--	--	--	--	--	--	--
8	--	--	--	--	--	--	--
9	6	16	6	6	6	6	--
10	--	--	--	--	--	--	4
11	24	21	24	19	24	41	--
12	--	--	--	--	--	--	--
13	--	--	--	--	--	--	--
14	--	--	--	--	--	--	--
15	--	--	--	--	--	--	4
16	5	3	3	8	3	6	--

17	--	--	--	--	--	--	4
18	6	9	9	14	9	9	--
19	--	--	--	--	--	--	4
Cycle Length	86	102	99	102	99	119	38

Table 4.3 - Phase times for intersection C2 in various scenarios

State Id	Low Traffic Scenario (s)	N-S Medium Traffic Scenario (Turn Left) (s)	N-S Medium Traffic Scenario (Straight) (s)	E-W Medium Traffic Scenario (Turn Left) (s)	E-W Medium Traffic Scenario (Straight) (s)	High Traffic Scenario (s)	Fixed Time (s)
0	--	--	--	--	--	--	8
1	--	--	--	--	--	--	6
2	6	9	14	14	14	12	--
3	4	0	4	4	4	4	--
4	3		6	6	6	6	--
5	--	--	--	--	--	--	4
6	--	4	--	--	--	--	--
7	--	5	--	--	--	--	--
8	--	4	--	--	--	--	--
9	6	9	9	6	9	9	--
10	--	--	--	--	--	--	4
11	24	21	24	19	24	41	--
12	--	--	--	--	--	--	4
13	5	5	5	9	5	5	--
14	--	--	--	--	--	--	4
15	--	--	--	--	--	--	--
16	--	--	--	--	--	--	--
17	--	--	--	--	--	--	--

18	6	6	6	12	6	6	--
19	4	12	4	4	4	6	--
Cycle Length	88	101	102	104	102	119	30

In order to observe the activation of phases more closely throughout the cycle, phase diagrams for high and low vehicle traffic simulations are represented in Figure 4.3 and Figure 4.4, respectively, for both intersections with the duration of one cycle. The numbers on the vertical axis of the diagram identify the traffic lights, shown in Figure 4.2 a), and the horizontal axis shows the time and moment at which the phases are activated throughout the cycle. The red lines indicate that the traffic lights are red and then turn green when the respective phase is started, also indicating the duration of the phase. It can be seen that the system manages to adapt the phase times depending on the traffic arriving at the junctions. For the higher traffic scenario, the active phase times end up being longer, which is as expected because the flow of vehicles is greater when compared to the lower traffic scenario.

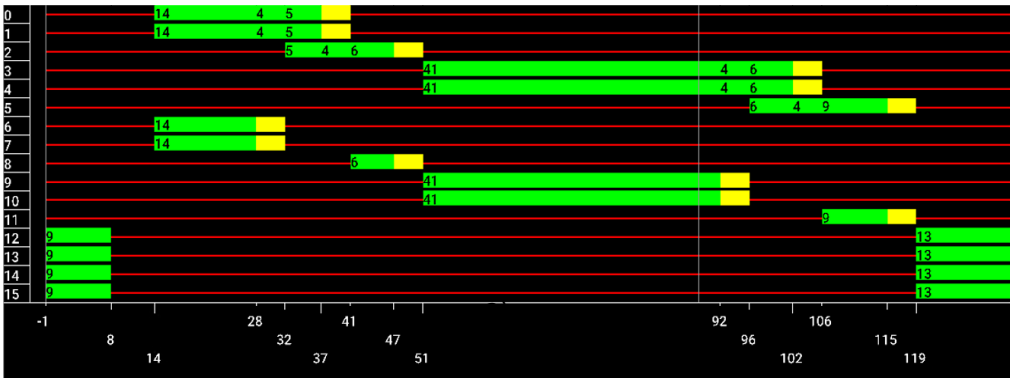

a)

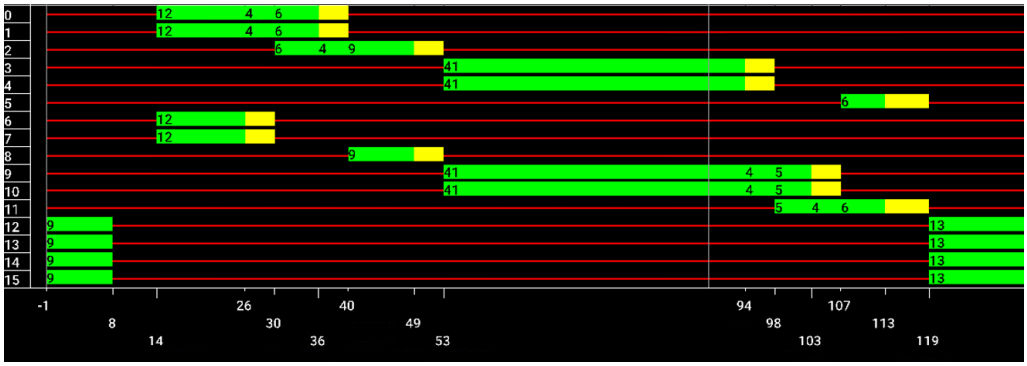

b)

Figure 4.3 - Phase diagram of active phases during cycle time for intersection C1 (a) and C2 (b) for the simulated high traffic scenario

In both simulations, more vehicles were generated in the West-East direction, resulting in a longer green light time at traffic lights 3-4 and 9-10. The West-East Straight phase is activated at the same time at both intersections, as can be seen in the diagram for each simulation, which results in a green wave that will dispatch vehicles from a critical lane, this being the lane that connects the intersections. This lane will have to be handled very carefully so that it is not completely filled with vehicles, causing great instability in the whole environment. This is why the phases are organised in this order, as can be seen in Figure 4.2 b). First, the North-South phase is activated so that some of the vehicles turning left or right, depending on the junction, enter this lane that connects the intersections. Next, the W-E phase is initiated, which uses this green wave to despatch vehicles that are already on this road, as well as those coming from the West-East direction. In this way it is possible for all vehicles to be dispatched from the environment quickly without the need for a second cycle.

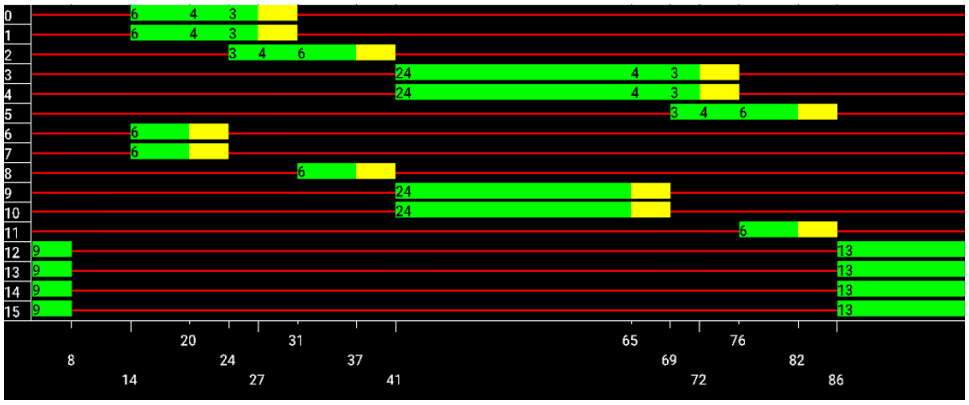

a)

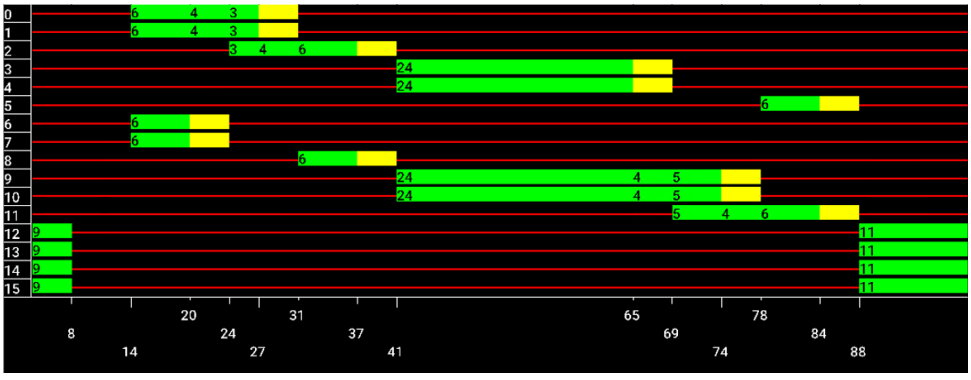

b)

Figure 4.4 - Phase diagram of active phases during cycle time for intersection C1 (a) and C2 (b) for the simulated low traffic scenario

Through this study of the various simulated scenarios for a cycle, it is then possible to estimate how many vehicles can be dispatched from the environment oven an hour. This will serve as a basis for the intelligent system to be implemented, in order to set a target value of vehicles and evaluate the

system's performance when compared to the dynamic system later on. For these estimations only the high and low traffic scenarios were used. With a duration of 120 seconds per cycle, for the highest traffic scenario, it is possible to run 30 cycles in an hour. In each cycle it was possible to dispatch 76 cars from the environment, which results in 2300 vehicles per hour.
For the low-traffic scenario, the same approach applies. With a cycle time of 86 seconds, in one hour it is possible to have approximately 42 cycles. In each of these, 44 cars are dispatched from the environment, which results in 1800 vehicles per hour.

4.3 Traffic scenarios with vehicles and pedestrians

Having studied the various vehicle scenarios, we then move on to analysing pedestrian traffic when inserted into the environment together with the vehicles in the dynamic traffic control system. For this purpose, the high and low vehicle traffic scenarios are used, with a cycle time of 120 and 86 seconds, respectively. For each of these, two pedestrian scenarios were implemented, as can be seen in the following Table 4.4, where a different pedestrian flow was generated for each intersection, considering an estimation of the number of pedestrians per hour that could be dispatched. This results in 4 different scenarios that will be analysed. Two scenarios of high vehicle traffic with high and low pedestrian traffic (High-High and High-Low) and two scenarios of low vehicle traffic with high and low pedestrian traffic (Low-High and Low-Low).
Pedestrians were only introduced in the North and South lanes (in both directions) at both junctions, at different distances from the traffic light, to simulate a scenario more similar to reality, rather than all starting from the same point. All pedestrians are introduced into the SUMO simulator at a speed of approximately 1m/s, which is equivalent to 3 Km/h, which is also close to reality.

Table 4.4 - High and low pedestrian traffic flows for each vehicle scenario

Scenarios	C1 [Pedestrians/Hour]	Middle Lane [Pedestrians/Hour]	C2 [Pedestrians/Hour]
High Pedestrians	7200	2000	4000
Low Pedestrians	3600	1000	2000

To examine the behaviour of pedestrians in the environment, two variables were considered. The average speed of pedestrians generated in the environment, where it will be possible to observe the influence of the duration of the cycles of each vehicle scenario and the halting, where it will be possible to analyse the number of people who stop in the waiting areas at all intersections over time.

Figure 4.5 a) and b) show comparisons between the average speed of pedestrians for the various vehicle scenarios in the high and low pedestrian traffic scenarios. The simulation begins in the first phase of the cycle, that of pedestrians, which at the start of both graphs results in an increase in average speed, up to approximately 8 seconds, this being the duration of the phase in question. The first influence of the vehicle cycle can then be seen. For the Low vehicle scenarios, the speed drops to approximately 90 seconds, which is approximately the duration of a cycle, indicating that the number of pedestrians stopped is increasing over time. The speed then rises rapidly, which means that a new cycle has started and the pedestrian phase is active. The same happens with the High vehicle scenario, but the speed continues to drop until approximately 120 seconds, which is how long the cycle lasts. The speeds drop again, which means that the pedestrians have walked through the environment and are now in the waiting areas. The average speed rises again, signalling the end of the second cycle and the start of the third. The average speed stabilises at 1.2 m/s, approximately 3 Km/h, as the pedestrians have all been dispatched from the environment.

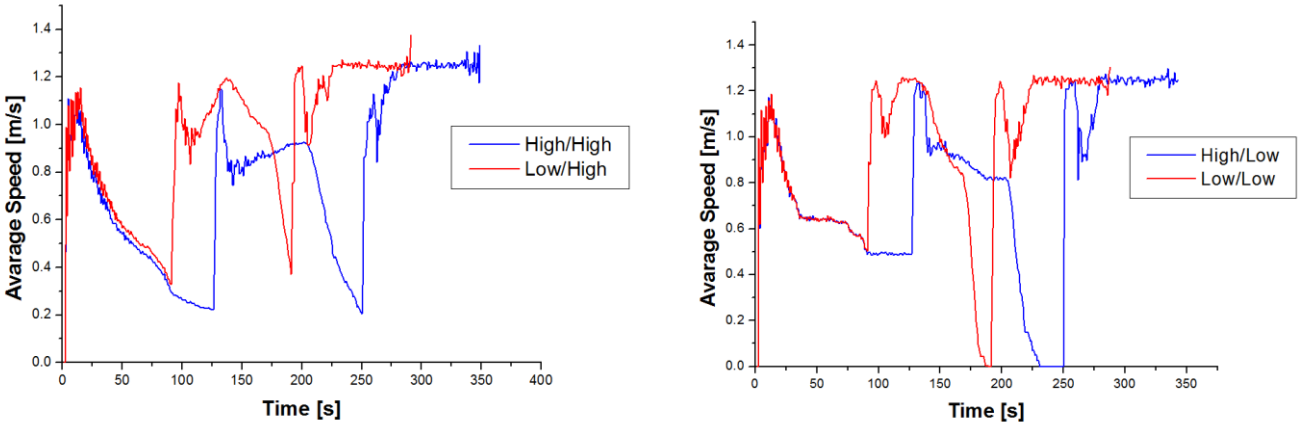

a) b)

Figure 4.5 - Analysis of the impact on average speed of pedestrians for the various vehicle scenarios in the high a) and low b) pedestrian traffic scenarios

Analysing Figure 4.6 a) and b), which show the halting for both vehicle scenarios in the high and low pedestrian traffic scenarios, it can be seen that the graph is in line with the previous analysis of the speed graphs. In both scenarios, up to 8 seconds there are no pedestrians stopped, as the pedestrian phase is currently active. From that time forward, the number of pedestrians in waiting areas waiting for their turn to cross the pedestrian crossing increases over time. It is possible to observe that there are different peaks at different times, which is due to the cycle time of the scenarios. Since the cycle of the high vehicle scenario lasts 120 seconds, it will gather more pedestrians in the waiting areas, thus explaining this difference in values between peaks. The start of the second cycle is visible when the halting value drops sharply. The first phase of the cycles is the pedestrian phase, causing the people

waiting to start moving. In this second cycle it can be seen that there are fewer people in the environment, since there are no longer as many waiting pedestrians, most of which have been dispatched in the first cycle and all in the third, where the halting value reaches zero by the end of the simulation.

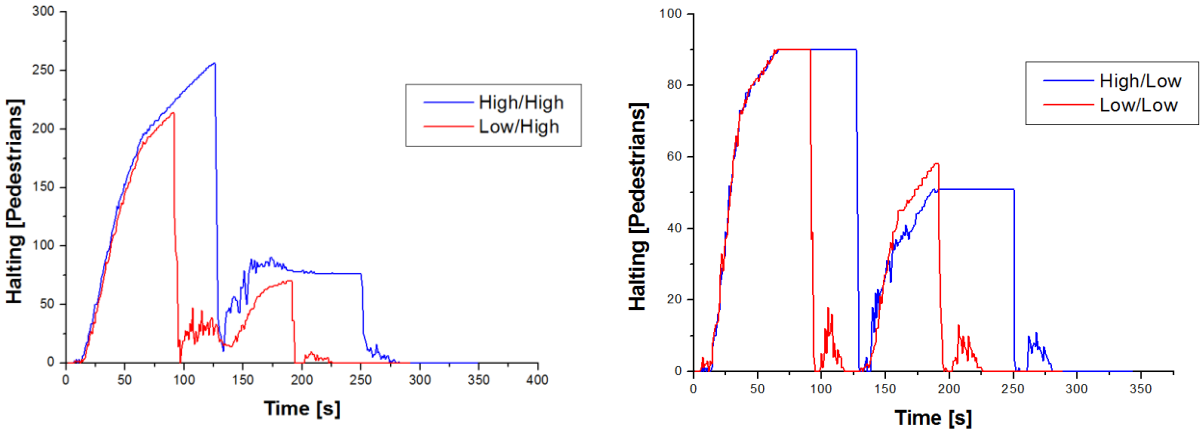

a) b)

Figure 4.6 - Analysis of the impact on the number of waiting pedestrians for the various vehicle scenarios in the high a) and low b) pedestrian traffic scenarios

In Figure 4.8 a) and b) represents the phase diagrams for the highest traffic scenario, for both vehicles and pedestrians. As can be seen in the diagrams, it is possible to distinguish the different cycles that occur during the simulation. It always starts with a pedestrian phase, where some will have the opportunity to cross the pedestrian crossing, turning red for them after 9 seconds. This is followed by phases dedicated to vehicles, until it ends at 123 seconds. This is when the second cycle begins, with the pedestrian phase once again active. The same process happens again until 247 seconds, which marks the end of this second cycle and the start of a third, but now only for the pedestrian phase as no more vehicles appear at the junctions.

Figure 4.8 a) and b) show the phase diagrams for both intersections, in the lower vehicle traffic scenario and the higher pedestrian traffic scenario. Compared to the graphs from Figure 4.8 a) and b), it is possible see that the duration of the two cycles is shorter, which is to be expected because the simulation is of the low vehicle scenario.

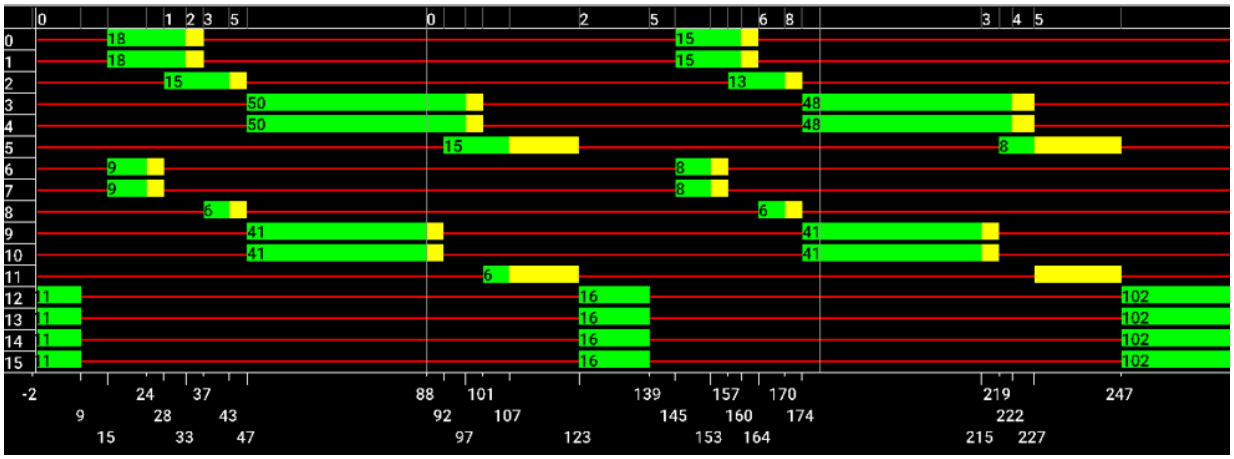

a)

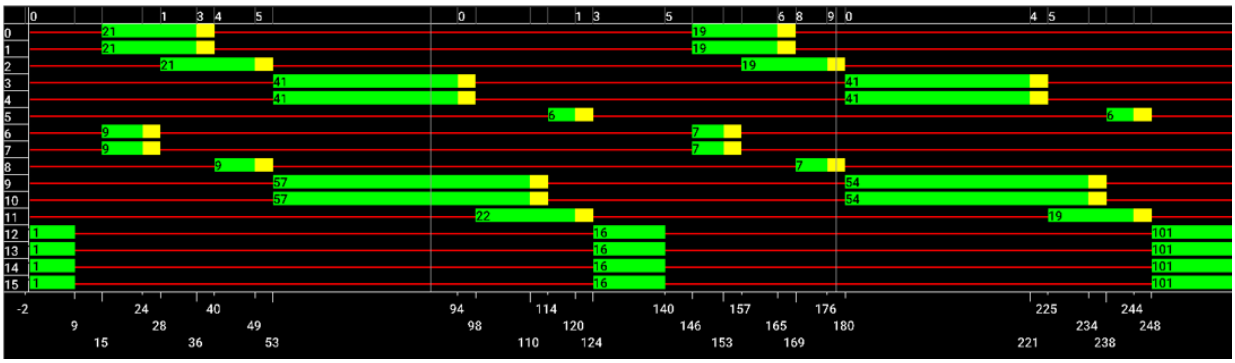

b)

Figure 4.7 - Phase diagram for high vehicle and pedestrian traffic scenario for first a) and second b) intersection

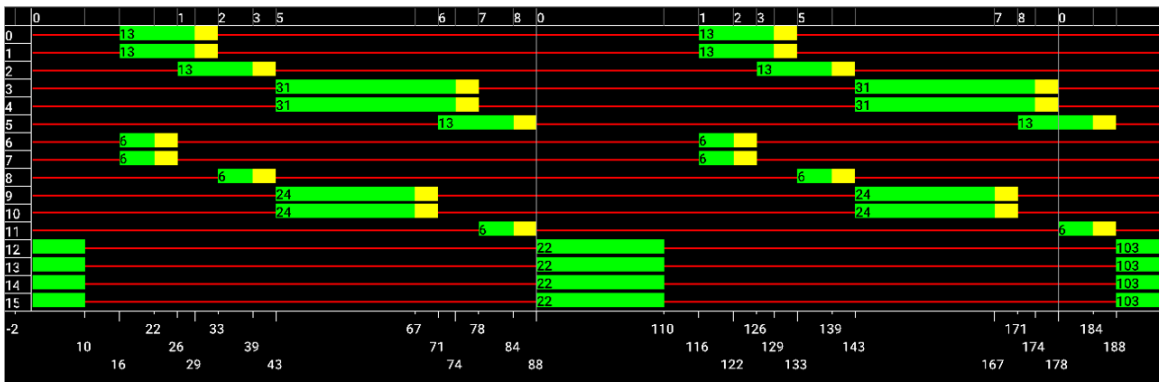

a)

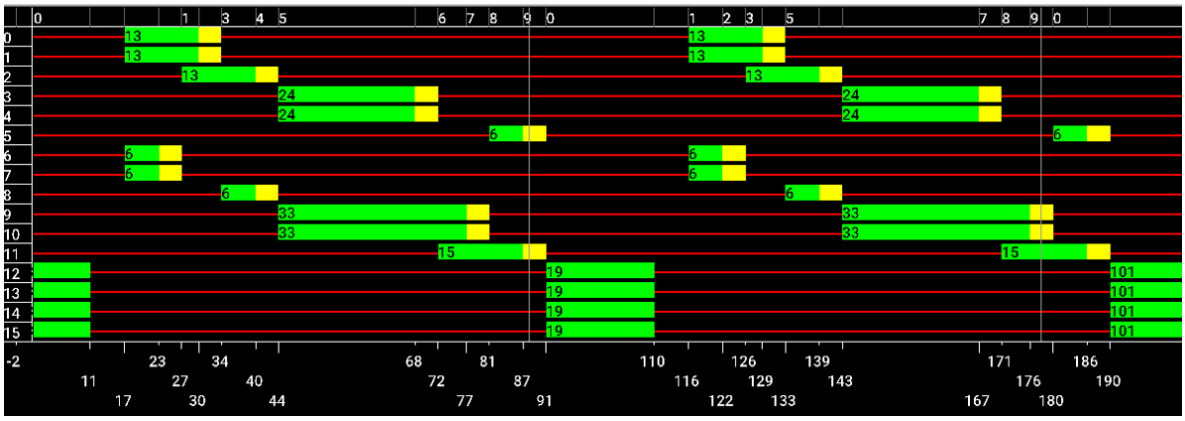

b)

Figure 4.8 - Phase diagram for low vehicle and pedestrian traffic scenario for first a) and second b) intersection

4.4 Variation in the length of the lane connecting the intersections

Having carried out the study on pedestrians in the environment, where the various metrics were analysed, we now move on to the study of the impact that the length of the roads between the two intersections can have on the circulation of vehicles and pedestrians. The same scenarios were used and these values will be compared for the various lane lengths. Distances of 160 (base distance, where the previous tests had already been carried out), 250 and 400 metres were considered.

As the length of the lanes increases, it is expected that pedestrians will take longer to get from one intersection to the next and will spend longer moving, which could lead to fewer people in the waiting areas. The graphs are then analysed to see if the results are in line with the expected behaviour.

Starting the analysis with the High-High scenario, Figure 4.9 shows a comparison of the average pedestrian speeds for the various lane lengths. It can be seen that the average speeds are similar at the start of the simulation, until approximately 120 seconds, when the second cycle begins and the first differences start to be noticed. These are directly related to the increase in lanes, where the 160m lane has a lower speed than the other two lanes, which are relatively identical. At around 240 seconds, where the second cycle ends and the third begins, it is possible to see a decline in speed, which indicates that most people are starting to wait in the waiting areas. This decline is less marked for the 400 metre lane where, due to its greater length, pedestrians will take longer to reach the waiting areas, spending more time in motion, which is in line with expectations.

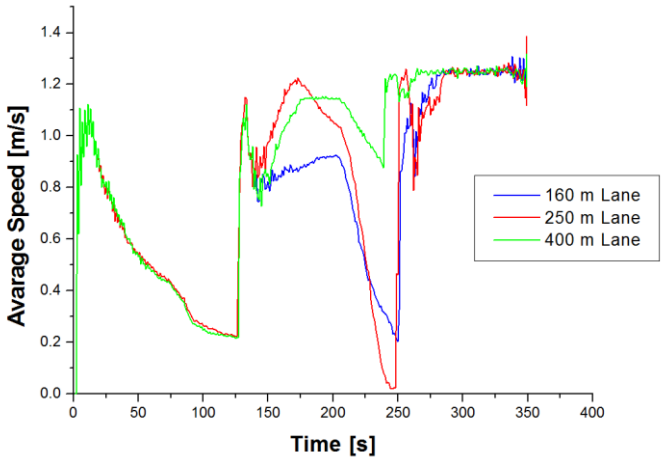

Figure 4.9 - A comparison of the average pedestrian speed observed for the High/High scenario for the different middle lane lengths

Figure 4.10 shows the halting graph, where it can be seen that in the first cycle there is the same progress in all lanes, since these numbers of waiting pedestrians are related to the generation of pedestrians, which is carried out in the same way in all simulations. In the second cycle there are differences due to the length of the lanes, where for the 160 metre lane there will be more people waiting, as they arrive at the other junction more quickly by staying in the waiting zone, and for the 400 metre lane there will be fewer people waiting. It should also be noted that at approximately 120 seconds, there is an increase in the number of people waiting, which at first glance may not make much sense, since people in waiting zones, when the pedestrian phase is activated, pass the pedestrian crossing following its path. However, this behaviour doesn't apply to all pedestrians, since in 8 seconds, which is the time allocated to them for the phase, it isn't enough to dispatch all the pedestrians in the waiting zones. At the end of these 8 seconds, there are still pedestrians waiting, which results in the increase seen in the graph.

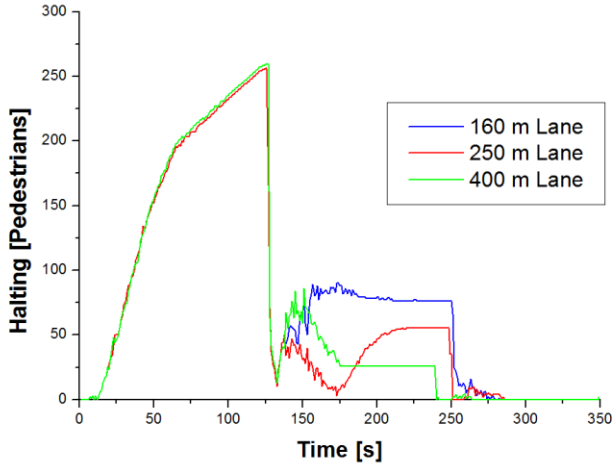

Figure 4.10 - A comparison of the observed pedestrian halting for the High/High scenario for the different middle lane lengths

For the High-Low scenario, there is a similar behaviour to the previous case. In the first cycle the avarage speeds are identical, due to the generation of pedestrians, but in the second cycle it can be seen that the speed of pedestrians decreases considerably in the 160 and 250 metre lanes, while in the 400 metre lane there is only a small decrease, since there are still pedestrians moving on the footpaths in the middle lanes, as can be seen in the Figure 4.11.

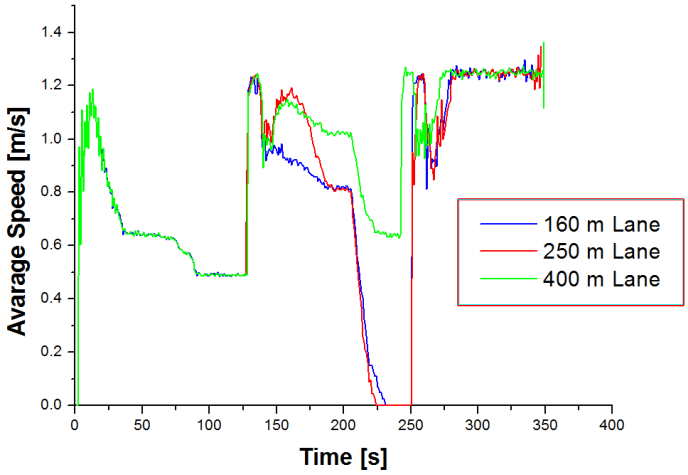

Figure 4.11 - A comparison of the average pedestrian speed observed for the High/Low scenario for the different middle lane lengths

For the graph in Figure 4.12, it can be seen that the behaviour is also in line with what was previously analysed, since there are more pedestrians moving on the 400-metre road, which leads to fewer

pedestrians in waiting areas, when compared to the 160-metre road. It should also be noted that the number of people waiting does not increase immediately after the pedestrian phase, when compared to Figure 4.10, but rather after some time, due to people passing from one crossing to the next and waiting in the waiting area. The behaviour seen in Figure 4.10 does not occur in this case, since there are fewer people in this scenario, which means that there is no disturbance in the waiting areas, allowing them to walk without problems.

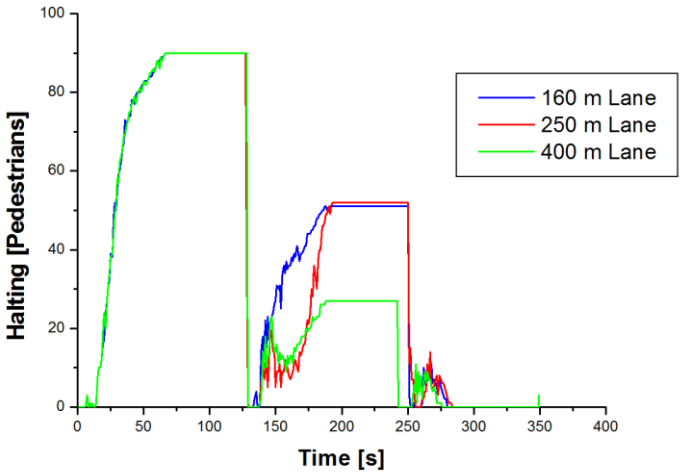

Figure 4.12 - A comparison of the observed pedestrian halting for the High/Low scenario for the different middle lane lengths

Moving on to analyse the Low/High scenario, in Figure 4.13, where the comparison between the average speeds is shown, it can be seen that there is already a small difference between the speeds in the first cycle. For the 160 and 250 metre lanes, the end of the first cycle is approximately 90 seconds, while for the 400 metre lane it is very close to 100 seconds, so there is a slight deviation between cycles. In the second cycle, it is possible to observe the same behaviour described above in the other scenarios. Both pedestrian speeds on the 160m and 250m routes are significantly lower than on the 400m route, with more people in waiting areas, as can be seen in figure 22, which shows the halting. In this figure it is also possible to observe the same behaviour as in Figure 4.10, where the number of people waiting increases immediately after the eviction phase, which indicates that not all people were able to cross the respective zebra crossings due to the high flow of pedestrians on them.

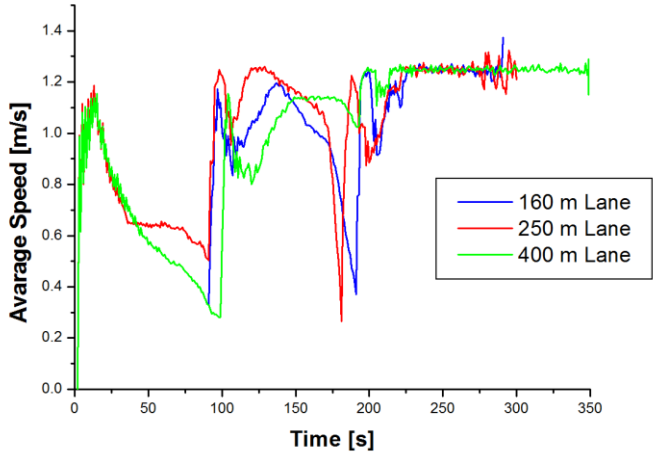

Figure 4.13 - A comparison of the average pedestrian speed observed for the Low/High scenario for the different middle lane lengths

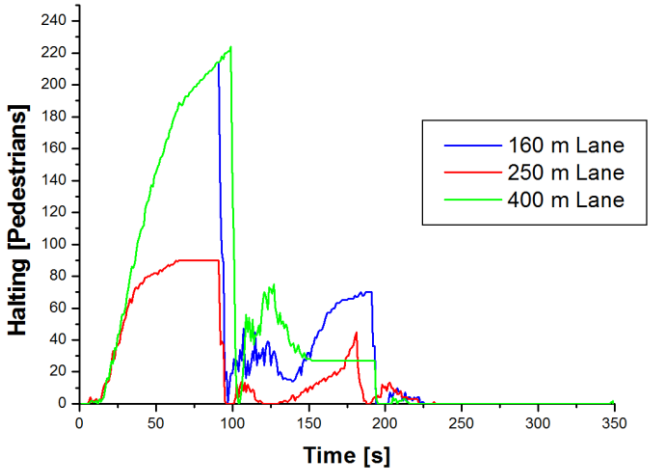

Figure 4.14 - A comparison of the observed pedestrian halting for the Low/High scenario for the different middle lane lengths

Finally, in the Low/Low scenario, the behaviour is identical to the analyses carried out previously. The speeds are identical in the first cycle, as is possible to see in Figure 4.15, but there is a small difference between them, which was already observed in the previous scenario. In the second cycle, the speed of the 400 metre road does not drop as sharply due to its great length, which means that it takes time for pedestrians to reach the other intersection.

With regard to the halting in Figure 4.16, it can be seen that there are fewer people waiting in the waiting areas in the larger lanes when compared to the 160m lane, which is behaviour that is in line with what was expected.

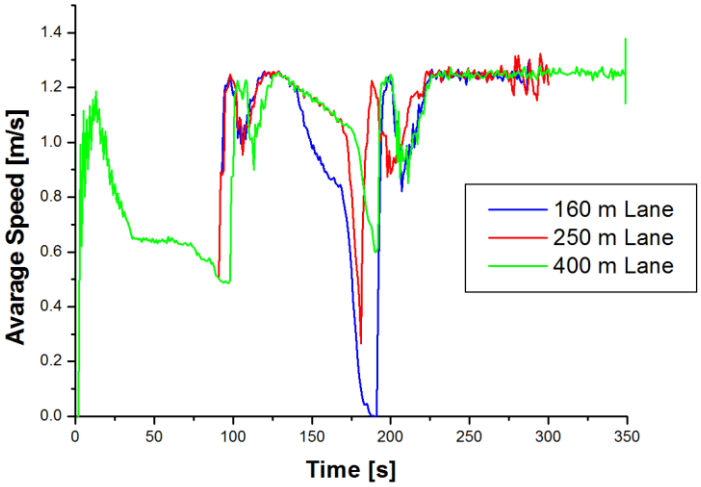

Figure 4.15 - A comparison of the average pedestrian speed observed for the Low/Low scenario for the different middle lane lengths

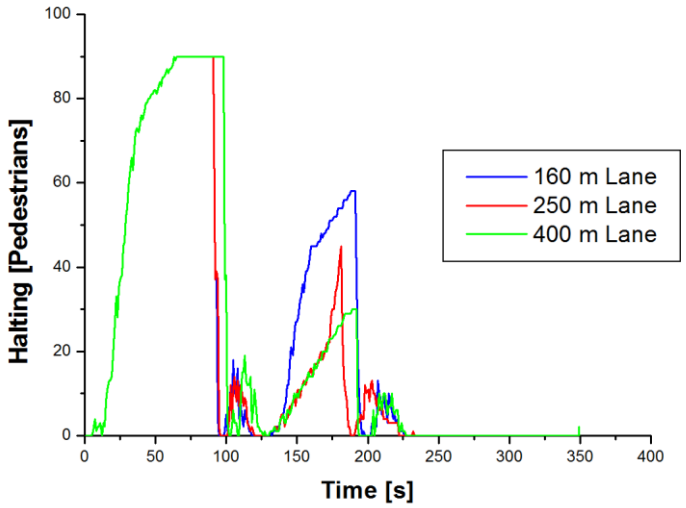

Figure 4.16 - A comparison of the observed pedestrian halting for the Low/low scenario for the different middle lane lengths

This concludes the study of the dynamic traffic control system. In this chapter, the various vehicle traffic counts were analysed and the times for the various traffic scenarios were defined, so that an estimate could be made of how many cars per hour would be dispatched at the intersections. Next, pedestrians were inserted into the environment, where their behaviour was studied, as well as the influence of the cycle of the scenario in question on pedestrian traffic flow. Finally, a variation in the length of the roadway connecting the intersections was carried out, where it was observed that this affects pedestrian movement as well as the number of people standing in waiting zones.
The next chapter begins the study of intelligent traffic control.

5 INTELLIGENT TRAFFIC CONTROL SYSTEM

This chapter will look at the implementation of an intelligent traffic control system. Firstly, we will see how it is implemented, how the states of the environment are observed and the reward considered. Then the various studies carried out with this system will be analysed. Firstly, the use of one or two agents to control the traffic scenario of two junctions will be compared. Next, the influence of varying the length of the road linking the two junctions on the flow of vehicles will be analysed. Finally, pedestrians will be introduced into the environment, which will be studied for various scenarios and the results compared with those obtained in the dynamic traffic control system.

5.1 Adjacent symmetric homogeneous reward

In order to implement the system, reinforcement learning is used, which is a type of machine learning where the agent learns to make decisions through interactions with the environment. For training the agent it is used a Deep Q-Learning network where Q-values are predicted by a neural network that takes the state of the environment as input and outputs Q-values for each action. The neural network used in this work is formed by an input layer of 80 neurons, representing the state of the environment, five hidden layers of 400 neurons, each with rectified linear unit (ReLU). Finally comes the output layer of 8 neurons, which will display the Q-Values for each possible action.

The agent's observation of the state in order to obtain a representation of its environment is based on dividing the lanes where vehicles travel to reach the intersection into cells. Each arm of the junction is made up of two lanes, one for going straight ahead and one for turning left. Each of these lanes is divided into 10 cells and, as the intersection is made up of four arms, 80 cells are obtained, where it is possible to describe the environment that the agent observes through its occupation. If a car is inside a cell, it will be filled with '1', otherwise with '0'. With this, the agent will decide about the action it will take, which through reward will be classified as a good or bad decision. The reward used to classify these actions is shown in equation 1, which considers vehicle waiting times.

The scenario under study is made up of two adjacent junctions, which have already been used in previous studies on the dynamic system, with some implications for their treatment, in relation to the lanes connecting the two intersections. These become critical lanes for balancing traffic flow between intersections. The traffic on these roads is the result of a decision made by an agent when activating a phase that allows vehicles to flow into them. Such a decision may be beneficial for one intersection,

but not for the other, as it could lead to an excessive increase in pressure at the intersection, affecting the overall environment, reducing traffic flow and increasing waiting times and queues.

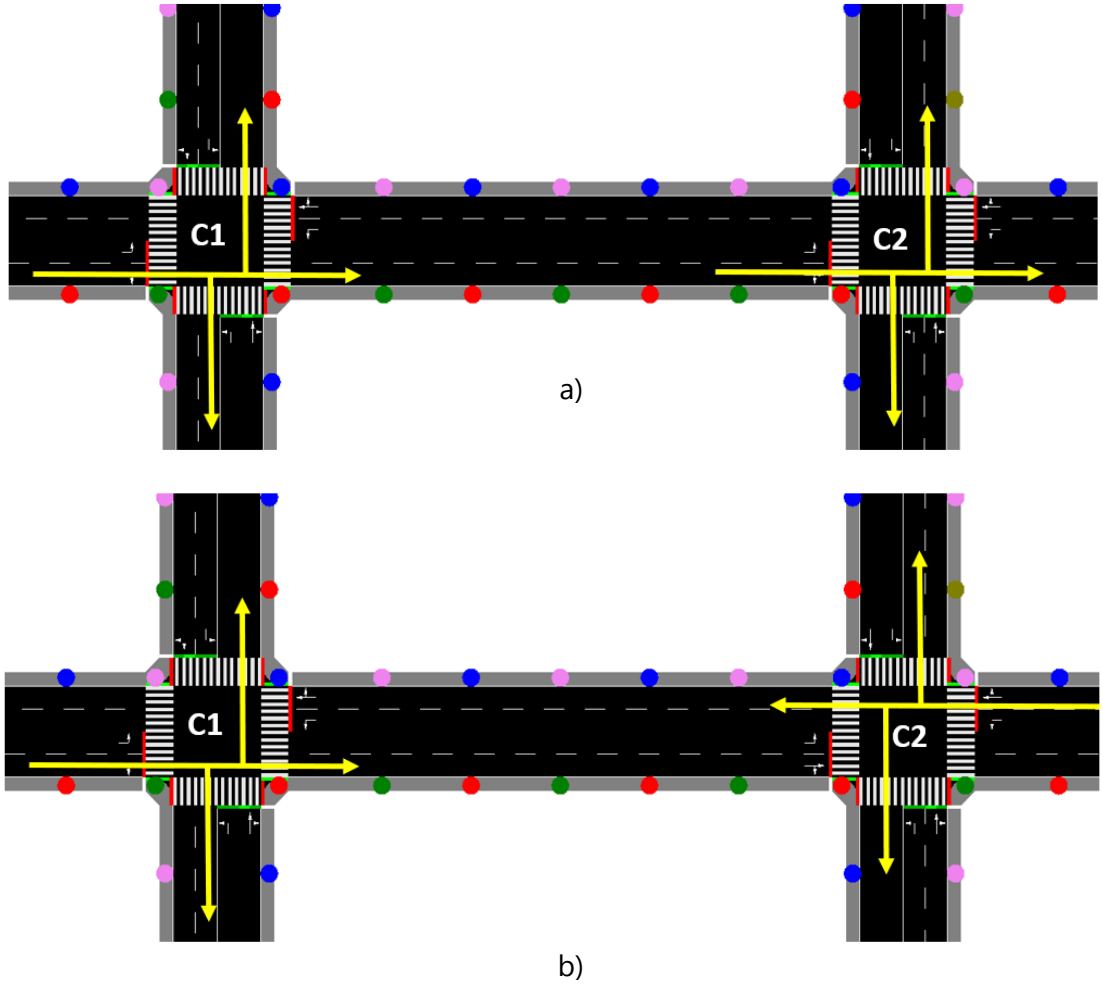

Figure 5.1 - Representation of phases at intersections with a) and without b) a relation between them

The observation made by the agent at each intersection is identical concerning the roadways and the occupancy of their cells. The distinction between the two intersections lies precisely in the decisions made by the agent. For instance, when the agent decides, at the first intersection (C1), to activate a green phase for the West direction in all directions, giving vehicles the possibility of going straight or turning right or left. This action will have a different impact on the environment when applied to the second intersection (C2), as can be seen in Figure 5.1 a). At the first intersection when this phase is activated, the cars that don't go straight will leave the environment, while those that do go straight will take a critical lane, heading for the adjacent intersection. When this phase is active at the second intersection, regardless of which direction the cars are travelling, they will all leave the environment and will not return to it. This difference will cause problems when training the network, as the

experiences observed at the first intersection will not be identical to those at the second. To address this issue, a phase relationship has been proposed between the first and second intersections, ensuring that both become entirely identical and homogeneous. This approach allows for the attainment of an adjacent symmetric homogeneous reward, where actions taken at the first intersection have the same impact as those at the second, significantly contributing to reward improvement. The West all direction action activated at the first intersection becomes equivalent to the East all direction action at the second, as it is possible to observe in Figure 5.1 b).

The effect of the adjacent intersections with the same structure is the so called adjacent symmetric homogenous reward. Such a cooperative mechanism helps to balance the traffic flow between intersections and learning better in both intersections with one agent in each intersection. The cumulative negative reward serves as an indicative measure of the performance of the RL agent(s) in optimizing traffic control strategies over the training episodes. In Figure 5.2 a) and b) it is represented the cumulative negative reward over the episodes. The network is trained over a set number of episodes, in this case 300, each lasting 1 hour. During this hour, a specific number of cars are generated along the junction, depending on the scenario. For the specific case in this study, 2300 cars were generated throughout the environment. The states used for training were obtained by either a single agent situated in C1 or C2, or by two agents, with one in C1 and the other in C2. This configuration suggests that the RL model was evaluated and trained under different scenarios, including the use of a single agent for each intersection and the coordination of two agents, each responsible for one of the intersections (C1 and C2).

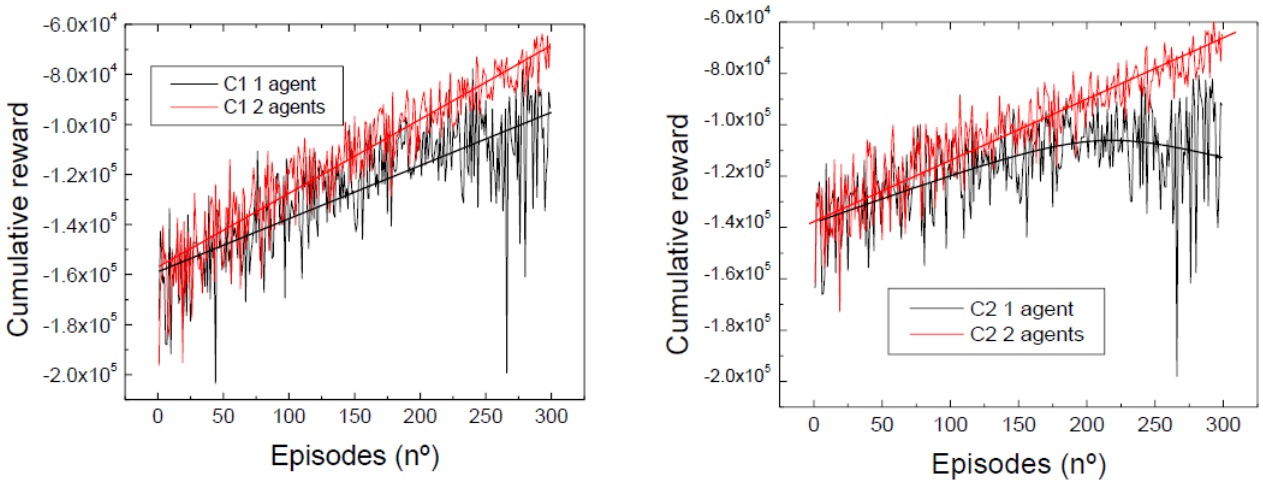

Figure 5.2 - Cumulative negative rewards across successive episodes obtained by either a single agent situated in C1 or C2, or by two agents, with one in C1 a) and C2 b)

The results indicate that incorporating a second agent enhances the learning velocity in the training process with less significant oscillations at the end of the process. This behavior suggests that the network has been well-trained, and the proposed solution has proven beneficial for the environment. Consequently, in the subsequent analysis and discussions, it is assumed that there are always two agents involved in the learning process. This implies that the collaborative efforts of agents in both C1 and C2 contribute positively to the overall learning dynamics, potentially facilitating more effective and efficient optimization of traffic control strategies in the multi-intersection environment.
In the next subchapter, the network controlled by the two agents will be tested for high and low traffic scenarios and various metrics will be taken to evaluate its operation.

5.2 Neural network tests for High and Low vehicular scenarios

Once all the optimisations have been carried out, the neural network is tested for high and low traffic scenarios where 2300 and 1800 vehicles per hour are generated, respectively. The aim is to observe the differences between these scenarios and compare them with the results obtained in the dynamic system, where simulation confirmed the feasibility of dispatching these quantities of cars within an hour. The neural networks for each scenario underwent training with 300 episodes, each lasting 3600 seconds. To characterize the scenarios, several variables related to traffic were employed to assess the system's performance. These variables include queue sizes, where individual intersections in each scenario were analyzed to compare the flow of cars in each. The average queue size for each scenario was also calculated to observe the impact of the number of cars on the environment and the system's response in each case. The average speed of cars was also considered, as vehicle speed provides insights into the fluidity of traffic. Lastly, the number of cars in halting (waiting) was analyzed, providing insights into the impact of the number of vehicles on the environment.
Figure 5.3 a) and b) depicts the queue length graph at both intersections (C1 and C2) for the scenario with 1800 and 2300 vehicles. It can be observed that until approximately 800 seconds, there is a significant increase in vehicles in the waiting queues, similar to a real-world rush hour scenario. There is a substantial influx of cars at both intersections, which gradually diminishes over time. During the neural network training, agents learn to make optimal decisions based on the observed environment. In testing, when agents are prompted to make these same decisions based on their observations, they respond accordingly, as evidenced by the decreasing number of cars in waiting queues over time. This results in clearing most of the vehicles from the intersections within the one-hour time frame.

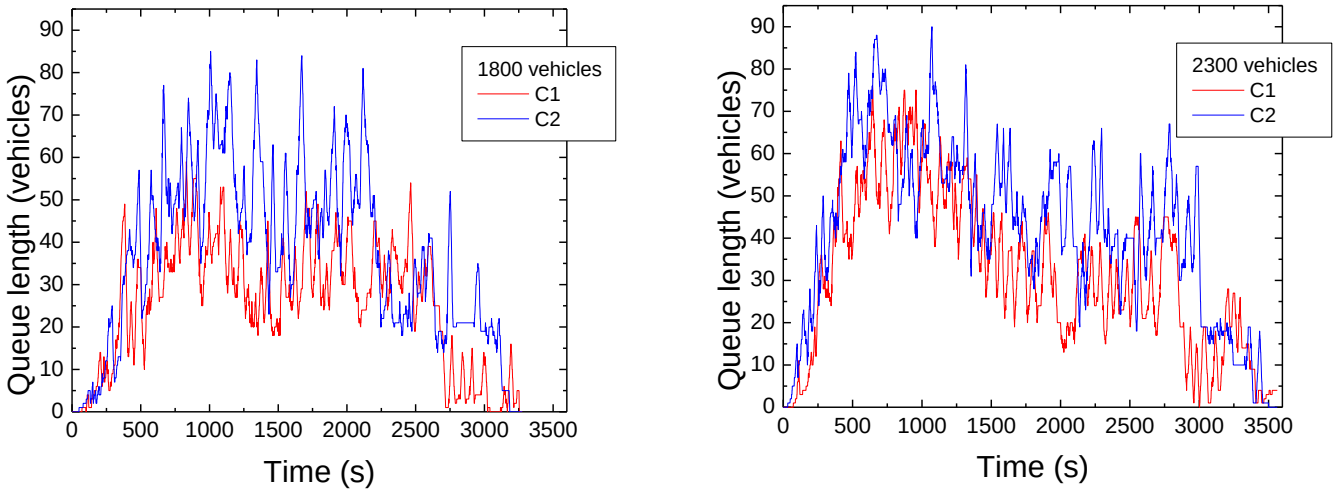

Figure 5.3 - Queue length as a function of time in a scenario of 1800 (left) and 2300 vehicles (right) for both intersections

In the low traffic scenario, with fewer vehicles in waiting queues, the intersections are less congested, aiding the agent in making better decisions and increasing the fluidity of vehicle movement throughout the environment. This translates to less time spent in waiting queues and more time in motion. Here, at around 3200 seconds, there were no longer any cars in the environment.

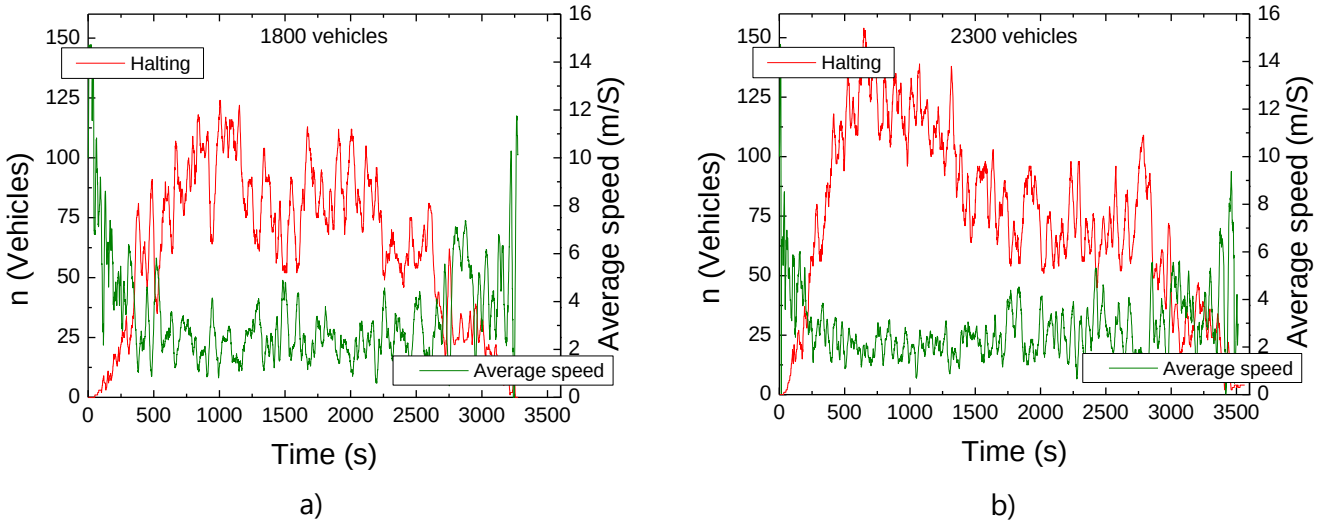

Figure 5.4 - Comparison of average speed and halting in both scenarios, a)1800 vehicles/hour and b) 2300 vehicles vehicles/hour

Figure 5.4 a) and b) depict a comparative analysis of average speeds and halting trends over time for both low and high traffic scenarios. As observed in the graphs, a notable peak in speed is evident at the initial stages of the halting simulations, gradually diminishing as the simulation progresses. This initial surge in speed can be attributed to the absence of vehicles at the intersections, providing ample space for faster movement. However, as the influx of cars intensifies, the average speed experiences a significant decline. This pattern repeats towards the conclusion of the simulation, where the clearance of cars from the environment affords remaining vehicles more space, resulting in an upturn in average speed, owing to reduced waiting queues. As expected, a higher volume of waiting cars corresponds to a decrease in speed, while a lower volume leads to an increase, aligning with anticipated traffic dynamics.

5.3 Variation in the length of critical lanes

After examining the environmental impact of varying the number of vehicles, our focus shifts to investigating the size of critical lanes connecting two junctions. Each agent oversees its junction, monitoring lanes and car volumes through cell occupation. Following optimization in terms of intersection phase relationships, both intersections become homogeneous, rendering the experience identical. Despite this, inadequate communication among agents may elevate car volumes on critical roads. Agent decisions generate rewards based on vehicle wait times at respective junctions. When an action facilitates vehicle movement to target roads, the agent perceives it as beneficial locally but may adversely affect the adjacent intersection. Enhanced communication could manage actions based on neighboring intersection pressure. However, implementing this communication might escalate system complexity, potentially requiring a neural network for information exchange and facing scalability issues with more adjacent intersections.

With a higher target road length, queue sizes decrease, alleviating pressure on the agent's junction and ensuring space for vehicle circulation. As seen in Figure 5.5 a) and b) three neural networks, trained with varying lane sizes, display expected reward behaviors. Figure 5.6 a) and b) illustrate average queue sizes during network training episodes. The 400m lane exhibits fewer queued cars than the other two, indicating minimal need for communication due to ample space for circulation. Conversely, for the 160m and 250m lanes, communication remains essential, as queue sizes are comparable to the 400m lane, necessitating coordination to manage traffic effectively.

After completing the Reinforcement Learning (RL) training, it can be seen fluctuations in the learning curve, indicating challenges in achieving convergence. Nevertheless, the model demonstrated gradual improvement, reaching a moderate level of performance over the training period.

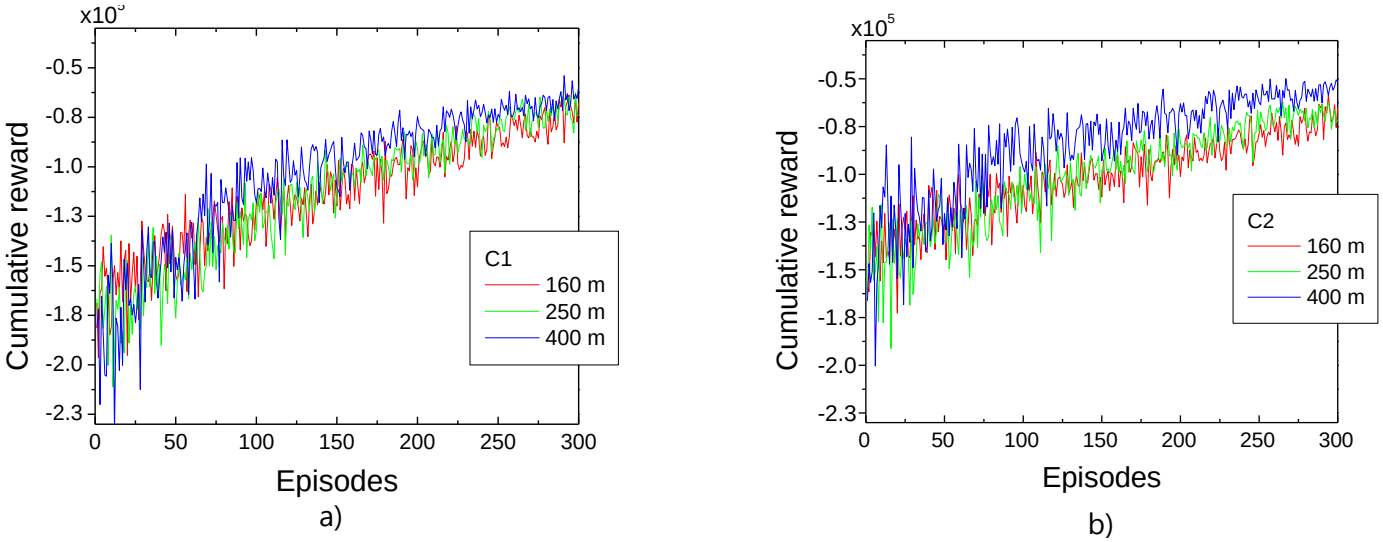

Figure 5.5 - Cumulative negative reward across successive episodes in the high traffic scenario (2300 vehicles/hour) and different target road length. a) C1 intersection. b) C2 intersection

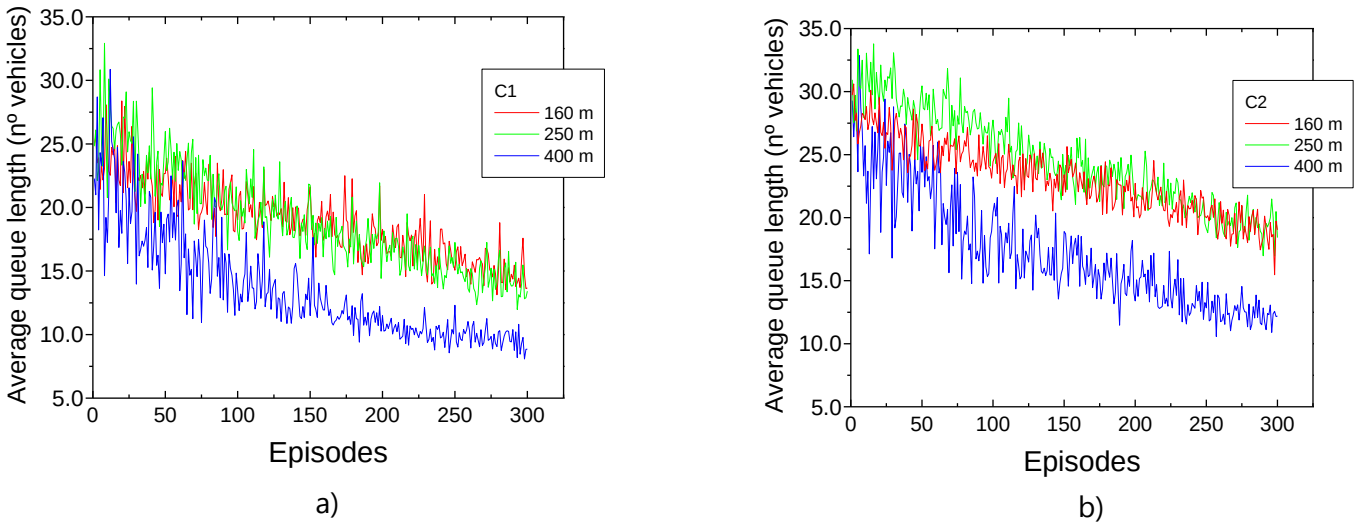

Figure 5.6 - Average queue length across successive episodes in the high traffic scenario (2300 vehicles/hour) and different target road lengths. a) C1 intersection. b) C2 intersection

The results revealed consistent trends in both cumulative negative reward and average queue length at both intersections. Importantly, there was no significant separation between the cumulative rewards for the three types of road networks, highlighting the scalability of the distributed approach across road networks of varying sizes. The observed stability in these metrics, with decreasing amplitude of oscillations as training progressed, suggests an enhancement in decision-making capabilities. Interestingly, in the shorter path, learning was faster initially but was later surpassed by longer paths as training advanced.

As anticipated, the average number of vehicles in the queue decreased at both intersections. Notably, the reduction in queue lengths was more pronounced and stable in the longer path at C1 compared to

C2. This discrepancy can be attributed to the decreasing resistance of traffic flow with increasing path length, contributing to the observed effects.

In Figure 5.7 a) and b), the average queue length across the time was tested for both intersection (C1 and C2) and different target road lengths.

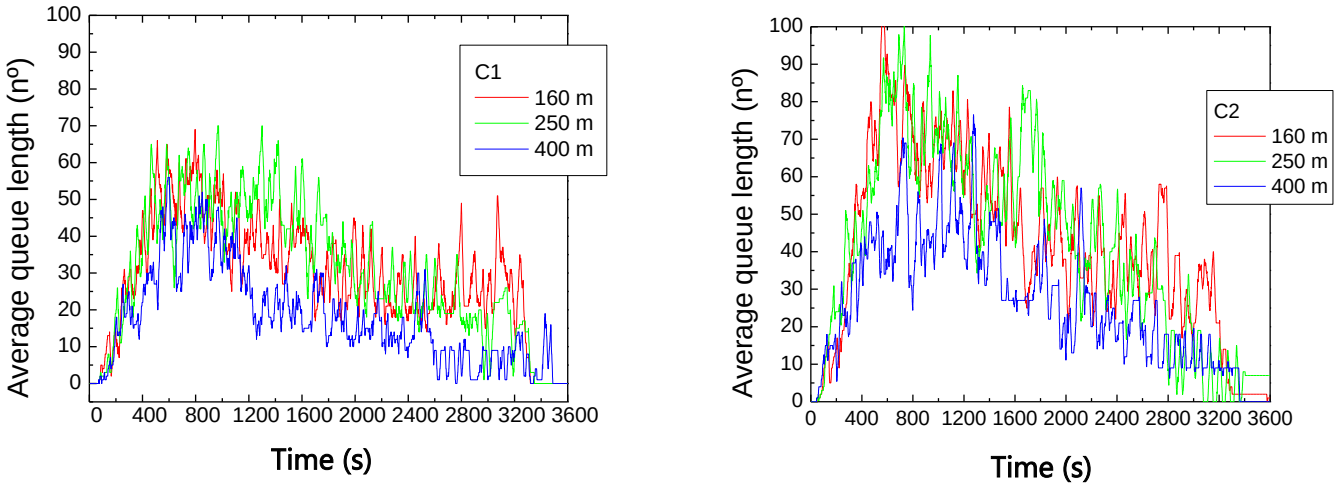

a) b)

Figure 5.7 - Average queue length test as a function of time in the high traffic scenario (2300 vehicles/hour) and different target road lengths. a) C1 intersection. b) C2 intersection

The observed average queue length can be explained by noting a notable surge in the number of vehicles in waiting queues until approximately 15 minutes, resembling a real-world rush hour scenario. Both intersections experience a substantial influx of cars, which gradually diminishes over time. Notably, as the road length increases, the queue length decreases at both intersections. Around the 45-minute mark of training, at C1, there are no cars waiting, while at C2, the queue disappears only at the end. So, as the road length increases, fewer vehicles remain in waiting queues, resulting in less congestion at the intersections. This reduction in congestion aids the agent in making better decisions, ultimately enhancing the fluidity of vehicle movement throughout the environment. Consequently, less time is spent in waiting queues, allowing for more time in motion.

Results show that the reinforcement learning can optimize traffic flow by dynamically adjusting traffic signals, pedestrian crossing times, and other traffic management parameters. This adaptability helps reduce congestion, improve overall traffic efficiency, and minimize delays for both pedestrians and vehicles.

5.4 Intelligent traffic control for vehicles and pedestrians

The previous section looked at various aspects of the neural network and the traffic environment, such as the introduction of a second agent and the relation between phases that are active, as well as the influence on traffic flow of the length of the critical lane that connects the intersections. This section then moves on to the introduction of pedestrians into the environment to check their impact on it. To do this, it is necessary to make a change in the reward equation so that it classifies both the flow of vehicles (*veh*) and pedestrians (*ped*) by their waiting times, as can be seen in the equation 2.

$$atwt_{veh,t} = \sum_{veh=1}^{n} wt_{(veh,t)} \qquad atwt_{ped,t} = \sum_{ped=1}^{n} wt_{(ped,t)} \tag{2}$$

$wt_{veh,t}$/ $wt_{ped,t}$ is the amount of time in seconds a vehicle or a pedestrian has a speed of less than 0.1 m/s at *t,* since the spawn into the environment. *n* represents the total number of vehicles/pedestrians in the environment in *t.* With this metric, the values of $atwt_t$ does not reset, until the vehicle or pedestrian cross the intersection.

The final reward equation, r_t, is defined in equation 3, where $atwt_t$ and $atwt_{t-1}$ are the accumulated total waiting time of all the cars/pedestrians in the intersection captured respectively at *t* and *t−1*. The weights of the p_{veh} and p_{ped} are set based on the desired priority that the agent should have towards vehicles and pedestrians during network training. The agent will learn a policy that benefits one more than the other, or keeps the system balanced if the weights are equal.

$$\mathrm{r_t} = p_{veh}\left(\mathrm{atwt}_{veh,t-1} - \mathrm{atwt}_{veh,t}\right) + p_{ped}\left(\mathrm{atwt}_{ped,t-1} - \mathrm{atwt}_{ped,t}\right) \tag{3}$$

Changes have also been made in terms of observing the environment. Previously, 80 cells were used per intersection to indicate the occupation of the lanes. When introducing pedestrians into the environment, the same process needs to be carried out, but for the waiting areas on the pavements, near the traffic lights, where pedestrians who wish to cross the pedestrian crossings will be stopped. Each waiting corner is divided into 5 cells, resulting in 20 pedestrian cells per intersection and 100 cells overall in the environment. These cells are filled with '1' or '0' to indicate pedestrian presence or vacancy, respectively.

Two neural networks were then trained, each considering vehicles and pedestrians in the environment but with different weight allocations at the reward level. In the first model (50/50), balanced weights are assigned to both groups, with 50% for vehicles and 50% for pedestrians. In contrast, the second model (25/75) features unbalanced weights, giving 75% importance to pedestrians and only 25% to

vehicles. Both models undergo training for 300 episodes and are tested with 2300 vehicles and 2000 pedestrians for over an hour.

Figure 5.8 illustrates the cumulative negative rewards during training in both models, with two different reward weight distributions obtained by agents in C1 (a) and C2 (b). Although both curves in the graphs are rewards, they cannot be directly compared. The difference between the two curves does not indicate that one system is better than the other, since different waiting times are being considered due to the weights assigned in the reward, and it is only possible to conclude that both agents trained relatively well.

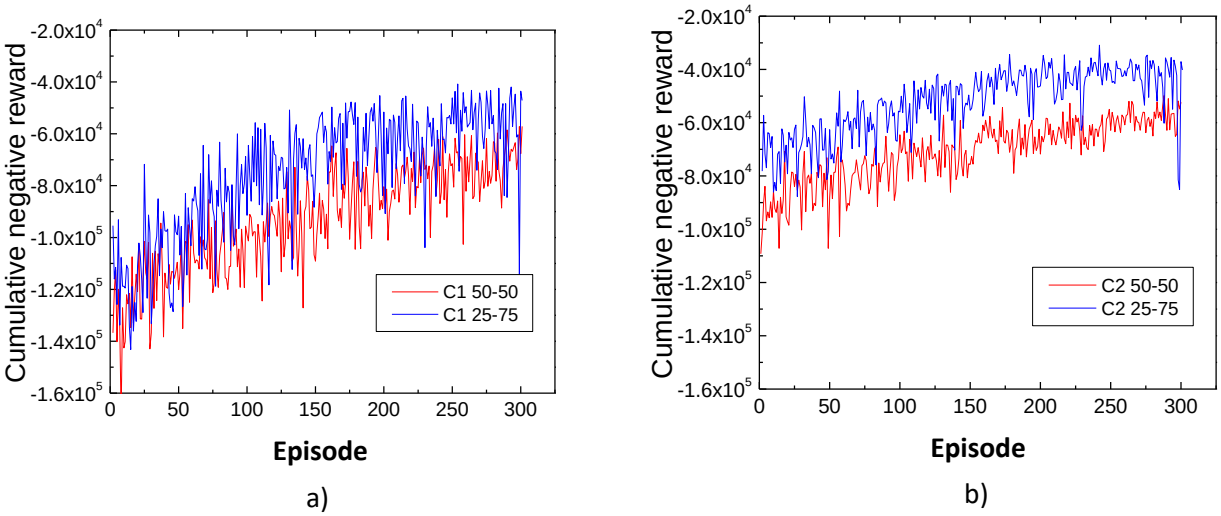

Figure 5.8 - Comparative cumulative negative rewards between two different reward weights obtained by two agents one in C1 (a) and the other in C2 (b)

Figure 5.9 depicts the average queue sizes along the successive episodes, for both intersections, C1 (a) and C2 (b) and for both weights model. Graphs exhibit expected behavior, with the curve allocating a weight of 25% to vehicles showing a higher number of cars waiting throughout the episodes. This outcome aligns with the greater importance given to pedestrians in the reward function, which naturally impacts vehicle traffic compared to the 50/50 curve, where a balance in importance is maintained between vehicles and pedestrians, or even in scenarios where only vehicles are considered.

In scenarios focusing solely on vehicles, optimization of vehicle traffic flow is achieved as it is the sole significant variable. However, this doesn't reflect real urban traffic scenarios where the presence of pedestrians unavoidably impacts vehicle flow. The integration of pedestrians into the environment and their phases invariably leads to delays in car flow, resulting in increased waiting times and queues. Nonetheless, this trade-off ensures the safety of both groups sharing the same environment, which is crucial in urban settings.

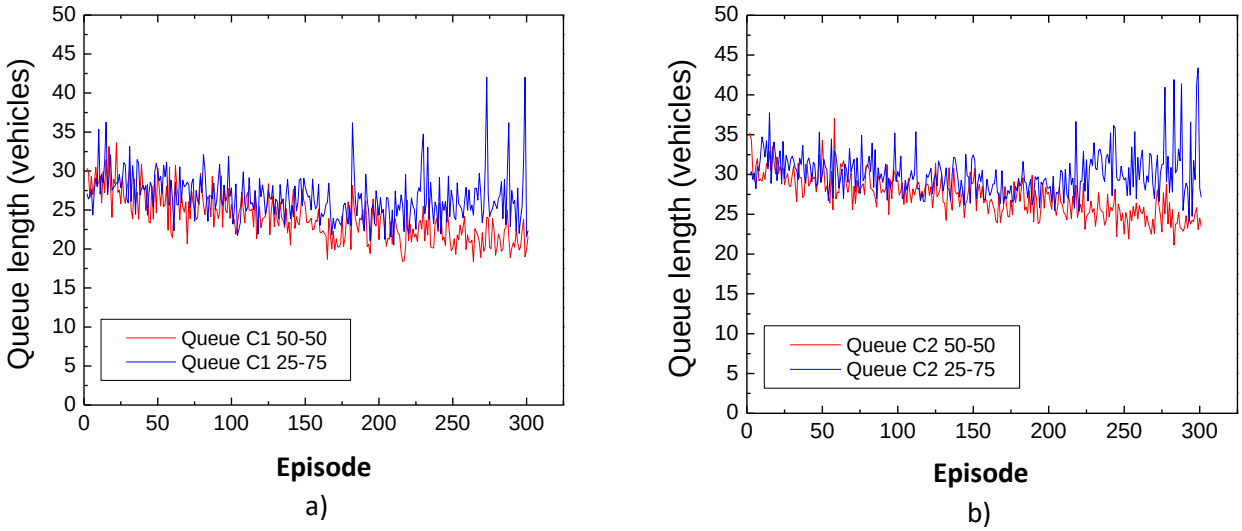

Figure 5.9 - Comparative queue length trends between two different reward weights obtained by two agents one in C1 (a) and the other in C2 (b)

Moving on to the analysis of the network test, Figure 5.10 shows the halting for the vehicles (a) and for the pedestrians (b) in both models. As expected, and in line with the previous analysis, the model that considers a lower weight for vehicles (25%) ends up with a greater number of cars waiting in the peak hour zone, but then manages to recover and even follow a similar behavior to the curve which represents the model with balanced weights.

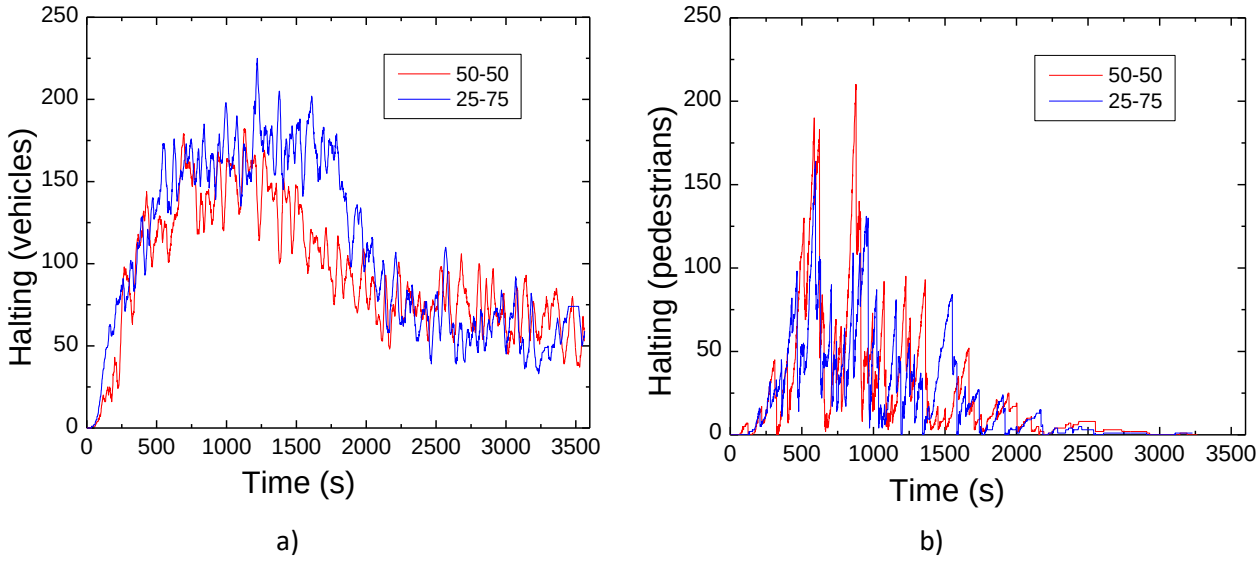

Figure 5.10 - Comparative halting trends between two different reward weights obtained by the agents for the vehicles (a) and for the pedestrians (b)

Even though it has less weight in the reward, the agent manages to optimize its decisions, giving more priority to pedestrians, but never letting the vehicles get too affected, while still managing to satisfy their request. This may indicate that, to have a balanced system between cars and pedestrians, it may not be necessary for the weights to be equal for both. The basis of the system and the set of actions that the agent can take ends up being unbalanced towards vehicles, since there are eight possible actions for them, with only one phase for pedestrians. There is a greater probability of one of these eight phases being active, which unbalances the system. By compensating in the reward, giving more importance to pedestrian waiting times, the agents learn a policy that leads to the pedestrian phase being activated more often.

In the analysis of pedestrian flow in the environment, Figure 5.10 b) illustrates pedestrian halting. Examining the graph representing the number of waiting pedestrians, it's clear that the 25/75 model has a lower count of waiting pedestrians. This observation aligns with the agents' training to prioritize pedestrian flow over vehicles, justifying the reduction in the importance of vehicles in the reward equation and leading to an enhancement in pedestrian flow in the environment.

This study underscores the inevitable impact of introducing pedestrians into the environment on vehicles, as the inclusion of pedestrian phases invariably increases waiting times and queues for vehicles. Effective system management in decision-making becomes crucial in this scenario. By assigning weights to the reward, agents are guided on who to prioritize when making phase activation decisions. Despite reducing the importance of vehicle flow, the system responds adequately, prioritizing pedestrians when their numbers exceed vehicles and then efficiently accommodating vehicle requests.

5.5 Comparison between dynamic and intelligent control systems for vehicle and pedestrian traffic scenarios

In order to evaluate the intelligent system, we then compare it with the dynamic control system for vehicle and pedestrian traffic. The same generation of vehicles and pedestrians was used for both systems.

The neural network used was previously analysed and trained for a reward with a 50% weighting of the waiting times for vehicles and pedestrians.

Four different scenarios were tested: High-High, High-Low, Low-High and Low-Low. For the High vehicle scenario, 2300 cars are generated over the course of an hour, while for the Low scenario, only 1800 are generated. For the High pedestrian scenario, 11000 pedestrians are generated and for the

Low scenario only 5600 are generated throughout the entire environment during the same hour. Next, the graphics are analysed, starting with High-High and High-Low traffic scenarios.

Figure 5.11 a) and b) shows the graphs for both scenarios indicating the number of pedestrians stopped in the waiting zones at the two intersections. Looking at the two graphs, it can be concluded that the intelligent system manages to meet the needs of pedestrians much better than the dynamic system. Figure 5.11 a) shows the biggest difference in the high scenario for vehicles and pedestrians. The dynamic system reaches a peak of approximately 1500 people simultaneously waiting in the first 25 minutes of the simulation, while the intelligent system only reaches a peak of 400 pedestrians for the same time interval. In Figure 5.11 b) the difference is not so great, where the dynamic system reaches a peak of approximately 275 people waiting during the first 15 minutes, while for the intelligent system, in the same time frame, there is a maximum of 150 pedestrians waiting.

These differences are related to the way the system works. While the intelligent system jumps between phases without any defined order, adapting to the traffic that is currently at the intersections, the dynamic system follows a well-defined cycle of phases, where at the end of each of these cycles, a pedestrian phase is active. This phase can be seen in both graphs. For the dynamic system, each time there is a pedestrian phase, there is a decrease in waiting pedestrians, which results in the peaks shown, spaced approximately 120 seconds apart, which is the cycle time for a high vehicle traffic scenario.

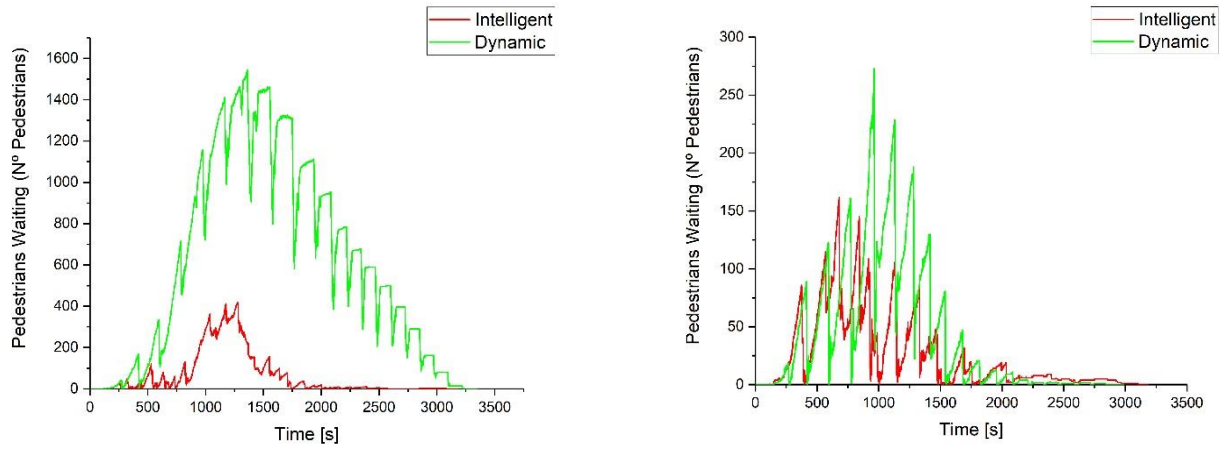

Figure 5.11 - Comparison of the number of pedestrians stopped waiting in both systems for the High-High (a) and High-Low (b) scenarios

The graphs in Figure 5.12 a) and b) show the average speed of pedestrians for both scenarios. It can be seen that in the graph in Figure 5.12 a) the differences between speeds are more significant, which is as expected, since for a scenario of greater pedestrian circulation at intersections, more pedestrians will be waiting, in the case of the dynamic system as analysed above, resulting in a drop in average

speed values. The graph in Figure 5.12 b) doesn't show such a marked difference, where the speeds end up being somewhat similar, since there are fewer people in the environment, with some variation at the end of the simulation, but this may have to do with just a few pedestrians still in the area.

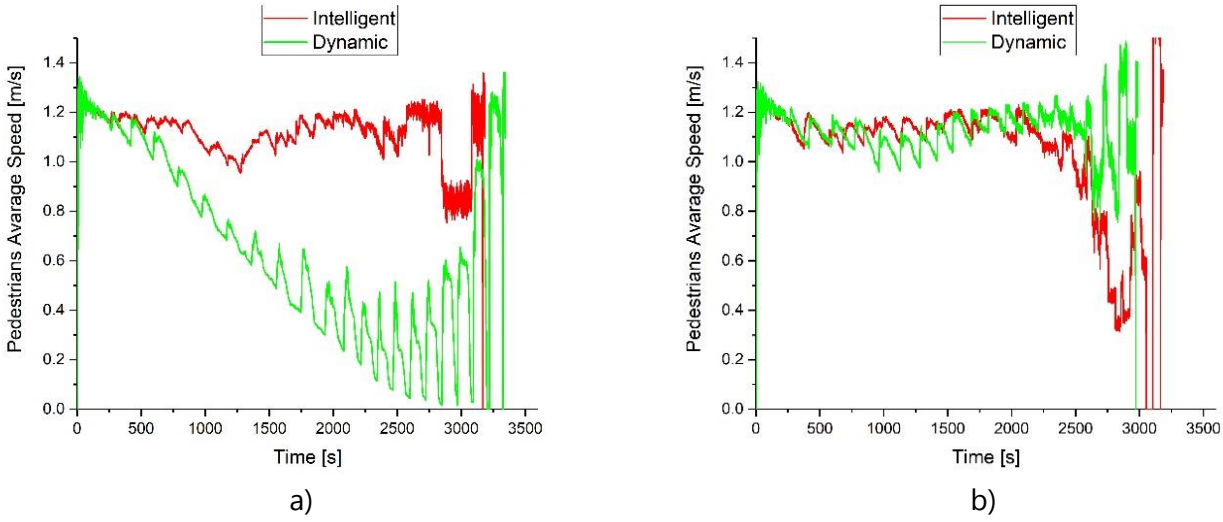

Figure 5.12 - Comparison of pedestrian speed through the environment in both systems for the High-High (a) and High-Low (b) scenarios

Now looking at the behaviour of vehicles, Figure 5.13 a) and b) shows the graphs of the number of cars waiting in the entire environment for both scenarios. In Figure 5.13 a) when compared with b) it is possible to see some differences despite the fact that the vehicle traffic scenario is high for both cases, which proves that the number of pedestrians influences the circulation of vehicles. With regard to the intelligent system, in Figure 5.13 a) it can be seen that a peak of vehicles is reached between the first 8 and 15 minutes of the simulation, while in Figure 5.13 b) a peak is reached at around 15 minutes. In the first case there are a greater number of pedestrians circulating in the environment, which causes the agent to trigger their phases, affecting the flow of vehicles, resulting in a greater number waiting. In the second case, with fewer pedestrians circulating, the system manages to better balance decisions between vehicles and pedestrians, resulting in fewer cars waiting. These values end up decreasing over time, remaining at approximately 50 vehicles waiting in the entire environment, but not managing to dispatch all 2300 cars.

As for the dynamic system, the behaviour is the same in both graphs, which is to be expected since the vehicle scenario is high in both cases, resulting in the same cycle time, 120 seconds. Even so, it can be seen that in figure 5.13 b) the system was able to dispatch more vehicles than in the first scenario, which indicates that with a high number of pedestrians it was also possible to affect the dynamic system. This difference may be due to the fact that for a high pedestrian scenario in the dynamic

system, many will be waiting, which can result in poor pedestrian behaviour, crossing on reds, which affects the flow of cars if they have to stop their movement at one of the crossings to avoid hitting the pedestrian.

Comparing the two systems in terms of vehicle flow, the dynamic system turns out to be slightly superior to the intelligent one in the first half hour, as it has fewer cars waiting. In the second half hour, the intelligent system, having already dispatched most of the pedestrians, manages to catch up and keep up, even showing better figures than the dynamic system.

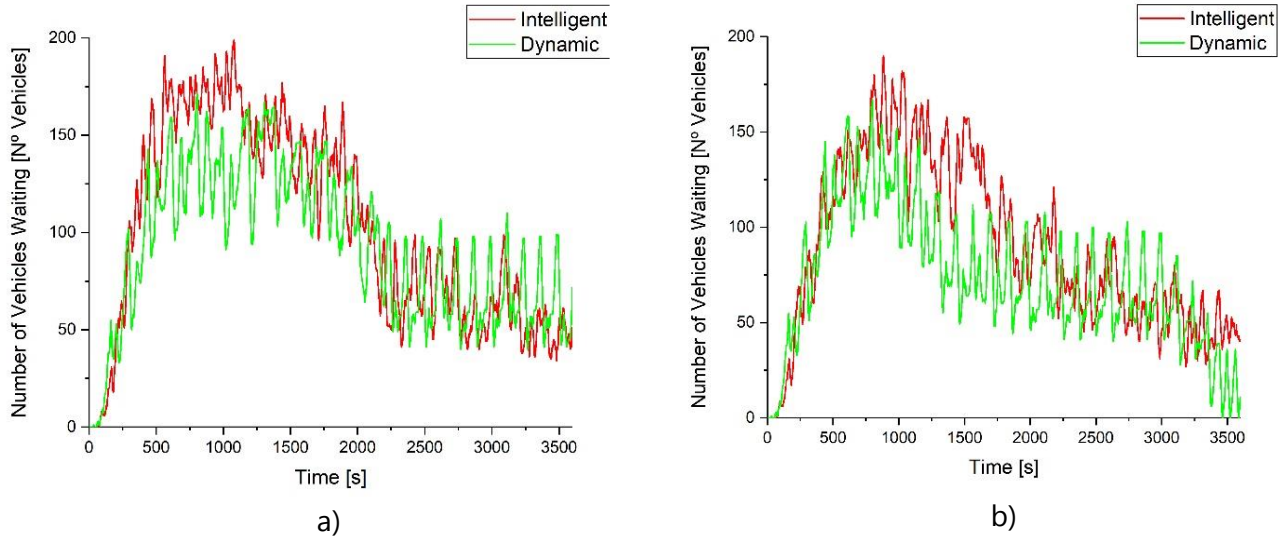

Figure 5.13 - Comparison of the number of cars in the entire environment for both systems for the High-High (a) and High-Low (b) scenarios

Figure 5.14 a) and b) shows the average vehicle speeds for both scenarios. In both figures it can be seen that in the first half hour, the speed of the dynamic system was slightly higher than that of the intelligent system, but in the second half hour, the speed of the intelligent system increases, since it has already dispatched all the pedestrians and is now giving full priority to the vehicles, managing on average to have a speed similar to or even higher than that of the dynamic system.

In both graphs, for the dynamic system it can be seen that it shows many variations in the average speed values throughout the simulation. This is due to the fact that the system strictly follows the phase cycle. When in the vehicle phase, this value rises, but after the 120 seconds of the cycle, it drops to 0 m/s, where all the cars at both intersections are stationary, because they are both active in the pedestrian phase.

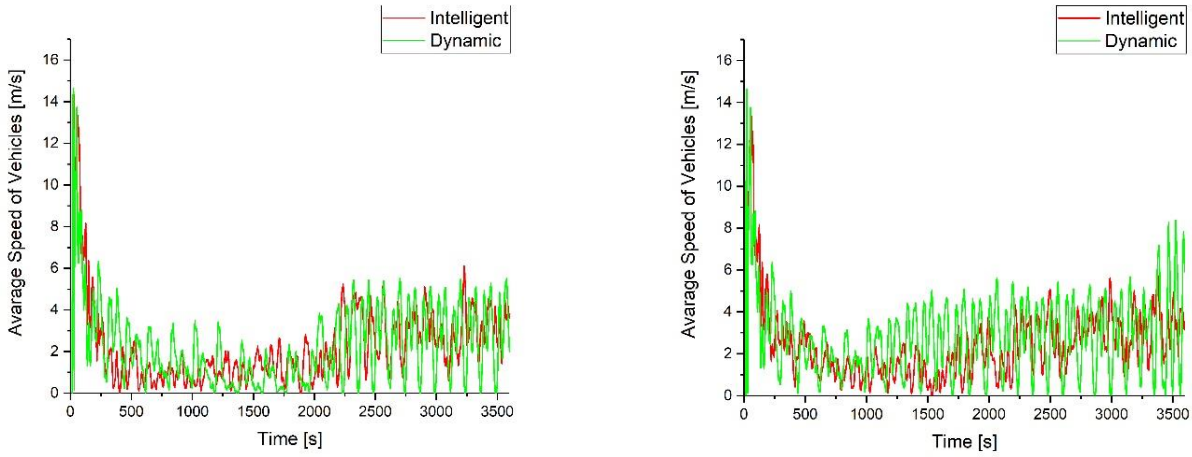

Figure 5.14 - Comparison of vehicle speeds throughout the environment for both systems for the High-High (a) and High-Low (b) scenarios

Figure 5.15 a) and b) shows the queue size graphs for the first intersection in both scenarios. For the intelligent system, it can be seen that in the first half hour of simulation, the queue is longer in the first scenario a) than in the second b). This is due to the fact that the high number of pedestrians circulating in the environment causes the system to prioritise them, affecting the flow of cars at the intersection and keeping them waiting. In the second scenario there are no longer as many cars waiting, since the number of pedestrians also decreases, making the system balanced. In the second half hour in the high pedestrian scenario, there are still cars at the intersection, while in the second scenario most of the cars are dispatched.

As for the dynamic system, it naturally has more cars waiting in the first scenario than the second, as mentioned above due to the greater number of pedestrians at the intersection. In the second half hour of simulation, the cars queuing at the first intersection remain around 30 on average, while for the low pedestrian traffic scenario, the system manages to dispatch all the cars at the intersection.

Comparing the systems, both behave similarly in terms of cars waiting at the intersection. In the first half hour, where the intelligent system prioritises pedestrians, it has more cars waiting, but quickly recovers in the second half hour, equalling or even lowering the number of vehicles queuing.

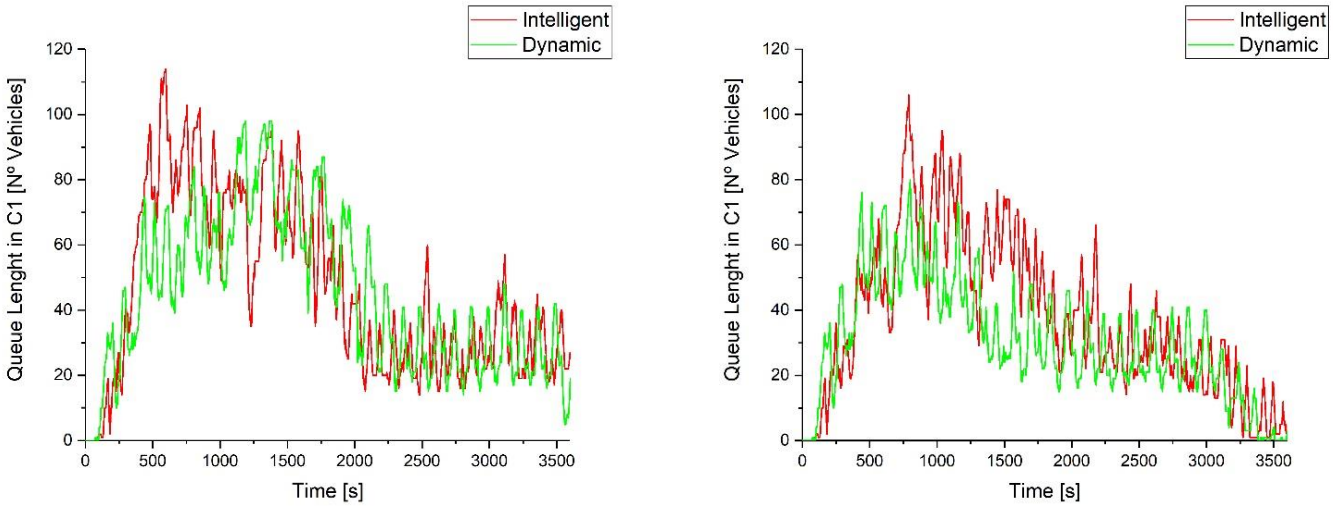

Figure 5.15 - Comparison of queue length at intersection C1 for both systems in the High-High (a) and High-Low (b) scenarios

Figure 5.16 a) and b) show the size of the queues at the second intersection for both scenarios. Starting with the intelligent system, it can be seen that in the high pedestrian traffic scenario it again has more cars waiting than the dynamic system. In the second half hour of simulation, the intelligent system manages to catch up by equalising and sometimes even obtaining fewer waiting cars. In the lower pedestrian flow scenario b), it can be seen that throughout the simulation the dynamic system managed the cars better than the intelligent system, even dispatching all the cars at the intersection.

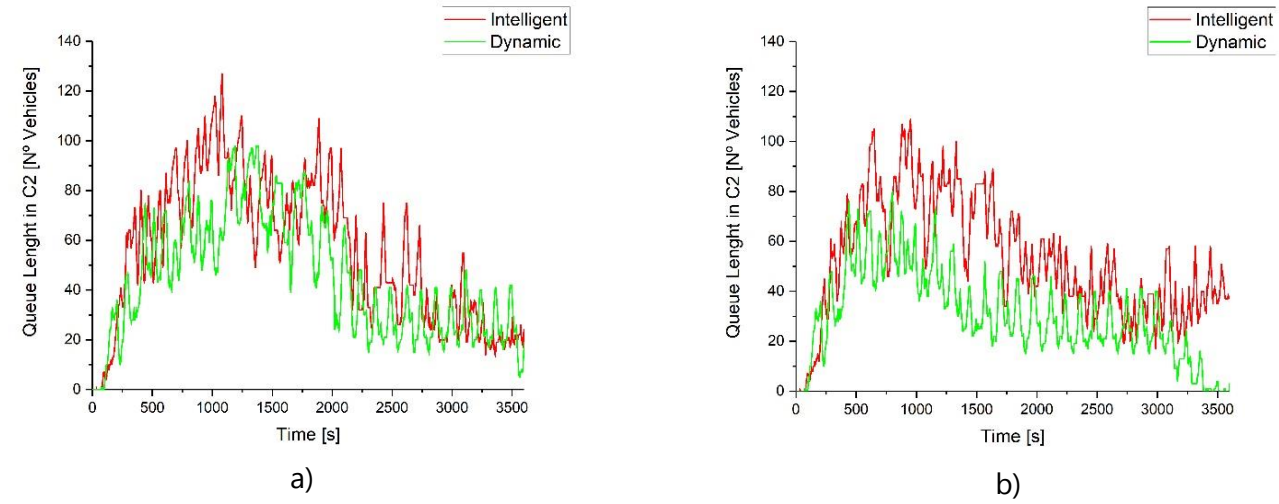

Figure 5.16 - Comparison of queue length at intersection C2 for both systems in the High-High (a) and High-Low (b) scenarios

We then move on to the analysis of the last two scenarios, Low-High and Low-Low, in order to observe the behaviour of the systems, maintaining a low number of vehicles on the roads while varying the number of pedestrians.

Figure 5.17 a) and b) shows the graphs of the number of pedestrians stopped in the waiting zones at both intersections for both scenarios. In the intelligent system, for the Low-High scenario (a), it can be seen that it manages to outperform the dynamic system, since it has a peak number of pedestrians waiting of only 400, while for the dynamic system this peak is much higher, reaching approximately 1200. For the second Low-Low b) scenario, the systems are more balanced, with the intelligent system still dispatching more pedestrians than the dynamic one.

This inequality in values is related to the difference between the two systems. While the intelligent system is able to decide to prioritise pedestrians at an early stage of the system, not having many pedestrians in the waiting areas standing still, adapting to both the flow of pedestrians and vehicles, jumping between the phases it deems best to activate at the time, the dynamic system follows a pre-defined cycle of phases, where only at the end of each one is the pedestrian phase activated, resulting in a high value of people waiting. In the dynamic system it is still possible to observe the various cycles over time. The various peaks of waiting pedestrians indicate the activation of the pedestrian phase, i.e. the indication of when the cycles end, and are spaced around 80 seconds apart, which is the duration of a cycle for low vehicle traffic. As this cycle is shorter, the value of waiting pedestrians no longer reaches 1500 in the graph for the High-High scenario, i.e. the system activates the pedestrian phase more quickly and doesn't let pedestrians accumulate to these higher values.

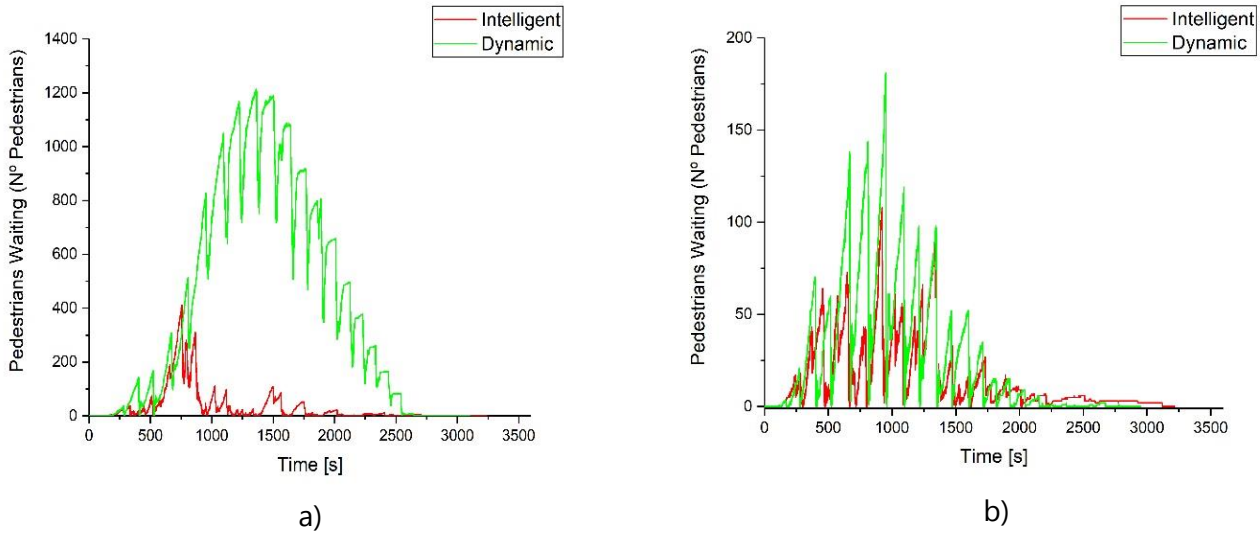

Figure 5.17 - Comparison of the number of pedestrians stopped waiting in both systems for the Low-High (a) and Low-Low (b) scenarios

Figure 5.18 a) and b) shows the average pedestrian speeds in the environment for both scenarios, where it can be seen that the behaviour is as expected. The intelligent system, for the first scenario a), being able to prioritise pedestrians more at an early stage of the simulation, manages to maintain the flow of pedestrians with a higher average speed, while the dynamic system has more pedestrians waiting, which causes the speed to decrease. In the second scenario, where the number of waiting pedestrians is similar, there is a better balance in pedestrian speeds over the course of the simulation.

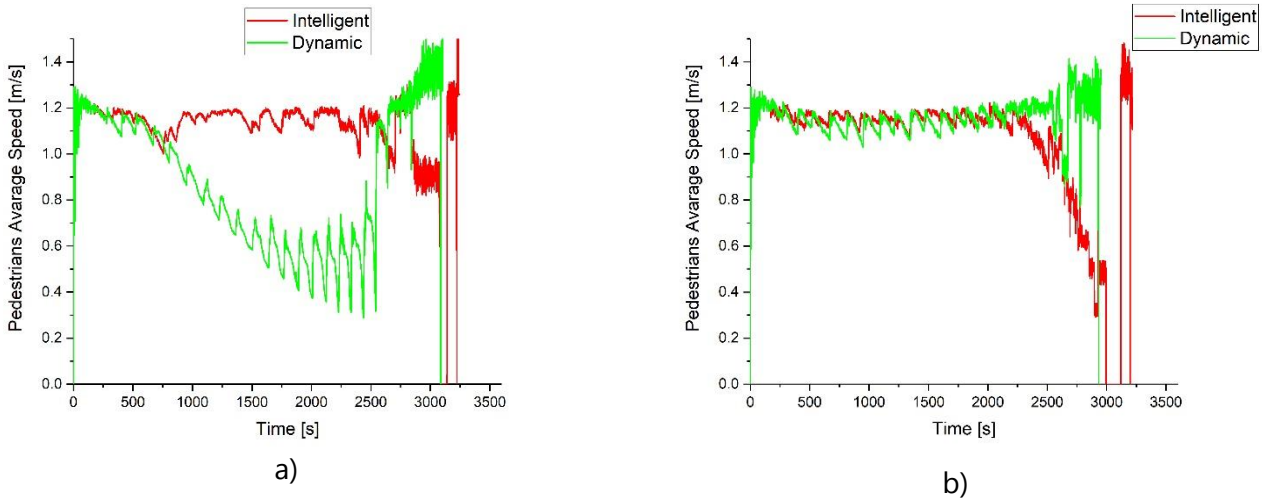

Figure 5.18 - Comparison of pedestrian speed through the environment in both systems for the Low -High (a) and Low -Low (b) scenarios

With regard to the behaviour of the systems for vehicle flow, figures 5.19 a) and b) show graphs of the number of cars waiting in the environment in both scenarios.

For the intelligent system, for the first scenario a), it can be seen that there are quite a few cars waiting when compared to the dynamic system. Somehow the system prioritised pedestrians at the start of the simulation but never managed to catch up, as seen in the previous graphs. The dynamic system, on the other hand, has a higher number of stopped cars in the first half hour, but then it decreases until it dispatches all the vehicles.

In the second scenario, the intelligent system again shows the expected behaviour. In the first half hour, prioritising pedestrians, the cars wait longer. In the second part of the simulation, the system manages to catch up and match the behaviour of the dynamic system, but never manages to dispatch all the cars in the environment. On the other hand, the dynamic system always manages to serve the cars, dispatching them even before the hour is up.

Figures 5.20 a) and b) show the average speed of the vehicles in the environment for both scenarios. It can be seen that the dynamic system, for both scenarios, has a higher average speed, since due to

its cycle of fixed vehicle phases it manages to have a greater flow of vehicles in the environment, with higher speed values.

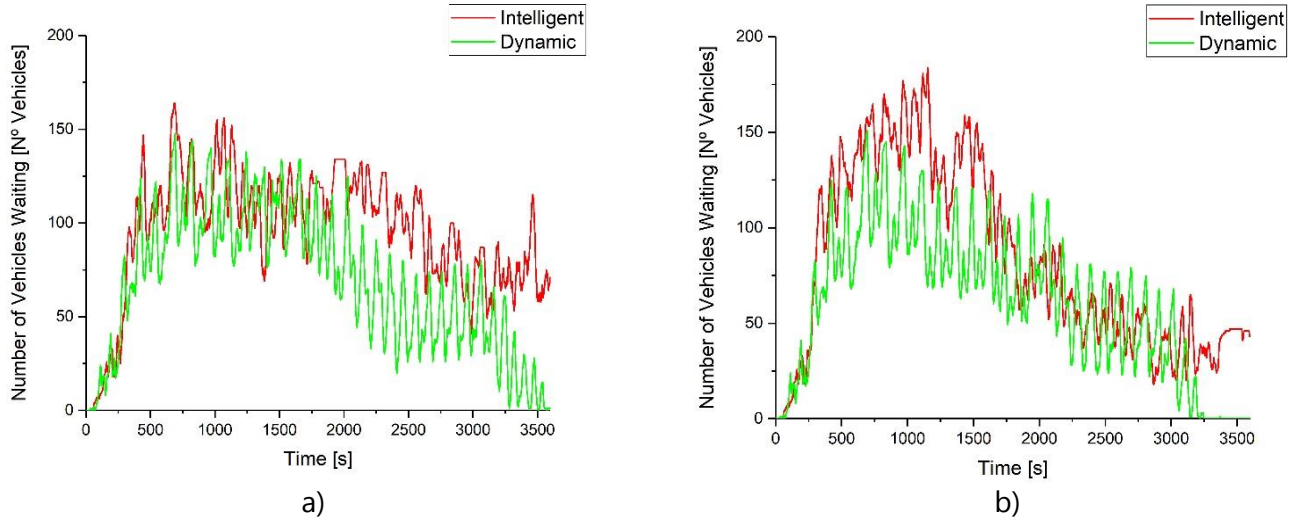

Figure 5.19 - Comparison of the number of cars in the entire environment for both systems for the Low-High (a) and Low-Low (b) scenarios

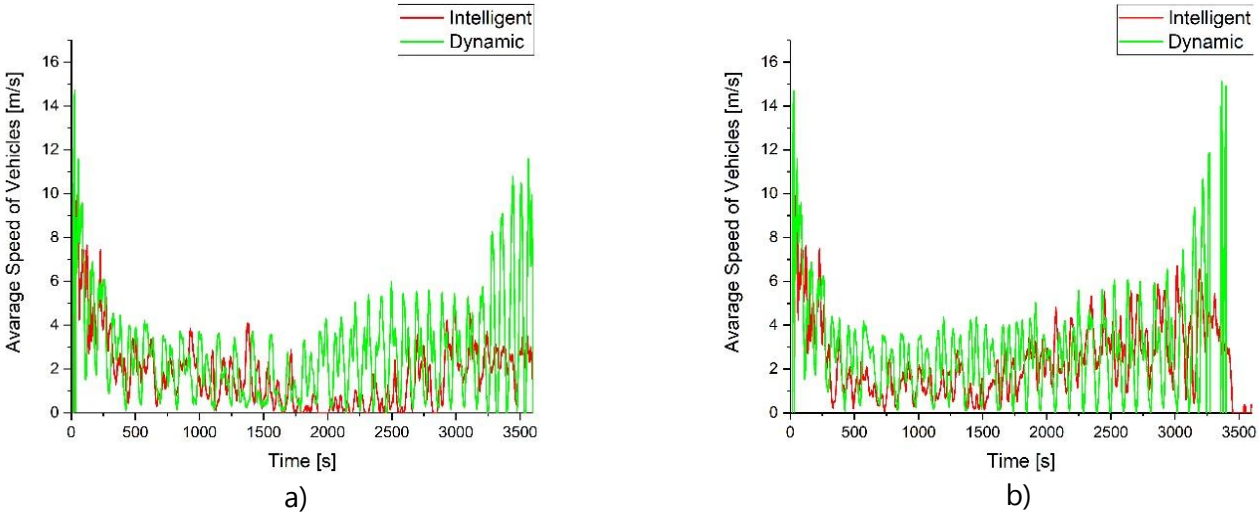

Figure 5.20 - Comparison of vehicle speeds throughout the environment for both systems for the Low-High (a) and Low-Low (b) scenarios

Figure 5.21 a) and b) shows the average queue size for the first intersection in both scenarios.
The same analysis can be made for the intelligent system in both scenarios. In the first half hour, a half hour in which there is a greater influx of pedestrians at the intersection, there is a greater priority for the system to satisfy their requests, affecting the flow of cars at the intersection, thus increasing the queues. In the second half hour, the values decrease, managing to dispatch almost all the cars at the

intersection, following the values of the dynamic system which shows a very similar behaviour, only with more peaks in the values, which indicates the end of each phase cycle.

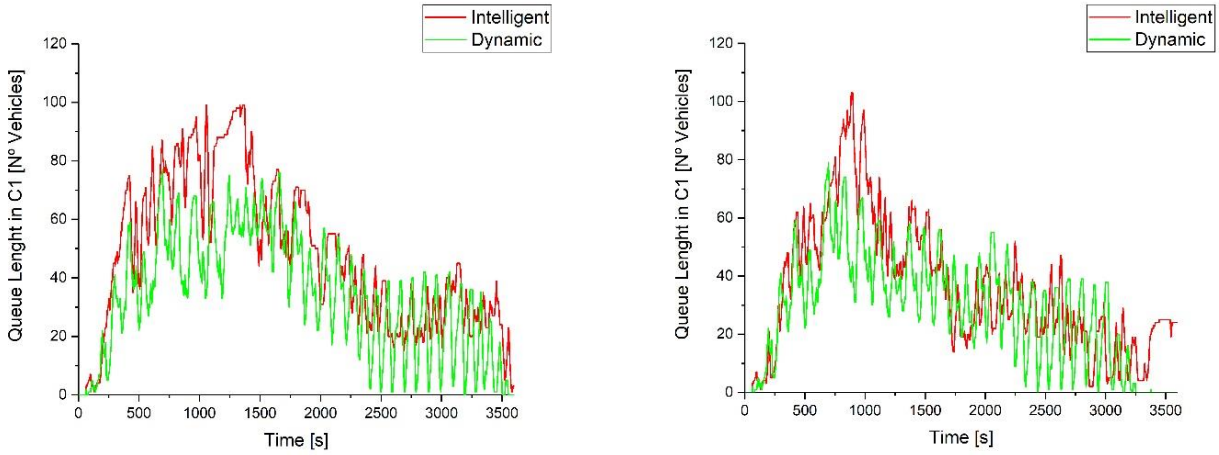

Figure 5.21 - Comparison of queue lengths at intersection C1 for both systems in the Low-High (a) and Low-Low (b) scenarios

The same analysis can be made for the second intersection. It can be seen that for the first scenario, both systems behave similarly, managing to dispatch most of the vehicles at the intersections. For the second scenario, however, the intelligent system has higher values in the first hour and lower values in the second hour, in line with the behaviour of the dynamic system.

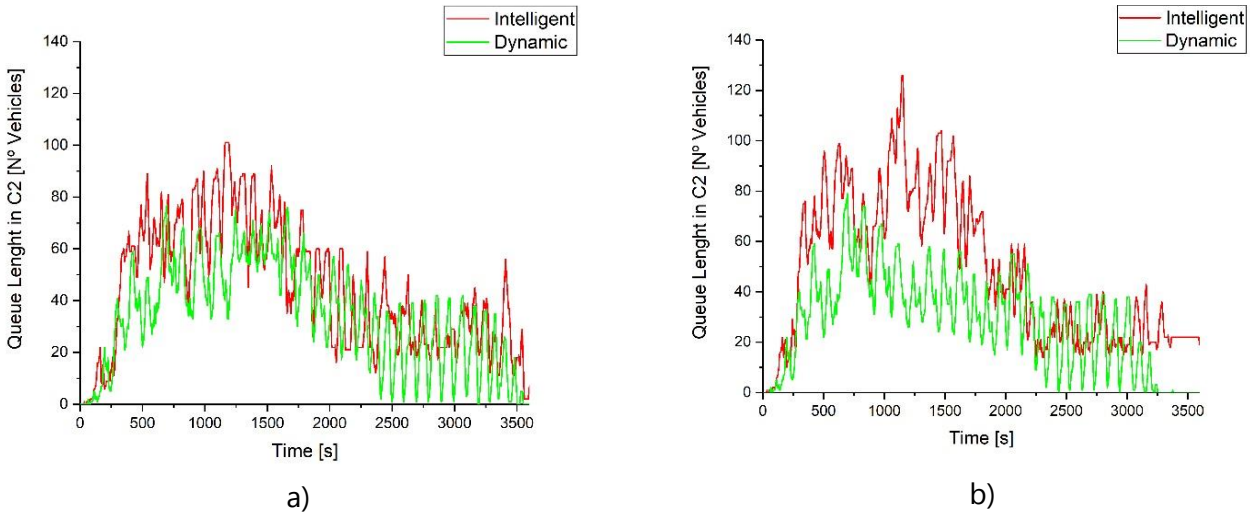

Figure 5.22 - Comparison of queue lengths at intersection C2 for both systems in the Low-High (a) and Low-Low (b) scenarios

After analysing the various scenarios and metrics taken from the study of traffic scenarios made up of different pedestrian and vehicle flows, it can be concluded that, in general, the intelligent system manages to outperform the dynamic system. The latter actually manages to obtain better values for the flow of cars, where it was observed that it obtained fewer waiting cars at both intersections, for the various scenarios. This difference turns out not to be very significant when compared to the values of the intelligent system, not least because it affects the flow of vehicles in the environment initially, but almost systematically manages to recover and give priority to vehicles again after the pedestrians have been mostly dispatched.

In order to have a system with pedestrians and vehicles, there has to be a balancing of the system so that it can respond to the needs of both groups in a more or less balanced way, with someone always being affected.

The dynamic system, with its fixed phase cycle of 120 seconds for larger vehicle flows and 80 seconds for smaller flows, ends up giving more priority to vehicles, since 10% and 15% of the time, respectively for each cycle, is reserved for pedestrians to pass, which ends up being short for high pedestrian flows as was observed, with many pedestrians standing still, filling up the waiting areas.

The intelligent system, on the other hand, with its real-time adaptation to the traffic observed at intersections, manages to decide to initially give more priority to pedestrians, since they were in large numbers in the environment, but never affecting vehicles too much, as was observed. The numbers of cars queuing and stopped throughout the environment were indeed higher, but the difference is not so significant as to justify waiting for so many pedestrians in waiting areas, as was observed in the dynamic system. It can therefore be concluded that the intelligent system performed better than the dynamic system for these scenarios under study.

6 CONCLUSION

The report is completed in this chapter. Because it was possible to properly develop and test what was designed, the suggested objectives were met. The most important takeaways from the project's development will be highlighted in this chapter, along with commentary on the outcomes. The following section is set aside to list potential future research in this field.

6.1 Final Comments

This thesis covers three main topics that have been addressed in the state of art: connected vehicles, visible light communication and reinforcement learning.

Connected and autonomous vehicles, with the advancement of technology, can circulate on roads by constantly monitoring their surroundings through implemented sensors that map the space around the vehicle. They can also exchange information with other vehicles (V2V) or infrastructures (V2I/I2V). This communication is crucial, especially for autonomous vehicles, which need reliable information exchange to navigate from one place to another without human intervention. To establish this communication, LEDs are used as transmitters, allowing visible light to be transmitted and modulated in intensity at high speeds, imperceptible to the human eye. A photodetector or camera sensor is used as a receiver to decode the signal.

With information collected through VLC, a system is needed to interpret the data to optimize the traffic flow, for example, at intersections, where the system adapts to observed traffic by activating phases that best suit the moment. The system is implemented using reinforcement learning, with deep Q-Learning algorithms to train an agent to make decisions regarding phase activation.

As part of the work, the system was implemented in a traffic environment consisting of two intersections. The positioning of lamps spaced 20 meters along the road, with modulated LED lights, will identify the position of vehicles along the road, mapping the surrounding environment of the intersections. This information is used by the Intersection Manager to make decisions about which phase to activate. Following the protocol established for the various communications, V2V, I2V/V2I for vehicles, and P2I/I2P communications for pedestrians were simulated.

Additionally, a dynamic traffic control system similar to those implemented in intersections today was developed. Various traffic scenarios, with vehicles and pedestrians, were simulated. This allowed an estimate of the number of cars that will be dispatched from the environment per hour, serving as a starting point for the intelligent system.

Finally, the intelligent traffic control system, where two agents control the two intersections to optimize traffic flow. When compared with the dynamic traffic control system, the results show that with the intelligent system is possible to optimize the vehicular traffic flow in the environment, as well as pedestrians traffic flow.

With the free choice of phases in the intelligent system, which does not follow a strict order as in the dynamic system, it is able to satisfy the needs of both vehicles and pedestrians in the environment.

By implementing this system, where traffic data is collected via VLC, the agent placed at the intersections is able to map the environment around it and then make the best phase activation decision, thus optimising traffic flow.

6.2 Future Work

The future work focuses on developing a vehicle and pedestrian management strategy for the city of Lisbon using AI agents equipped with Visible Light Communication (VLC) sensors. This strategy will be based on a detailed study of two adjacent and symmetrical intersections, addressing sections with either surplus or deficit traffic flow. The goal is to resolve conflicts arising from incompatible actions, prioritize levels of urgency, and establish rules to determine which traffic connection proposals need to be adjusted.

An integrated VLC and AI system bring benefits in vehicle and pedestrian management. AI agents can use VLC data to monitor and control traffic in real-time, ensuring safety and efficiency. AI can also implement rules to determine priority levels among traffic connections, adjusting proposals to manage the most critical areas first. VLC ensures these adjustments are communicated instantaneously. The integration of VLC and AI creates a responsive traffic management system that adapts to changing conditions, reduces congestion, and enhances overall safety for all road users.

By integrating VLC sensors and AI agents, this approach aims to create a dynamic and responsive traffic management system, improving overall traffic flow and reducing congestion in urban areas like Lisbon.

In summary, the synergy between VLC and AI provides a powerful toolset for managing urban traffic. VLC enables real-time, high-bandwidth communication, while AI offers intelligent analysis and adaptive control. Together, they can significantly improve traffic flow, reduce congestion, and enhance safety in urban environments.

The future working scenario envisions a systematic expansion of intersections, forming new agent connections in various configurations such as radial, circular, square, or roundabout road structures. Intersections will be connected in different patterns - two, three, four, or five intersections at a time adapting to various road structures.

This expansion will be guided by a multi-agent network that studies and learns general control strategies and travel models for both vehicles and pedestrians, enhancing traffic management and flow. Specific strategies will also be developed for priority vehicles (e.g., emergency services) to ensure their smooth transit through fluid road sections.

REFERENCES

[1] E. Uhlemann, "Introducing connected vehicles [Connected vehicles]," *IEEE Vehicular Technology Magazine*, vol. 10, no. 1. Institute of Electrical and Electronics Engineers Inc., Mar. 01, 2015. doi: 10.1109/MVT.2015.2390920.

[2] N. Lu, N. Cheng, N. Zhang, X. Shen, and J. W. Mark, "Connected vehicles: Solutions and challenges," *IEEE Internet of Things Journal*, vol. 1, no. 4. Institute of Electrical and Electronics Engineers Inc., pp. 289–299, Aug. 01, 2014. doi: 10.1109/JIOT.2014.2327587.

[3] M. M. Rana and K. Hossain, "Connected and Autonomous Vehicles and Infrastructures: A Literature Review," *International Journal of Pavement Research and Technology*, vol. 16, no. 2. Springer, pp. 264–284, Mar. 01, 2023. doi: 10.1007/s42947-021-00130-1.

[4] "Connected Automated Driving Roadmap Status: final for publication."

[5] "AI IN THE DRIVING SEAT: KEY CHALLENGES FOR THE FUTURE OF ADVANCED DRIVER ASSISTANCE SYSTEMS (ADAS)," 2019.

[6] H. S. M. Lim and A. Taeihagh, "Autonomous vehicles for smart and sustainable cities: An in-depth exploration of privacy and cybersecurity implications," *Energies (Basel)*, vol. 11, no. 5, 2018, doi: 10.3390/en11051062.

[7] R. Hoogendoorn, B. Van Arem, and S. Hoogendoorn, "Automated driving, traffic flow efficiency, and human factors," *Transp Res Rec*, vol. 2422, pp. 113–120, 2014, doi: 10.3141/2422-13.

[8] S. E. Shladover, D. Su, and X. Y. Lu, "Impacts of cooperative adaptive cruise control on freeway traffic flow," *Transp Res Rec*, vol. 2324, pp. 63–70, 2012, doi: 10.3141/2324-08.

[9] D. Milakis, B. Van Arem, and B. Van Wee, "Policy and society related implications of automated driving: A review of literature and directions for future research," *Journal of Intelligent Transportation Systems: Technology, Planning, and Operations*, vol. 21, no. 4, pp. 324–348, 2017, doi: 10.1080/15472450.2017.1291351.

[10] F. Report, C. M. Poe, P. J. Edward Seymour, S. Kuciemba WSP USA Washington, and D. Shelley Row, "CONNECTED ROADWAY CLASSIFICATION SYSTEM DEVELOPMENT," 2019.

[11] R. R. Slavescu, S. Nedevschi, R. Potolea, Universitatea Tehnicǎ din Cluj-Napoca. Computer Science Department, IEEE Romania Section, and Institute of Electrical and Electronics Engineers, *Proceedings, 2019 IEEE 15th International Conference on Intelligent Computer Communication and Processing (ICCP) : Cluj-Napoca, Romania, September 5-7, 2019*.

[12] "IEEE Standard for Information technology-- Local and metropolitan area networks-- Specific requirements-- Part 11: Wireless LAN Medium Access Control (MAC) and Physical Layer (PHY) Specifications Amendment 6: Wireless Access in Vehicular Environments," 2010. doi: 10.1109/IEEESTD.2010.5514475.

[13] S. A. A. Shah, E. Ahmed, M. Imran, and S. Zeadally, "5G for Vehicular Communications," *IEEE Communications Magazine*, vol. 56, no. 1, pp. 111–117, Jan. 2018, doi: 10.1109/MCOM.2018.1700467.

[14] Institute of Electrical and Electronics Engineers, *IEEE PIMRC 2016.*

[15] M. and L. P. and V. P. and F. R. Vieira Manuel Augusto and Vieira, "Adaptive Traffic Control Using Cooperative Communication Through Visible Light," in *Internet of Things. IoT through a Multi-disciplinary Perspective*, L. and S. L. Camarinha-Matos Luis M. and Ribeiro, Ed., Cham: Springer International Publishing, 2022, pp. 315–331.

[16] R. Fernandes, M. A. Vieira, M. Vieira, P. Vieira, P. Louro, and M. Véstias, "Using visible light communication to implement intelligent traffic signals and cooperative trajectories at urban intersections," in *Light-Emitting Devices, Materials, and Applications XXVII*, J. K. Kim, M. R. Krames, and M. Strassburg, Eds., SPIE, 2023, p. 124410G. doi: 10.1117/12.2647862.

[17] M. A. Vieira, M. Vieira, P. Vieira, R. Fernandes, and P. Louro, "Dynamic vehicular visible light communication for traffic management," in *Next-Generation Optical Communication: Components, Sub-Systems, and Systems XII*, G. Li, K. Nakajima, and A. K. Srivastava, Eds., SPIE, 2023, p. 124290O. doi: 10.1117/12.2647866.

[18] P. H. Pathak, X. Feng, P. Hu, and P. Mohapatra, "Visible Light Communication, Networking, and Sensing: A Survey, Potential and Challenges," *IEEE Communications Surveys and Tutorials*, vol. 17, no. 4. Institute of Electrical and Electronics Engineers Inc., pp. 2047–2077, Oct. 01, 2015. doi: 10.1109/COMST.2015.2476474.

[19] "Frequency of Target Crashes for IntelliDrive Safety Systems," 2010. [Online]. Available: www.ntis.gov

[20] M. A. Vieira, M. Vieira, P. Louro, P. Vieira, and A. Fantoni, "Vehicular Visible Light Communication for Intersection Management," *Signals*, vol. 4, no. 2, pp. 457–477, 2023, doi: 10.3390/signals4020024.

[21] A. M. Cailean and M. Dimian, "Current Challenges for Visible Light Communications Usage in Vehicle Applications: A Survey," *IEEE Communications Surveys and Tutorials*, vol. 19, no. 4. Institute of Electrical and Electronics Engineers Inc., pp. 2681–2703, Oct. 01, 2017. doi: 10.1109/COMST.2017.2706940.

[22] A. Memedi and F. Dressler, "Vehicular visible light communications: A survey," *IEEE Communications Surveys and Tutorials*, vol. 23, no. 1, pp. 161–181, Jan. 2021, doi: 10.1109/COMST.2020.3034224.

[23] J. He, K. Tang, J. He, and J. Shi, "Effective vehicle-to-vehicle positioning method using monocular camera based on VLC," *Opt Express*, vol. 28, no. 4, p. 4433, Feb. 2020, doi: 10.1364/oe.382482.

[24] J. Oskarbski, L. Guminska, M. Miszewski, and I. Oskarbska, "Analysis of Signalized Intersections in the Context of Pedestrian Traffic," in *Transportation Research Procedia*, Elsevier B.V., 2016, pp. 2138–2147. doi: 10.1016/j.trpro.2016.05.229.

[25] A. M. Căilean, C. Beguni, S. A. Avătămăniței, M. Dimian, and V. Popa, "Design, Implementation and Experimental Investigation of a Pedestrian Street Crossing Assistance System Based on Visible Light Communications," *Sensors*, vol. 22, no. 15, Aug. 2022, doi: 10.3390/s22155481.

[26] E. Plascencia, H. Guan, L. Chassagne, O. Barrois, O. Shagdar, and A. M. Căilean, "A Comprehensive Investigation on Multi-User Interference Effects in Vehicular Visible Light Communications," *Sensors*, vol. 23, no. 5, Mar. 2023, doi: 10.3390/s23052553.

[27] A. Cailean, B. Cagneau, L. Chassagne, M. Dimian, and V. Popa, "Novel Receiver Sensor for Visible Light Communications in Automotive Applications," *IEEE Sens J*, vol. 15, no. 8, pp. 4632–4639, 2015, doi: 10.1109/JSEN.2015.2425473ï.

[28] G. A. Zhang, J. Y. Gu, Z. H. Bao, C. Xu, and S. B. Zhang, "Joint routing and channel assignment algorithms in cognitive wireless mesh networks," *Transactions on emerging telecommunications technologies*, vol. 25, no. 3, pp. 294–307, 2014, doi: 10.1002/ett.

[29] "Vehicle Safety Communications Project Task 3 Final Report Identify Intelligent Vehicle Safety Applications Enabled by DSRC," 2005.

[30] T. Nawaz, M. Seminara, S. Caputo, L. Mucchi, and J. Catani, "Low-latency VLC system with fresnel receiver for I2V ITS applications," *Journal of Sensor and Actuator Networks*, vol. 9, no. 3, Jul. 2020, doi: 10.3390/JSAN9030035.

[31] G. Galvão, M. Vieira, P. Louro, M. Vieira, M. Véstias, and P. Vieira, "Visible Light Communication at Urban Intersections to Improve Traffic Signaling and Cooperative Trajectories," Apr. 2023, pp. 60–65. doi: 10.1109/YEF-ECE58420.2023.10209320.

[32] M. A. Vieira, M. Vieira, P. Louro, P. Vieira, and R. Fernandes, "Adaptive Traffic Control Using Cooperative Communication Through Visible Light," *SN Comput Sci*, vol. 5, no. 1, p. 159, 2024, doi: 10.1007/s42979-023-02483-9.

[33] A. Vidali, L. Crociani, G. Vizzari, and S. Bandini, "A Deep Reinforcement Learning Approach to Adaptive Traffic Lights Management." [Online]. Available: https://population.un.org/wup/

[34] A. Tigga, L. Hota, S. Patel, and A. Kumar, "A Deep Q-Learning-Based Adaptive Traffic Light Control System for Urban Safety," in *Proceedings - 2022 4th International Conference on Advances in Computing, Communication Control and Networking, ICAC3N 2022*, Institute of Electrical and Electronics Engineers Inc., 2022, pp. 2430–2435. doi: 10.1109/ICAC3N56670.2022.10074123.

[35] R. Michelucci, "Deep Q-learning From a single agent to a multi-agent perspective for Traffic Signal Control."

[36] M. A. Vieira, G. Galvão, M. Vieira, P. Louro, M. Vestias, and P. Vieira, "Enhancing Urban Intersection Efficiency: Visible Light Communication and Learning-Based Control for Traffic Signal Optimization and Vehicle Management," *Symmetry (Basel)*, vol. 16, no. 2, 2024, doi: 10.3390/sym16020240.

[37] L. B. Bus¸oniu, R. Babuška, and B. De Schutter, "Multi-Agent Reinforcement Learning: A Survey," 2006.

[38] H. Ge, Y. Song, C. Wu, J. Ren, and G. Tan, "Cooperative deep Q-learning with Q-value transfer for multi-intersection signal control," *IEEE Access*, vol. 7, pp. 40797–40809, 2019, doi: 10.1109/ACCESS.2019.2907618.

[39] A. Yousefpour *et al.*, "All one needs to know about fog computing and related edge computing paradigms: A complete survey," *Journal of Systems Architecture*, vol. 98. Elsevier B.V., pp. 289–330, Sep. 01, 2019. doi: 10.1016/j.sysarc.2019.02.009.

[40] M. A. Vieira, G. Galvão, M. Vieira, M. Véstias, P. Vieira, and P. Louro, "Traffic Signaling and Cooperative Trajectories based on Visible Light Communication," *Sensors and Electronic Instrumentation Advances*, p. 23, 2023.

[41] M. A. Vieira, M. Vieira, P. Louro, and P. Vieira, "Optical vehicular communication based on a-SiC:H technology," *Science and Technology of Materials*, vol. 30, no. 3, pp. 151–156, Sep. 2018, doi: 10.1016/J.STMAT.2018.05.003.

[42] M. Vieira, M. A. Vieira, G. Galvão, P. Louro, M. Véstias, and P. Vieira, "Enhancing Urban Intersection Efficiency: Utilizing Visible Light Communication and Learning-Driven Control for Improved Traffic Signal Performance," *Vehicles*, vol. 6, no. 2, pp. 666–692, 2024, doi: 10.3390/vehicles6020031.

[43] G. Galvão, M. A. Vieira, M. Vieira, P. Vieira, P. Louro, M. Vestias, P. Lourenço, "Traffic signals and cooperative trajectories at urban intersections: leveraging visible light communication for implementation," Proc. SPIE 12906, Light-Emitting Devices, Materials, and Applications XXVIII, 129060O (13 March 2024); doi : 10.1117/12.3000529

[44] M. A. Vieira, G. Galvão, M. Vieira, M. Véstias, P. Vieira, and P. Louro, "Sensors & Transducers Enhancing Traffic Management through Visible Light Communication-Driven Signaling and Cooperative Trajectories," 2023. [Online]. Available: http://www.sensorsportal.com

[45] Manuel Augusto Vieira, Manuela Vieira, Paula Louro, Gonçalo Galvão, Pedro Vieira, "Smarter Intersections with Cooperative Vehicular Visible Light Communication", SENSORDEVICES 2023 : The Fourteenth International Conference on Sensor Device Technologies and Applications, September 25, 2023 to September 29, 2023, Porto-Portugal, pp. 7-12, Copyright (c) IARIA, 2023. ISBN: 978-1-68558-091-9.